Three-Dimensional Aromaticity in Polyhedral Boranes and Related Molecules

R. Bruce King

Department of Chemistry, University of Georgia, Athens, Georgia 30602

Received July 10, 2000

Contents

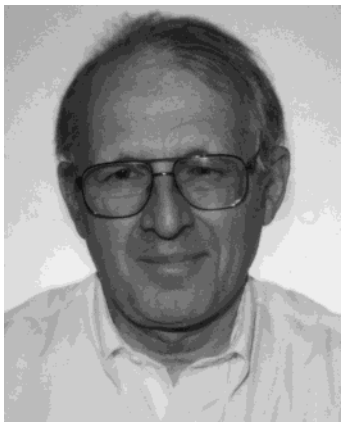

R. Bruce King was born in Rochester, NH, in 1938, attended Oberlin College (B.A. 1957), and was an NSF Predoctoral Fellow with Professor F. G. A. Stone at Harvard University (Ph.D. 1961). After 1 year at du Pont and 4.5 years at the Mellon Institute, he joined the faculty of the University of Georgia, where he is now Regents' Professor of Chemistry. His research interests have ranged from synthetic organometallic and organophosphorus chemistry to applications of topology and graph theory in inorganic chemistry and the inorganic chemistry of nuclear waste treatment. Professor King was the American Regional Editor of the *Journal of Organometallic Chemistry* from 1981 to 1998 as well as Editor-in-Chief of the *Encyclopedia of Inorganic Chemistry* published in 1994. He is the recipient of American Chemical Society Awards in Pure Chemistry (1971) and Inorganic Chemistry (1991). During the past decade, he has published books entitled *Applications of Graph Theory and Topology in Inorganic Cluster and Coordination Chemistry* (1993), *Inorganic Main Group Element Chemistry* (1994), and *Beyond the Quartic Equation* (1996). All three of these books have icosahedra on their covers similar to the $B_{12}H_{12}^{2-}$ structure discussed in this review. Professor King's hobbies include contract bridge, music, and travel.

I. Introduction

The capacity of boron to catenate and form self-bonded complex molecular networks is as extensive as any element except for carbon. However, the principles of structure and bonding in the binary compounds of boron and hydrogen, namely, the boranes, are so different from those of hydrocarbons that hydrocarbon chemistry has historically provided very little guidance for the understanding of borane chemistry. The high reactivity of the neutral boranes required the development of special techniques for handling them by Alfred Stock[1] before any of their formulas could be reliably determined.

This pioneering work of Stock led to the identification of the neutral boron hydrides B_2H_6, B_4H_{10}, B_5H_9, B_5H_{11}, and B_6H_{10} as toxic and air- and water-sensitive gases or volatile liquids as well as the more stable volatile solid $B_{10}H_{14}$ (Figure 1). However, even after the unambiguous identification of these substances,

10.1021/cr000442t CCC: $36.00
Published on Web 03/03/2001

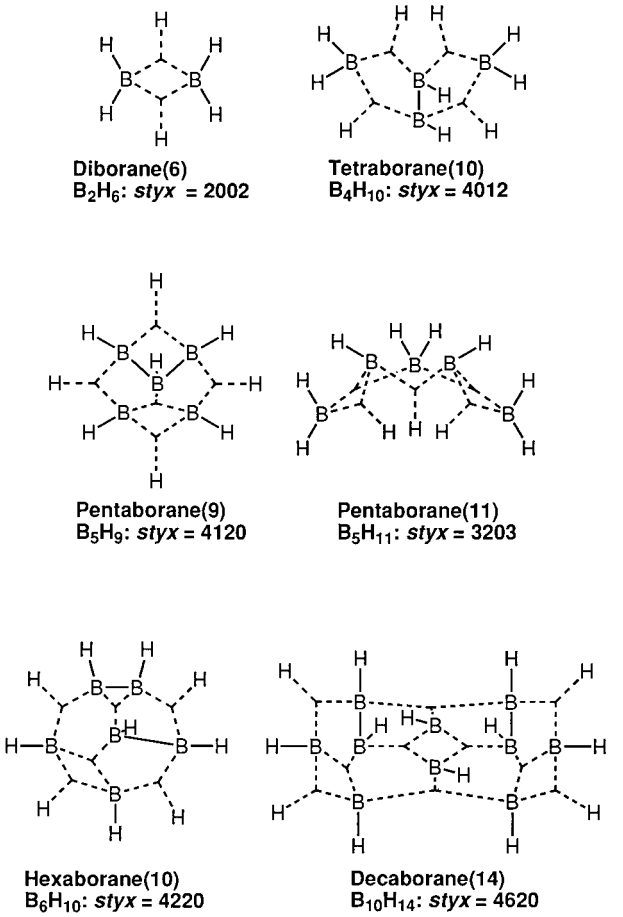

Figure 1. The six boranes originally characterized by Stock.

which clearly provided an indication of the catenation ability of boron in molecular compounds, there remained the question of their structure and bonding. This dilemma was most apparent in the simplest boron hydride diborane, B_2H_6, which has the stoichiometry of the hydrocarbon ethane, C_2H_6, but two electrons fewer. In addition, for a long time it was not clear why BF_3, BCl_3, and $B(CH_3)_3$ were stable as monomers with apparently trivalent boron whereas BH_3 dimerizes spontaneously to B_2H_6.

The structure of diborane now known to be correct, namely, $B_2H_4(\mu\text{-}H)_2$ (Figure 1), was first predicted by Dilthey[2] in 1921 but only considered seriously in the early 1940s after evidence supporting this structure was obtained from infrared spectra.[3,4] However, even after some initial experimental data relating to the structure of diborane became available, some important members of the chemical community were reluctant to accept the $B_2H_4(\mu\text{-}H)_2$ structure, which involved ideas of chemical bonding unprecedented at that time. For example, correspondence made public only recently[5] show that even Linus Pauling as late as 1945 preferred an ethane-like $H_3B{-}BH_3$ structure for diborane rather than the correct $B_2H_4(\mu\text{-}H)_2$ structure. However, the correct $B_2H_4(\mu\text{-}H)$ structure for diborane was subsequently confirmed beyond any reasonable doubt by electron-diffraction studies[6] and low-temperature X-ray diffraction work.[7] Consideration of the chemical bonding in the correct diborane structure first led to the concept of the "protonated double bond", initially proposed by Pitzer[8] in 1945.

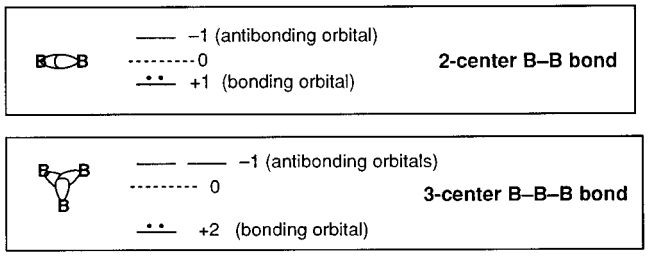

Figure 2. Comparison of 2c-2e B−B and 3c-2e B−B−B bonding.

Subsequent work by Lipscomb and collaborators[9] led in 1954 to the concept of three-center two-electron (3c-2e) bonding (Figure 2), which in the case of diborane consists of two 3c-2e B−H−B bonds involving the bridging hydrogen atoms. Further theoretical work by Lipscomb[7] led to the topological models for the structures of all of the known boranes in which 3c-2e B−H−B bonds are key building blocks. Initially Lipscomb[7] proposed that the structures of all of the then known neutral boron hydrides (Figure 1) were based on icosahedral fragments except for B_5H_9, whose square pyramidal structure was clearly derived from an octahedron by removal of a single vertex. Eventually, after considerable additional experimental information became available, Williams[10] corrected this suggestion of Lipscomb in a seminal paper describing the "most spherical" deltahedra which are the key structural units in boron structures containing boron polyhedra or polyhedral fragments.

Chemically bonded aggregates of boron atoms are found not only in molecular boranes, but also in solid-state borides. Pioneering X-ray diffraction structural work by Allard[11] and by Pauling and Weinbaum[12] in the 1930s indicated the presence of regular octahedra of boron atoms in several metal hexaborides of the general formula MB_6. This very early work represents the first experimental demonstration of closed boron polyhedra in a chemical structure. In subsequent related work, Longuet-Higgins and Roberts[13] used molecular orbital theory to show that the $[B_6]^{2-}$ ion had a "closed-shell" arrangement of high stability and predicted that divalent metal borides of the type MB_6 should be insulators whereas hexaborides in which the metal ion has a higher charge should exhibit metallic conductivity. Their predictions were in accord with experimental evidence. Longuet-Higgins and Roberts[14] then used a similar approach to study icosahedra of boron atoms, a dominant structural feature of the various allotropes of solid elemental boron.[15] Their work[14] indicated that a B_{12} icosahedron has 13 bonding orbitals available for holding the icosahedron together (such orbitals have subsequently been called *skeletal orbitals*) in addition to the 12 outward pointing equivalent orbitals, i.e., the *external orbitals*, on the separate boron atoms. A conclusion of this work was that a borane of formula $B_{12}H_{12}$ would be stable only as a dianion $B_{12}H_{12}^{2-}$. This prediction was verified experimentally by Hawthorne and Pitochelli in 1960,[16] one year after they had prepared salts of the borane anion[17] $B_{10}H_{10}^{2-}$. Both of these anions were significantly more chemically and thermally stable than any previously

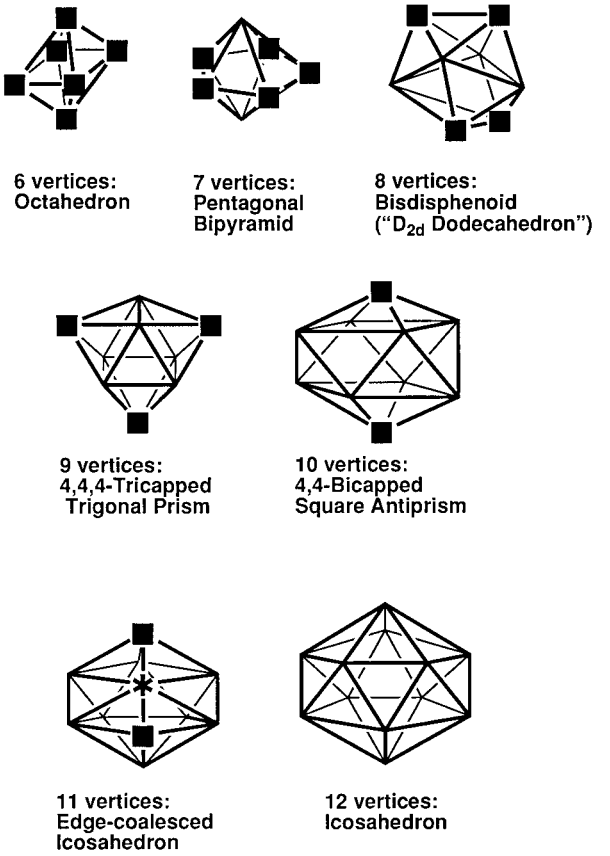

Figure 3. The most spherical deltahedra found in the boranes $B_nH_n^{2-}$ ($6 \leq n \leq 12$) and related compounds. Degree 4 vertices are indicated by a solid box (■), and degree 6 vertices are indicated by an asterisk (*).

known B−H derivatives. Determination of their structures by X-ray diffraction indicated closed polyhedral structures for both of these anions with $B_{12}H_{12}^{2-}$ being a regular icosahedron[18] and $B_{10}H_{10}^{2-}$ a bicapped square antiprism of D_{4d} idealized symmetry.[19] Subsequent work led to the syntheses of salts of the analogous anions $B_{11}H_{11}^{2-}$ (ref 20), $B_9H_9^{2-}$ (ref 20), $B_8H_8^{2-}$ (ref 21), $B_7H_7^{2-}$ (ref 21), and $B_6H_6^{2-}$ (ref 22). Structural determinations on these borane anions by X-ray diffraction indicated in all cases the presence of boron polyhedra in which all of the faces are triangles (Figure 3). Such polyhedra are conveniently called *deltahedra*. Furthermore, the vertices in all of these experimentally observed borane deltahedra with one exception were found to have degrees 4 or 5, where the degree of a vertex is the number of edges meeting at that vertex. The one exception was the presence of a single degree 6 vertex in the 11-vertex deltahedron found in $B_{11}H_{11}^{2-}$. Subsequent work by King and Duijvestijn[23] provided proof of the nontrivial fact that an 11-vertex deltahedron cannot be constructed with only degree 4 and 5 vertices; at least one degree 6 vertex is necessary. The stoichiometry of the stable borane anion deltahedra $B_nH_n^{2-}$ ($6 \leq n \leq 12$) corresponds to the presence of $n + 1$ skeletal bonding orbitals leading to $2n + 2$ skeletal electrons.[24,25,26,27]

Related deltahedral structures are exhibited by *neutral* ternary compounds of carbon, boron, and hydrogen of the general formula $C_2B_{n-2}H_n$ known as carboranes.[28] The first carboranes to be discovered were $C_2B_3H_5$, $C_2B_4H_6$, and $C_2B_5H_7$, whose structures were deduced to contain C_2B_{n-2} deltahedra, i.e., the trigonal bipyramid, octahedron, and pentagonal bipyramid for $n = 5$, 6, and 7, respectively.[29] Subsequent work led to the discovery of the three isomers of the regular icosahedral $C_2B_{10}H_{12}$ (often known as the *ortho*, *meta*, and *para* isomers by analogy to the three types of disubstituted benzene).[30,31] The neutral deltahedral carboranes $C_2B_{n-2}H_n$ are clearly isoelectronic with the corresponding deltahedral borane dianions $B_nH_n^{2-}$ through the isoelectronic substitution of C by B^-, and many of the corresponding monoanionic monocarbon carboranes $CB_{n-1}H_n^-$ have subsequently been prepared. The only unusual feature of this deltahedral borane−carborane isoelectronic relationship is that $B_5H_5^{2-}$ isoelectronic with the known[29] $C_2B_3H_5$ has never been prepared despite numerous attempts.

The compounds containing boron deltahedra, whether borane anions $B_nH_n^{2-}$, the isoelectronic carboranes $C_2B_{n-2}H_n$, or metal borides containing boron deltahedra, are characterized by unusual stability compared with the reactive and frequently unstable neutral boron hydrides such as those originally obtained by Stock.[1] The compounds with boron icosahedra appear to be the most stable and least chemically reactive of the deltahedral boron species as indicated, for example, by the stability of the $C_2B_{10}H_{12}$ isomers at temperatures around 500 °C, the low toxicity of $B_{12}H_{12}^{2-}$ salts of unreactive countercations, and the refractory nature of elemental boron and metal borides containing B_{12} icosahedra. This suggests that the concept of aromaticity, originally developed for two-dimensional polygonal molecules and ions to account, for example, for the unusual stability of benzene relative to polyolefins, might be extended to three-dimensional polyhedral molecules and ions to account for the unusual stability of deltahedral boranes and carboranes relative to boron hydrides having open structures, e.g., the original neutral binary boron hydrides discovered by Stock (Figure 1).[1] An explicit suggestion of three-dimensional aromaticity in deltahedral boranes was made by Aihara[32] in 1978, who used a graph-theoretical method to find significant positive resonance energies for deltahedral $B_nH_n^{2-}$ ($6 \leq n \leq 12$) with the experimentally very stable $B_{12}H_{12}^{2-}$ having the highest resonance energy. Meanwhile, King and Rouvray[33] used methods also derived from graph theory to demonstrate the analogy between the delocalization in two-dimensional planar polygonal aromatic hydrocarbons such as benzene and that in three-dimensional deltahedral boranes. Shortly thereafter, Stone and Alderton[34] approximated borane deltahedra by spheres so that tensor surface harmonic theory mathematically similar to that used to generate atomic orbitals for (spherical) atoms could be used to generate the skeletal molecular orbitals for borane deltahedra. This review summarizes these and other approaches to the chemical bonding in deltahedral boranes and related species showing how the concept of aromaticity originally developed for two-dimensional carbon compounds can be extended to the third dimension in boron chemistry.

II. Topological Aspects of the Chemical Bonding in Boranes

A. Three-Center Bonding in Boranes: Lipscomb's Topological Models

The feature of particular interest distinguishing three-dimensional boranes from two-dimensional planar hydrocarbons is the presence of three-center bonds. In the usual 2c-2e covalent bond, two atoms supply two orbitals, one centered on each atom. These atomic orbitals interact to form one bonding orbital and one antibonding orbital so that if two electrons are available, they will just fill the bonding orbitals and constitute the standard covalent bond such as the C−C and C−H σ-bonds typically found in hydrocarbons (Figure 2). The usual 2c-2e bond of this type provides a place for as many electrons as atomic orbitals. Thus, if n atomic orbitals form a bonding network using exclusively 2c-2e bonds such as in the saturated hydrocarbons, they form $n/2$ bonding orbitals which accommodate n electrons. For example, the chemical bonding in ethane, C_2H_6, consists of one C−C and six C−H 2c-2e bonds formed by the 14 atomic orbitals originating from the eight valence orbitals of the two carbon atoms and the six valence orbitals of the six hydrogen atoms. These 14 atomic orbitals effectively use these 14 valence electrons consisting of four valence electrons from each of the carbon atoms and a single valence electron from each of the hydrogen atoms. In the 3c-2e bonding found in boranes, three atoms supply three orbitals, one on each atom. These atomic orbitals interact to form one bonding and two antibonding orbitals so that two electrons may thus fill the bonding orbital to form a 3c-2e bond (Figure 2). If n atomic orbitals interact to form only 3c-2e bonds, they form only $n/3$ bonding orbitals which can accommodate only $2n/3$ electrons. Thus, 3c-2e bonding is used in the so-called "electron-deficient" compounds in which there are fewer bonding electrons than atomic orbitals. Diborane, B_2H_6, is a simple example of such an electron-deficient compound since the combination of two boron and six hydrogen atoms provides the same 14 atomic orbitals as the two carbon and six hydrogen atoms of ethane. However, the combination of two boron atoms and six hydrogen atoms provides only 12 valence electrons, leading to the electron deficiency of diborane. The availability of 14 atomic orbitals but only 12 valence electrons in diborane leads to the structure $B_2H_4(\mu\text{-}H)_2$ consisting of four 2c-2e B−H bonds to the external hydrogens and two 3c-2e bonds B−H−B bonds involving the bridging hydrogens (Figure 1). Since doubly deprotonated diborane, $B_2H_4^{2-}$, is isoelectronic with ethylene, C_2H_4, the set of the two 3c-2e B−H−B bonds in diborane can also be viewed as a protonated B═B double bond.[8] In this sense, diborane is more closely related to ethylene than to ethane.

Lipscomb[7,35,36] has studied the topology of the distribution of 2c-2e B−B and 3c-2e B−B−B bonds in networks of boron atoms using principles completely analogous to those discussed above for the balance of valence electrons and orbitals in diborane. The following assumptions are inherent in Lipscomb's methods. (1) Only the 1s orbital of hydrogen and the four sp^3 orbitals of boron are used. (2) Each external (i.e.., terminal) B−H bond is regarded as a typical 2c-2e single bond requiring the hydrogen 1s orbital, one hybridized boron orbital, and one electron each from the hydrogen and boron atoms. Because of the very small electronegativity difference between hydrogen and boron, these bonds are assumed to be nonpolar. In polynuclear boron hydrides, every boron atom may form 0 or 1 but never more than 2 such external bonds. (3) Each B−H−B 3c-2e "bridge" bond corresponds to a filled three-center localized bonding orbital requiring the hydrogen orbital and one hybrid orbital from each boron atom. (4) The orbitals and electrons of any particular boron atom are allocated to satisfy first the requirement of the external B−H single bonds and the bridge B−H−B bonds. The remaining orbitals and electrons are allocated to the skeletal molecular orbitals of the boron framework.

The relative amounts of orbitals, electrons, hydrogen, and boron atoms as well as bonds of various types can be expressed in a systematic way.[7,35,36] For a neutral boron hydride B_pH_{p+q} containing s *bridging* hydrogen atoms, x *extra* 2c-2e B−H bonds in terminal BH_2 groups rather than BH groups, t 3c-2e B−B−B bonds, and y 2c-2e B−B bonds, balancing the hydrogen atoms leads to $s + x = q$ assuming that each boron atom is bonded to at least one hydrogen atom. Since each boron atom supplies four orbitals but only three electrons, the total number of 3c-2e bonds in the molecule is the same as the number of boron atoms, namely, $s + t = p$. This leads to the following equations of balance:

$$2s + 3t + 2y + x = 3p \quad \text{(orbital balance with three orbitals/BH vertex)} \tag{1a}$$

$$s + 2t + 2y + x = 2p \quad \text{(electron balance with two } \textit{skeletal} \text{ electrons/BH vertex)} \tag{1b}$$

Using this approach, the structure of a given borane can be expressed by a four-digit *styx number* corresponding to the numbers of 3c-2e B−H−B bonds, 3c-2e B−B−B bonds, 2c-2e B−B bonds, and BH_2 groups, respectively. For example, the *styx* numbers for the structures for the boranes originally discovered by Stock are 2002 for B_2H_6, 4012 for B_4H_{10}, 4120 for B_5H_9, 3203 for B_5H_{11}, 4220 for B_6H_{10}, and 4620 for $B_{10}H_{14}$ (Figure 1).

B. Deltahedral Boranes and Polyhedral Skeletal Electron Pair Theory: The Wade–Mingos Rules

Structural information on the boranes $B_nH_n^{2-}$ ($6 \leq n \leq 12$)[18−22] show all of these ions to have the deltahedral structures (Figure 3) as suggested by Williams in 1971.[10] This group of deltahedra have been described by Williams[37] as the "most spherical" deltahedra since they are those with the most uniformly or most homogeneously connected vertices. This corresponds to deltahedra having exclusively degree 4 and 5 vertices for $B_nH_n^{2-}$ ($n = 6$, 7, 8, 9, 10, and 12) and having all degree 4 and 5 vertices except for a single degree 6 vertex in $B_{11}H_{11}^{2-}$. In addition,

Williams[10] also recognized that the loss of boron vertices from these most spherical *closo* deltahedra generates the structures of the known boranes B_nH_{n+4} and B_nH_{n+6} (Figure 1). Thus, the so-called *nido* boranes B_nH_{n+4} and isoelectronic carboranes have structures which can be derived from the corresponding $B_{n+1}H_{n+1}^{2-}$ structure by the loss of the vertex of highest degree (i.e., the most highly connected vertex). Similarly, the so-called *arachno* boranes B_nH_{n+6} are related to those of the corresponding $B_{n+2}H_{n+2}^{2-}$ structure by the loss of a pair of adjacent vertices of relatively high degree. Williams[10] thus first recognized the relationship between the *closo* ($B_nH_n^{2-}$), *nido* (B_nH_{n+4}), and *arachno* (B_nH_{n+6}) borane structures, which is a key aspect of the commonly accepted theory for polyhedral boron species. Furthermore, the role of the most spherical deltahedra in all of these structures suggest that they are particularly stable structural units in borane chemistry similar to the planar benzenoid rings in the chemistry of aromatic hydrocarbons and their derivatives.

The next important contribution in this area was made shortly thereafter by Wade,[24] who recognized that this structural relationship could be related to the number of valence electrons associated with skeletal bonding in the boranes. Thus, deprotonation of all of the bridging hydrogens from the related series of boranes $B_nH_n^{2-}$, $B_{n-1}H_{(n-1)+4}$, and $B_{n-2}H_{(n-2)+6}$ gives the ions $B_nH_n^{2-}$, $B_{n-1}H_{n-1}^{4-}$, and $B_{n-2}H_{n-2}^{6-}$, which can readily be seen to have the same number of skeletal electron pairs, namely, $n + 1$, corresponding to $2n + 2$ skeletal electrons. Consequently, Wade[24] provided an electronic rationale for the observations of Williams,[10] namely, that the *closo*, *nido*, and *arachno* structures are related because they share a common number of bonding molecular orbitals associated with the boron skeleton. Rudolph and Pretzer[38,39] subsequently provided the first attempt to account for the structural and electronic relationships proposed by Williams and Wade using semiempirical molecular orbital calculations. Mingos[40,41] incorporated these ideas into his "polyhedral skeletal electron pair approach", which provides a simple way to understand the structural diversity shown by polynuclear molecules. Because of the seminal work of Wade and Mingos in understanding electron counting in polyhedral molecules, the rules assigning $2n + 2$ skeletal electrons to deltahedral boranes and related *nido* and *arachno* derivatives as well as other similar polyhedral molecules (e.g., certain transition-metal clusters) are frequently called the "Wade−Mingos Rules."

C. Localized Bonding Models for Deltahedral Boranes: Three-Dimensional Analogues of Kekulé Structures

A central idea in the aromaticity of planar benzenoid hydrocarbons is the contribution of two or more different structures of equivalent energy consisting of alternating C−C single and C=C double bonds known as *Kekulé structures* to a lower energy averaged structure known as a *resonance hybrid*.[42] In benzene itself the two equivalent Kekulé structures contain three double and three single bonds alternating along the six edges of the C_6 hexagon.

The 2c-2e B−B bonds and 3c-2e B−B−B bonds in polyhedral boranes can be components of Kekulé-type structures similar to the C−C single and C=C double bonds in planar hydrocarbons. Thus, consider the deltahedral boranes $B_nH_n^{2-}$ ($6 \leq n \leq 12$). Such deltahedral boranes cannot have any terminal BH_2 groups or 3c-2e B−H−B bonds and have two "extra" electrons for the −2 charge on the ion, so that $s = x = 0$ in the equations of balance (eqs 1a and 1b), which then reduce to the following equations in which n is the number of boron atoms in the deltahedron corresponding to p in eqs 1a and 1b

$$3t + 2y = 3n \quad \text{(orbital balance for } B_nH_n^{2-}\text{)} \quad (2a)$$

$$2t + 2y = 2n + 2 \quad \text{(electron balance for } B_nH_n^{2-}\text{)} \quad (2b)$$

Solving the simultaneous eqs 2a and 2b leads to $y = 3$ and $t = n - 2$, implying the presence of three 2c-2e B−B bonds and $n - 2$ 3c-2e B−B−B bonds. Since a deltahedron with n vertices has $2n - 4$ faces, the $n - 2$ 3c-2e B−B−B bonds cover exactly one-half of the faces. In that sense a Kekulé-type structure for the deltahedral boranes $B_nH_n^{2-}$ has exactly one-half of the faces covered by 3c-2e B−B−B bonds just like a Kekulé structure for a benzenoid hydrocarbon has one-half of the edges covered by C=C double bonds.

An initial attempt was made by Lipscomb and coworkers[43] to generate Kekulé-type localized bonding structures for the deltahedral boranes using wave functions calculated in the approximation of differential overlap. Their 1977 paper presents a variety of such localized bonding structures for the deltahedral boranes containing networks of 2c-2e B−B and 3c-2e B−B−B bonds. Subsequently in 1984 O'Neill and Wade[44] examined such localized bonding schemes using the following fundamental assumptions. (1) Each skeletal atom is assumed to participate in three skeletal bonds in addition to the external bond, typically to a hydrogen atom.(2) Each edge of the skeletal B_n polyhedron must correspond to a 2c-2e B−B bond or a 3c-2e B−B−B bond. (3) A pair of boron atoms cannot be simultaneously bonded to each other both by a 2c-2e B−B bond and one or two 3c-2e B−B−B bonds since these arrangements would require too close an alignment of the atomic orbitals involved. (4) Cross-polyhedral interactions, which are significantly longer than polyhedral edge interactions, are considered to be nonbonding. (5) When individual bond networks do not match the symmetry of the polyhedron in question, resonance between plausible canonical forms needs to be invoked.

These assumptions, particularly assumption 3, pose certain restrictions on the combinations of 2c-2e B−B and 3c-2e B−B−B bonds meeting at polyhedral vertices of various degrees (Figure 4).[44] (1) Degree 3 vertices: The only possibilities are three 2c-2e B−B bonds along the polyhedral edges corresponding to edge-localized bonding or three 3c-2e B−B−B bonds in the polyhedral faces. (2) Degree 4

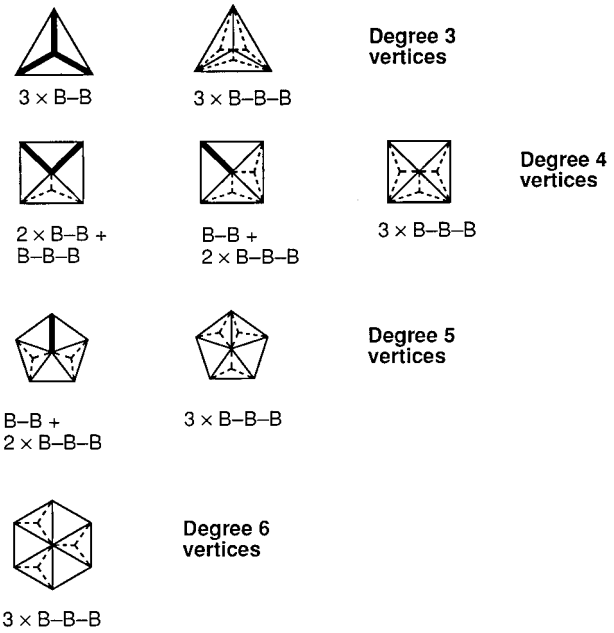

Figure 4. Bonding networks by which atoms at vertices of particular degrees can bond to their skeletal neighbors indicating 2c-2e B−B bonds by bold edges and 3c-2e B−B−B bonds by dotted lines meeting in the center of a face.

vertices: At least one 3c-2e bond must meet at each degree 4 vertex since there are not enough internal orbitals to form exclusively 2c-2e B−B bonds along each of the four edges of a degree 4 vertex. (3) Degree 5 vertices: A minimum of two 3c-2e bonds must meet at each degree 5 vertex. (4) Degree 6 vertices: All three internal bonds at each degree 6 vertex must be 3c-2e B−B−B bonds.

O'Neill and Wade[44] also consider the feasibility of *deltahedral* structures isoelectronic and isolobal with B_nH_n which are either neutral such as the B_nX_n halides,[45] have a −2 charge such as the stable deltahedral borane anions $B_nH_n^{2-}$, or are isoelectronic and isolobal with $B_nH_n^{4-}$ such as the 8-vertex species $(C_5H_5)_4Ni_4B_4H_4$.[46] They relate to the following two criteria for the feasibility of deltahedral structures: (1) The ability to draw a satisfactory Kekulé-type structure using 2c-2e B−B and 3c-2e B−B−B bonds and (2) the degeneracies of the highest occupied and lowest unoccupied molecular orbitals (HOMO's and LUMO's, respectively).

The latter criterion relates to the closed-shell configuration for the dinegative anions $B_nH_n^{2-}$ and thus the requirements of a nondegenerate HOMO for neutral B_nH_n also to have a closed-shell configuration and a nondegenerate LUMO for tetranegative $B_nH_n^{4-}$ also to have a closed-shell configuration. The conclusions from this study are summarized in Table 1. From these observations, the deltahedral species B_nH_n (n = 8, 9, and 11) are seen to be potentially stable with 0, −2, and −4 charges whereas the deltahedral species B_nH_n (n = 6, 7, 10, and 12) are seen to be stable only with a −2 charge. This is in approximate accord with the stability of the neutral halide species B_nX_n.[45]

Gillespie, Porterfield, and Wade[47] subsequently developed an alternative predominantly localized electron pair scheme for describing the electron distribution and bonding in the deltahedral anions $B_nH_n^{2-}$ and related species. In their scheme a skeletal electron pair is assumed to remain localized on each vertex, thereby using $2n$ of the $2n + 2$ skeletal electrons. The remaining electron pair is regarded as delocalized just inside the roughly spherical surface on which the skeletal atoms lie. This scheme provides a clearer picture of the electron distribution than that conveyed by resonating Kekulé-type structures and also preserves the symmetry of the deltahedron.

Table 1. Feasibility of Deltahedral B_nH_n Species with 0, −2, and −4 Charges

		degeneracies		existence of Kekulé structure for $B_nH_n^z$		
deltahedron	formula	HOMO	LUMO	0	−2	−4
octahedron	B_6H_6	3	3	+	+	+
pentagonal bipyramid	B_7H_7	2	2	−	+	−
bisdisphenoid	B_8H_8	1	1	+	+	+
tricapped trigonal prism	B_9H_9	1	1	+	+	+
bicapped square antiprism	$B_{10}H_{10}$	2	2	−	+	−
edge-coalesced icosahedron	$B_{11}H_{11}$	1	1	+	+	+
icosahedron	$B_{12}H_{12}$	4	4	+	+	+

D. Resonance Stabilization of Deltahedral Boranes: Graph-Theoretical Approaches to Three-Dimensional Aromaticity in Borane Deltahedra

The existence of Kekulé structures consisting of 2c-2e B−B bonds and 3c-2e B−B−B bonds is not sufficient to account for the special stability of deltahedral boranes just as the existence of Kekulé structures consisting of C−C single and C=C double bonds fails to account for the special stabilities of benzene and other benzenoid hydrocarbons. Thus, any of the deltahedral borane anions $B_nH_n^{2-}$ ($6 \leq n \leq 12$) is much more stable toward air, heat, moisture, and many chemical reagents than the typically highly inflammable and otherwise highly reactive neutral boranes with open structures. Furthermore, the configurations of the 2c-2e B−B bonds and 3c-2e B−B−B bonds in individual Kekulé structures of the most symmetrical deltahedral boranes such as the octahedral $B_6H_6^{2-}$ and the icosahedral $B_{12}H_{12}^{2-}$ do not conform to the experimentally observed high symmetry of these ions just as an individual Kekulé structure of benzene does not have the full C_6 symmetry observed experimentally. Other methods are needed to determine the resonance stabilization of these deltahedral ions leading to aromaticity. Such methods ultimately derive from Hückel theory but use graph theory to model the interaction between the atomic orbitals participating in the delocalization leading to the aromatic stabilization. These graph-theoretical approaches, which were first applied to the study of the aromaticity in benzenoid hydrocarbons by Ruedenberg[48] and Schmidtke,[49] are most useful in demonstrating the close analogy between the bonding in two-dimensional planar aromatic systems such as benzene and the three-dimensional deltahedral systems such as the boranes and carboranes.

Table 2. Delocalized versus Localized Bonding and the "Matching Rule" (assumes three internal orbitals per vertex atom)

structure type	vertex degrees	matching	localization	examples
planar polygons	2	no	delocalized	benzene, $C_5H_5^-$, $C_7H_7^+$
"simple polyhedra"	3	yes	localized	polyhedranes: C_4H_4, C_8H_8, $C_{20}H_{20}$
deltahedra	4, 5 (6)	no	delocalized	polyhedral boranes and carboranes

Graph-theoretical methods for the study of aromatic systems use a graph G to describe the overlap of the atomic orbitals participating in the delocalized bonding in which the vertices V correspond to orbitals and the edges E correspond to orbital overlaps. The adjacency matrix[50] **A** of such a graph can be defined as follows

$$A_{ij} = \begin{cases} 0 \text{ if } i = j \\ 1 \text{ if } i \text{ and } j \text{ are connected by an edge} \\ 0 \text{ if } i \text{ and } j \text{ are not connected by an edge} \end{cases} \quad (3)$$

The eigenvalues of the adjacency matrix are obtained from the following determinantal equation

$$|\mathbf{A} - x\mathbf{I}| = 0 \quad (4)$$

in which **I** is the unit matrix ($I_{ii} = 1$ and $I_{ij} = 0$ for $i \neq j$). These topologically derived eigenvalues are closely related to the energy levels as determined by Hückel theory which uses the secular equation

$$|\mathbf{H} - E\mathbf{S}| = 0 \quad (5)$$

Note the general similarities between eqs 4 and 5. In eq 5 the energy matrix **H** and the overlap matrix **S** can be resolved into the identity matrix **I** and the adjacency matrix **A** as follows

$$\mathbf{H} = \alpha\mathbf{I} + \beta\mathbf{A} \quad (6a)$$

$$\mathbf{S} = \mathbf{I} + S\mathbf{A} \quad (6b)$$

The energy levels of the Hückel molecular orbitals (eq 5) are thus related to the eigenvalues x_k of the adjacency matrix **A** (eq 4) by the following equation

$$E_k = \frac{\alpha + x_k\beta}{1 + x_k S} \quad (7)$$

In eq 7, α is the standard Coulomb integral, assumed to be the same for all atoms, β is the resonance integral taken to be the same for all bonds, and S is the overlap integral between atomic orbitals on neighboring atoms. Because of the relationship of the set of the eigenvalues of a graph to the energy levels of the molecular orbitals of a structure represented by the graph in question as indicated by eqs 4−7, the set of eigenvalues of a graph is called the *spectrum* of the graph, even by mathematicians solely concerned with graph theory without interest in its chemical applications.

The two extreme types of skeletal chemical bonding in polygonal or polyhedral molecules may be called *edge-localized* and *globally delocalized*.[31,51−53] An edge-localized polygon or polyhedron has 2c-2e bonds along each edge and is favored when the number of internal orbitals from each vertex atom matches the degree of the corresponding vertex. A globally delocalized polygon or polyhedron has a multicenter bond involving all of the vertex atoms; such global delocalization is a feature of fully aromatic systems. Delocalization is favored when the numbers of internal orbitals do *not* match the vertex degrees.

Consideration of the properties of vertex groups leads to the following very simple rule to determine whether polygonal or polyhedral molecules exhibit delocalized bonding or edge-localized bonding: *Delocalization occurs when there is a mismatch between the vertex degree of the polygon or polyhedron and the number of internal orbitals provided by the vertex atom.*

This rule is illustrated in Table 2 for normal vertex atoms providing three internal orbitals. This rule implies that fully edge-localized bonding occurs in a polyhedral molecule in which all vertices have degree 3. Such is the case for the polyhedranes $C_{2n}H_{2n}$ such as tetrahedrane ($n = 2$), cubane ($n = 4$), and dodecahedrane ($n = 10$), in which the vertex degrees are all three thereby matching the three available internal orbitals and leading to edge-localized bonding represented by the $3n/2$ two-center carbon−carbon bonds of the skeleton. In the planar polygonal molecules $C_nH_n^{(n-6)+}$ ($n = 5, 6, 7$), the vertex degrees are all 2 and thus do not match the available three internal orbitals, thereby leading to globally delocalized two-dimensional aromatic systems. Furthermore, polyhedral molecules having all normal vertex atoms are globally delocalized if all vertices of the polyhedron have degrees 4 or larger; the simplest such polyhedron is the regular octahedron with six vertices, all of degree 4. Such globally delocalized polyhedra are characteristic of three-dimensional aromatic systems as exemplified by the deltahedral boranes $B_nH_n^{2-}$ ($6 \leq n \leq 12$) and isoelectronic carboranes (Figure 3). Furthermore, tetrahedral chambers in deltahedra, which lead to isolated degree 3 vertices, provide sites of localization in an otherwise delocalized molecule provided, of course, that all vertex atoms use the normal three internal orbitals.

Aromatic systems can be classified by the nodality of the orbitals participating in the delocalization. Thus, the deltahedral boranes are examples of aromatic systems constructed from anodal sp hybrid orbitals (Figure 5a) in contrast to the planar polygonal hydrocarbons, which are examples of aromatic systems constructed from uninodal p orbitals (Figure 5b). In both cases the three internal orbitals on each vertex atom are partitioned into two twin internal orbitals (also[25] called *tangential* orbitals) and a unique internal orbital (also[25] called a *radial* orbital). Pairwise overlap between the $2n$ twin internal orbitals is responsible for the formation of the polygonal or deltahedral framework and leads to the splitting of these $2n$ orbitals into n bonding and n antibonding orbitals. The magnitude of this splitting can be designated as $2\beta_s$, where β_s refers to the parameter

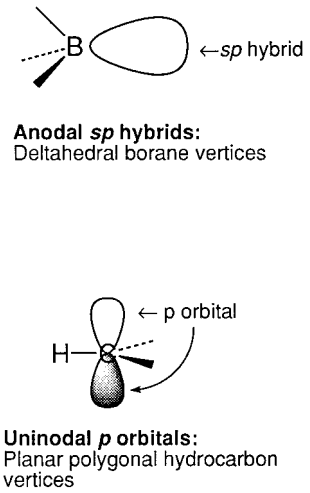

Figure 5. Types of vertex orbitals participating in the delocalization of aromatic systems of various types as classified by their nodalities: (a) The anodal sp hybrid unique internal (radial) orbitals of a B−H vertex in the deltahedral boranes; (b) the uninodal p orbital of a C−H vertex in planar polygonal aromatic hydrocarbons such as benzene.

β in eqs 6a and 7 as applied to surface bonding. This portion of the chemical bonding topology can be described by a disconnected graph G_s having $2n$ vertices corresponding to the $2n$ twin internal orbitals and n isolated K_2 components; a K_2 component has only two vertices joined by a single edge. The dimensionality of this bonding of the twin internal orbitals is one less than the dimensionality of the globally delocalized system. Thus, in the case of the two-dimensional planar polygonal systems, such as benzene, the pairwise overlap of the $2n$ twin internal orbitals leads to the σ-bonding network, which may be regarded as a set of one-dimensional bonds along the perimeter of the polygon using adjacent pairs of polygonal vertices. The n bonding and n antibonding orbitals thus correspond to the σ-bonding and σ*-antibonding orbitals, respectively. In the case of the three-dimensional deltahedral systems, the pairwise overlap of the $2n$ twin internal orbitals results in bonding over the two-dimensional surface of the deltahedron, which may be regarded as topologically homeomorphic to the sphere.[54]

The equal numbers of bonding and antibonding orbitals formed by pairwise overlap of the twin internal orbitals are supplemented by additional bonding and antibonding orbitals formed by the global mutual overlap of the n unique internal orbitals. The bonding topology of the n unique internal orbitals, whether the uninodal p orbitals in the planar polygonal aromatic hydrocarbons (Figure 5b) or the anodal sp hybrids in the three-dimensional deltahedral boranes (Figure 5a), can be described by a graph G_c in which the vertices correspond to the vertex atoms of the polygon or deltahedron, or equivalently their unique internal orbitals, and the edges represent pairs of overlapping unique internal orbitals. The energy parameters of the additional molecular orbitals arising from such overlap of the unique internal orbitals are determined from the eigenvalues of the adjacency matrix $\mathbf{A_c}$ of the graph G_c using β_c as the energy unit where β_c refers to the

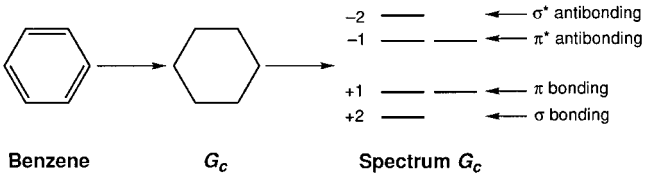

Figure 6. Benzene and the corresponding spectrum of G_c (the C_6 cyclic graph).

parameter β in eqs 6a and 7 as applied to core bonding. In the case of the two-dimensional aromatic system benzene, the graph G_c is the C_6 cyclic graph (the 1-skeleton[55] of the hexagon) which has three positive (+2, +1, +1) and three negative (−2, −1, −1) eigenvalues corresponding to the three π-bonding and three π*-antibonding orbitals, respectively (Figure 6). The spectra of the cyclic graphs C_n all have odd numbers of positive eigenvalues[50] leading to the familiar $4k + 2$ (k = integer) π-electrons[56] for planar aromatic hydrocarbons. The total benzene skeleton thus has 9 bonding orbitals (6σ and 3π) which are filled by the 18 skeletal electrons which arise when each of the CH vertices contributes three skeletal electrons. Twelve of these skeletal electrons are used for the σ-bonding and the remaining six electrons for the π-bonding.

Figure 7a illustrates how the delocalized bonding in benzene from the C_6 overlap of the unique internal orbitals, namely, the p orbitals, leads to aromatic stabilization. In a hypothetical localized "cyclohexatriene" structure in which the interactions between the p orbitals on each carbon atom are pairwise interactions, the corresponding graph G consists of three disconnected line segments (i.e., $3 \times K_2$). This graph has three +1 eigenvalues and three −1 eigenvalues. Filling each of the corresponding three bonding orbitals with an electron pair leads to an energy of 6β from this π bonding. In a delocalized "benzene" structure in which the delocalized interactions between the p orbitals on each carbon atom are described by the cyclic C_6 graph, filling the three bonding orbitals with an electron pair each leads to an energy of 8β. This corresponds to a resonance stabilization of $8\beta - 6\beta = 2\beta$ arising from the delocalized bonding of the carbon p orbitals in benzene corresponding to the two-dimensional aromaticity in benzene. We will see below how similar ideas can be used to describe the three-dimensional aromaticity in deltahedral boranes.

An important question is the nature of the core bonding graph G_c for the deltahedral boranes $B_nH_n^{2-}$. The two limiting possibilities for G_c are the complete graph K_n and the deltahedral graph D_n, and the corresponding core bonding topologies can be called the *complete* and *deltahedral* topologies, respectively. In the complete graph K_n, each vertex has an edge going to every other vertex leading to a total of $n(n - 1)/2$ edges.[57] For any value of n, the corresponding complete graph K_n has only one positive eigenvalue, namely, $n - 1$, and $n - 1$ negative eigenvalues, namely, −1 each. The deltahedral graph D_n is identical to the 1-skeleton[55] of the borane deltahedron. Thus, two vertices of D_n are connected by an edge if, and only if, the corresponding vertices of the deltahedron are connected by an edge.

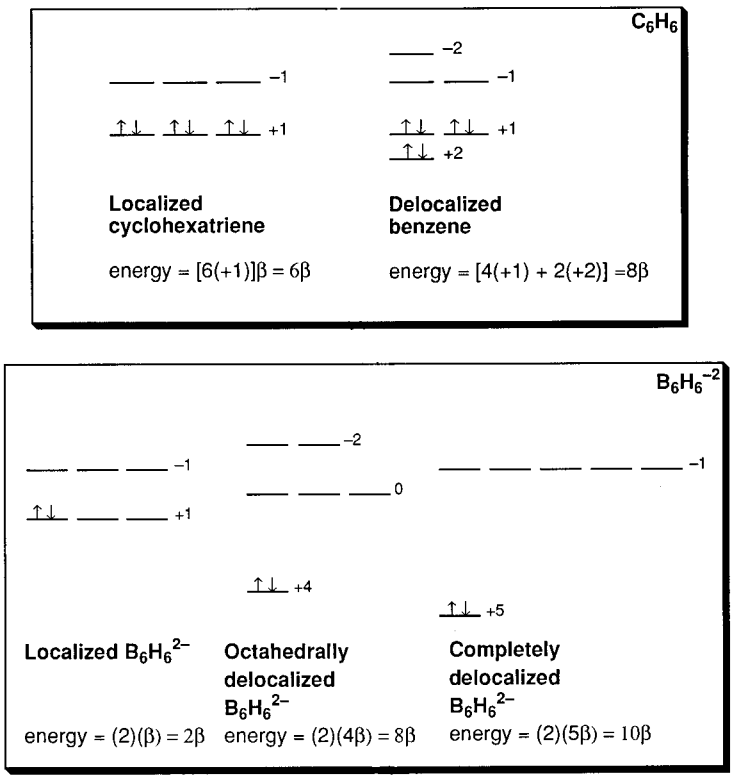

Figure 7. (a) Aromatic stabilization of benzene relative to the hypothetical localized triolefin cyclohexatriene. (b) Aromatic stabilization of $B_6H_6^{2-}$ considering both complete and deltahedral (octahedral) delocalization for the core bonding.

The graphs D_n for the deltahedra of interest with six or more vertices all have at least four zero or positive eigenvalues in their spectra (Figure 8). However, in all cases there is a unique positive eigenvalue which is much more positive than any other of the positive eigenvalues. This unique positive eigenvalue can be called conveniently the *principal eigenvalue* and corresponds to the fully symmetric $A_{(1)(g)}$ irreducible representation of the symmetry group of G_c. The molecular orbital corresponding to the principal eigenvalue of G_c may be called the *principal* core orbital. Since deltahedral boranes of stoichiometry $B_nH_n^{2-}$ have $2n + 2$ skeletal electrons of which $2n$ are used for the surface bonding, as noted above, there are only two skeletal electrons remaining for core bonding corresponding to a single core bonding molecular orbital and a single positive eigenvalue for G_c. Thus, deltahedral boranes are three-dimensional aromatic systems having $4k + 2 = 2$ core bonding electrons for $k = 0$ analogous to the $4k + 2$ π electrons for $k = 0$ ($C_3H_3^+$), $k = 1$ ($C_5H_5^-$, C_6H_6, $C_7H_7^+$), or $k = 2$ ($C_8H_8^{2-}$) for planar two-dimensional polygonal aromatic systems. Furthermore, only if G_c is taken to be the corresponding complete graph K_n will the simple model given above for globally delocalized deltahedra provide the correct number of skeletal electrons in all cases, namely, $2n + 2$ skeletal electrons for $6 \leq n \leq 12$. Such a model with complete core bonding topology is a convenient working basis for the chemical bonding topology in deltahedral boranes exhibiting three-dimensional aromaticity. However, deltahedral core bonding topology can also account for the observed $2n + 2$ skeletal electrons in the $B_nH_n^{2-}$ deltahedral boranes if there is a mechanism for raising the energies of all of the core molecular orbitals other than the principal core orbital to antibonding energy levels.

The distinction between complete (K_n) and deltahedral (D_n) core bonding topology is illustrated for octahedral $B_6H_6^{2-}$ in Figure 9. Among the $(6)(6 - 1)/2 = 15$ pairs of six vertices in an octahedron (D_6 graph), 12 pairs correspond to edges of the octahedron (cis interactions) and the remaining three pairs correspond to antipodal vertices related by the inversion center and *not* connected by an edge (trans interactions). However, all of the 15 pairs of six vertices in a complete K_6 graph correspond to edges of equal weight. In an octahedral array of six points, a parameter t can be defined as the ratio of the trans interactions to the cis interactions. This parameter t is 0 for the pure octahedral topology (D_6) and 1 for pure complete topology (K_6). Values of t between 0 and 1 can be used to measure gradations of topologies between D_6 and K_6 corresponding to the weighting of edges representing trans interactions relative to those representing cis interactions in the underlying graph G_c. In group-theoretical terms, pure complete core bonding topology (i.e., $t = 1$) uses the symmetric permutation group[58] S_6 with 720 operations rather than its subgroup O_h with 48 operations (the symmetry point group of the octahedron) to describe the symmetry of the core bonding manifold in $B_6H_6^{2-}$. The actual O_h point group rather than a higher S_6 permutational symmetry of $B_6H_6^{2-}$ results in the partial removal of the 5-fold degeneracy of the core antibonding orbitals implied by the complete core bonding topology (Figure 9).

Multicenter core bonding such as that implied by the K_n topology of the n-vertex complete graph has been shown by Aihara[59] to lead to considerable

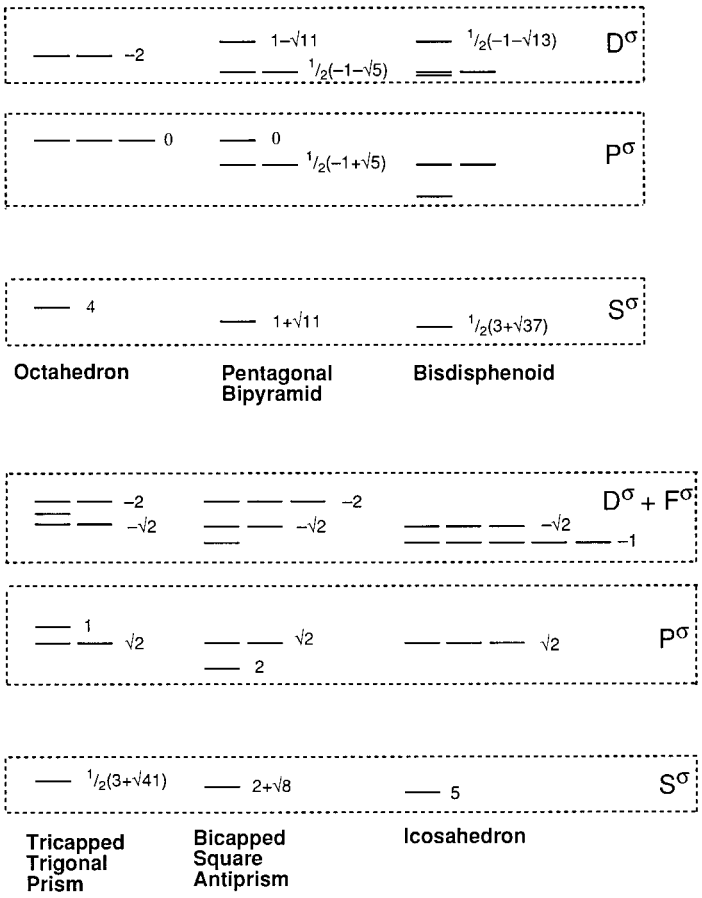

Figure 8. Eigenvalues of the borane deltahedra (Figure 3) having 6, 7, 8, 9, 10, and 12 vertices.

resonance stabilization as illustrated in Figure 7b for $B_6H_6^{2-}$. In a hypothetical localized structure in which the interactions between the radial sp hybrids are pairwise interactions, the spectrum of the corresponding graph G_c consists of three disconnected line segments (i.e., $3 \times K_2$). The spectrum of this disconnected graph has three $+1$ eigenvalues and three -1 eigenvalues. Filling one of the resulting three bonding orbitals with the available two core bonding electrons leads to an energy of 2β from the core bonding. In a completely delocalized structure in which the core bonding is described by the complete graph K_6, this electron pair resides in a bonding orbital with an eigenvalue of $+5$ corresponding to an energy of $(2)(5\beta) = 10\beta$ (Figure 7b). The aromatic stabilization of completely delocalized $B_6H_6^{2-}$ is thus $10\beta - 2\beta = 8\beta$ assuming the same β unit for both the localized and completely delocalized structures. In an octahedrally delocalized $B_6H_6^{2-}$ in which the core bonding is described by the deltahedral graph D_6 corresponding to the 1-skeleton[27] of the octahedron, the core bonding electron pair resides in a bonding orbital with an eigenvalue of $+4$ corresponding to an energy of $(2)(4\beta) = 8\beta$ (Figure 7b). The aromatic stabilization of octahedrally delocalized $B_6H_6^{2-}$ is thus $8\beta - 2\beta = 6\beta$. Thus, the aromatic stabilization of $B_6H_6^{2-}$ is considerable regardless of whether the delocalized core bonding is considered to have the complete topology represented by the complete graph K_6 or the octahedral topology represented by the deltahedral graph D_6.

There are several implications of this bonding model for delocalized deltahedral structures having n vertices using the complete core bonding topology described by the corresponding K_n complete graph. (1) The overlap of the n unique internal orbitals to form an n-center core bond may be hard to visualize since its topology corresponds to that of the complete graph K_n, which for $n \geq 5$ is nonplanar by Kuratowski's theorem[60] and thus cannot correspond to the 1-skeleton[55] of a polyhedron realizable in three-dimensional space. However, the overlap of these unique internal orbitals does not occur along the edges of the deltahedron or any other three-dimensional polyhedron. For this reason, the topology of the overlap of the unique internal orbitals in the core bonding of a deltahedral cluster need not correspond to a graph representing a 1-skeleton of a three-dimensional polyhedron. The only implication of the K_n graph description of the bonding topology of the unique internal orbitals is that the deltahedron is topologically homeomorphic[54] to the sphere as noted above. (2) The equality of the interactions between all possible pairs of unique internal orbitals required by the K_n model for the core bonding is obviously a very crude assumption since in any deltahedron with five or more vertices not all pairwise relationships of the vertices are equivalent. The example of the nonequivalence of the cis and trans vertex pairs in an octahedral structure such as $B_6H_6^{2-}$ has already been discussed. However, the single eigenvalue of the K_n graph is so strongly positive that severe inequali-

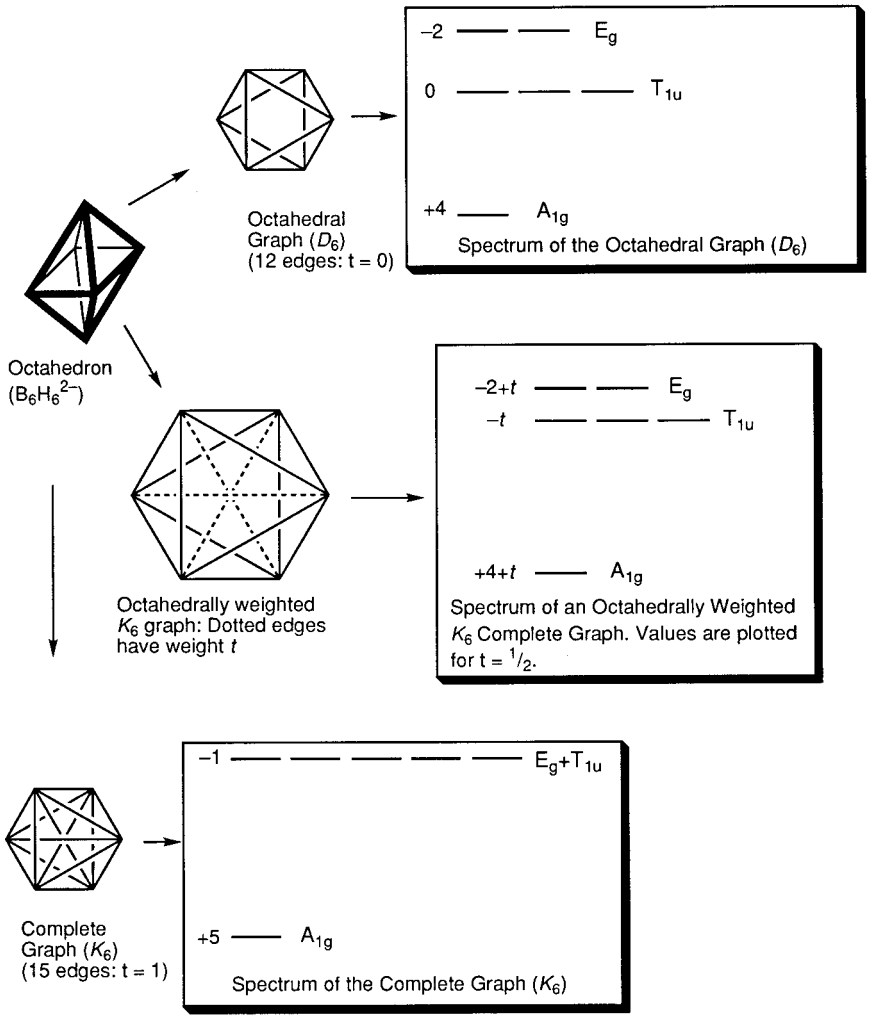

Figure 9. Distinction between complete (K_6) and deltahedral (D_6) core bonding topology for octahedral $B_6H_6^{2-}$.

ties in the different vertex pair relationships are required before the spectrum of the graph representing precisely the unique internal orbital overlap contains more than one positive eigenvalue.

Aihara[32] described an alternative graph-theoretical approach to modeling the aromaticity in the deltahedral boranes at about the same time as the original publication by King and Rouvray[33] outlined above. Aihara's paper was also significant in being the first to emphasize the three-dimensional aromaticity of polyhedral boranes even in its title. He used a Hückel-type molecular orbital (MO) theory with the three-center bond formalism of Kettle and Tomlinson[61] so that localized 3c-2e B−B−B bonding orbitals were used as basis functions. Such localized 3c-2e B−B−B bonds were assumed to be in every face of the $B_nH_n^{2-}$ deltahedron at variance with the topological methods of Lipscomb noted above,[7,35,36,43] which restrict the number of 3c-2e B−B−B bonds in a deltahedral structure to those that can be formed with the three skeletal orbitals available to each boron atom in the deltahedron. Nevertheless, Aihara[32] provided reasonable numerical estimates of the resonance energies of the $B_nH_n^{z-}$ deltahedra ($z = 2$ for $5 \leq n \leq 12$; $z = 0$ for $n = 4$) in terms of β units. In this connection, the B_4H_4 tetrahedron and the $B_5H_5^{2-}$ trigonal bipyramid were found to have no resonance energy and the $B_{12}H_{12}^{2-}$ icosahedron was found to have the largest resonance energy.

These estimates of B_nH_n resonance energies by Aihara[32] confirm the observation that degrees 4 or greater for all deltahedral vertices appear to be essential for the stability of deltahedral boranes of the type $B_nH_n^{2-}$ and the isoelectronic carboranes. Thus, although the borane anions $B_nH_n^{2-}$ ($6 \leq n \leq 12$) are very stable, the five-boron deltahedral borane $B_5H_5^{2-}$ based on a trigonal pyramidal structure with two (apical) degree 3 vertices has never been prepared. Such degree 3 vertices in boron polyhedra lead to two-electron two-center bonds along each of the three edges meeting at the degree 3 vertex and leave no internal orbitals from degree 3 vertices for the multicenter core bond responsible for aromatic delocalization. However, the dicarbaborane 1,5-$C_2B_3H_5$ isoelectronic with $B_5H_5^{2-}$ with the carbon atoms in the degree 3 apical vertices of the trigonal bipyramid can be isolated.[62] The B−C bonds along the 6 B−C edges of the C_2B_3 trigonal bipyramid in 1,5-$C_2B_3H_5$ can be interpreted as edge-localized B−C bonds leading to three-coordinate boron atoms with a local environment similar to the boron environment in trimethylboron, $(CH_3)_3B$ (Figure 10a). This localized bonding model for trigonal bipyramidal boranes is sometimes called the "classical" model in contrast

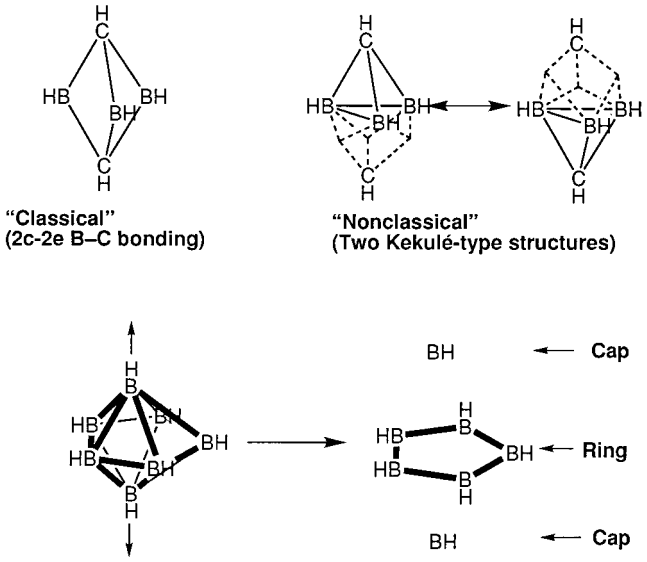

Figure 10. (a) "Classical" versus "nonclassical" structures for trigonal bipyramidal 1,5-$C_2B_3H_5$. (b) Dissection of pentagonal bipyramidal B_7H_7 into a B_5H_5 "ring" and two BH "caps."

to a "nonclassical" delocalized bonding model similar to the bonding in the larger deltahedra without degree 3 vertices. In Figure 10a, the "nonclassical" delocalized bonding model for 1,5-$C_2B_3H_5$ is depicted as a resonance hybrid of two equivalent Kekulé-type structures.

Another observation by Aihara[32] is the unusually high resonance energy of the $B_{12}H_{12}^{2-}$ icosahedron compared with the other borane deltahedra. This is in accord with experimental observations that structures containing boron icosahedra are the most stable and least chemically reactive relative to those based on other boron deltahedra as exemplified by the ionic $B_{12}H_{12}^{2-}$ and $CB_{11}H_{12}^{-}$, the molecular $C_2B_{10}H_{12}$, the stable allotropes of elemental boron, and many of the most stable metal borides. This unusual stability of boron deltahedra suggests that nonicosahedral boron deltahedra can be described in terms of their deviation of the local surroundings of their vertices from those found in ideal icosahedra. In this connection, the characteristic feature of the geometry of the regular icosahedron is the presence of 12 equivalent vertices of degree 5 where the degree of a vertex is the number of edges meeting at that vertex. If the unusual stability of borane icosahedra can be attributed to the special stability of degree 5 boron vertices, then vertices of degrees other than 5 can be considered to be defects in the deltahedral structure.[63] The most favorable borane deltahedra will be those with a minimum number of such defective vertices and with the defective vertices as widely spaced as possible.

This idea of defective vertices is not new but was used by Frank and Kasper more than 40 years ago to study polyhedra found in metal alloy structures.[64] In such systems the defective vertices are vertices of degree 6. Frank and Kasper showed that there are only four polyhedra (Figure 11) with only degree 5 and 6 vertices and with "isolated" degree 6 vertices, i.e., no pair of degree 6 vertices is connected by an edge. The four Frank−Kasper polyhedra are

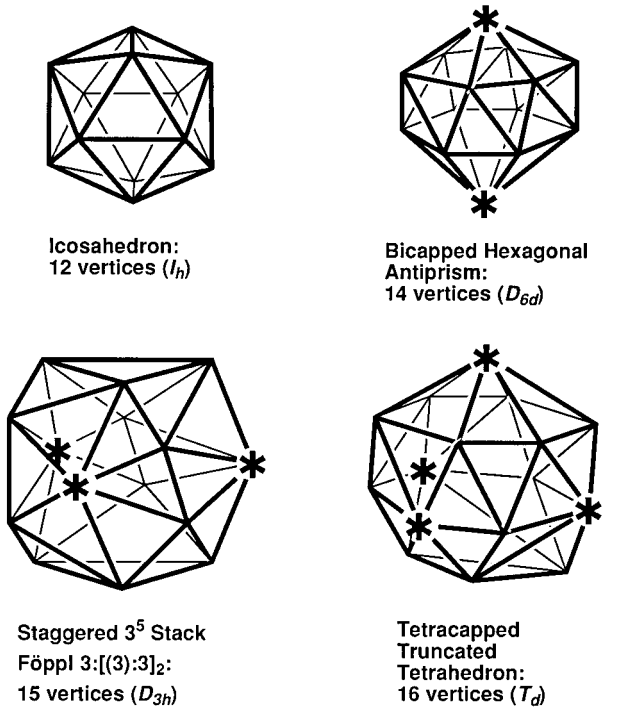

Figure 11. The four Frank−Kaspar polyhedra with their degree 6 vertices indicated by an asterisk (*).

significant not only in metal alloy structures, but also in metal carbonyl cluster chemistry in describing the polyhedra formed by the carbonyl ligands in polynuclear metal carbonyls.[65]

Ideas analogous to those applied by Frank and Kasper to deltahedra with degree 5 and 6 vertices can also be applied to the borane deltahedra with degree 4 and 5 vertices. In such borane deltahedra the defective vertices can be considered to be the vertices of degree 4. Among borane deltahedra (Figure 3) other than the icosahedron, only the bicapped square antiprism of $B_{10}H_{10}^{2-}$ and the tricapped trigonal prism of $B_9H_9^{2-}$ are seen to meet a Frank−Kasper-like criterion of nonadjacent degree 4 vertices. This topological observation can be related to the experimentally observed chemistry of the deltahedral borane anions in the following ways. (1) The decrease of the hydrolytic stability of the deltahedral boranes in the following sequence[66]

$$B_{12}H_{12}^{2-} > B_{10}H_{10}^{2-} > B_{11}H_{11}^{2-} > B_9H_9^{2-} \sim B_8H_8^{2-} \sim B_6H_6^{2-} > B_7H_7^{2-}$$

(2) The only deltahedral boranes formed from the pyrolysis of CsB_3H_8 are $B_{12}H_{12}^{2-}$, $B_{10}H_{10}^{2-}$, and $B_9H_9^{2-}$, which are the only deltahedral boranes without adjacent degree 4 vertices.

E. Tensor Surface Harmonic Theory: Approximation of Borane Deltahedra by Spheres

The graph-theory-derived model for the skeletal bonding of a deltahedral borane with n vertices with complete core bonding topology discussed above uses the corresponding complete graph K_n to describe the topology of the multicenter core bond leading to the global delocalization responsible for the three-dimen-

sional aromaticity of such structures. The precise topology of the cluster deltahedron does not enter directly into such models but only the absence of degree 3 vertices. In other words, graph-theory-derived models of the skeletal bonding of globally delocalized deltahedral clusters consider such deltahedra to be topologically homeomorphic to the sphere.[54]

The topological homeomorphism of a deltahedron to a sphere used in the graph-theory-derived models is also the basis of the tensor surface harmonic theory developed by Stone.[67] The tensor surface harmonic (TSH) theory defines the vertices of a deltahedral borane as lying on the surface of a single sphere with the atom positions described by the standard angular coordinates θ and ϕ related to latitude and longitude. The second-order differential equations for the angular dependence of the molecular orbitals from the core bonding become identical to the equations for the angular dependence of the atomic orbitals obtained by solution of the Schrödinger equation, with both sets of equations using the spherical harmonics $Y_{LM}(\theta,\phi)$.

In TSH theory, as applied to deltahedral boranes, the internal orbitals of the vertex atoms are classified by the number of nodes with respect to the radial vector connecting the vertex atom with the center of the deltahedron.[68] The unique internal orbitals are anodal or σ-type (Figure 5a) and lead to core bonding and antibonding molecular orbitals described by the scalar spherical harmonics $\Theta(\theta)\cdot\Phi(\phi) = Y_{LM}(\theta,\phi)$, which for deltahedra having n vertices correspond successively to a single anodal S^σ orbital (Y_{00}) the three uninodal P^σ orbitals (Y_{10}, Y_{11c}, Y_{11s}), the five binodal D^σ orbitals (Y_{20}, Y_{21c}, Y_{21s}, Y_{22c}, Y_{22s}), the seven trinodal F^σ orbitals (Y_{30}, Y_{31c}, Y_{31s}, Y_{32c}, Y_{32s}, Y_{33c}, Y_{33s}), etc., of increasing energy. The S^σ, P^σ, D^σ, F^σ orbitals, etc., correspond to the molecular orbitals arising from the n-center core bond of the deltahedron. The energy levels of these orbitals for the core bonding in the seven deltahedra depicted in Figure 3 correspond to the spectra of the corresponding deltahedral graphs D_n (Figure 8). In the deltahedra found in boranes, the S^σ and P^σ molecular orbitals appear in well-separated groups whereas the clearly antibonding D^σ and F^σ molecular orbitals appear clustered around eigenvalues of -1 to -2 without a clear separation.

The twin internal orbitals are uninodal (i.e., π-type) and lead to surface bonding described by the vector surface harmonics. Two vector surface harmonic functions can be generated from each Y_{LM} as follows

$$V_{LM} = \nabla Y_{LM} \tag{9a}$$

$$V_{LM} = \mathbf{r} \times \nabla Y_{LM} \tag{9b}$$

In eqs 9a and 9b, ∇ is the vector operator

$$\nabla = \left(\frac{\partial}{\partial\theta}, \frac{1}{\sin\theta}\frac{\partial}{\partial\phi}\right) \tag{10}$$

$\times$ is the vector cross-product, and the $\bar{V}_{LM}$ of eq 9b is the parity inverse of the V_{LM} of eq 9a, corresponding to a rotation of each atomic π-function by 90° about the radial vector $\mathbf{r}$. The V_{LM} and $\bar{V}_{LM}$ correspond to the equal numbers of bonding and antibonding surface orbitals in a globally delocalized deltahedral cluster leading to three P^π, five D^π, seven F^π, etc., bonding/antibonding orbital pairs of increasing energy and nodality. Since Y_{00} is a constant, $\nabla Y_{00} = 0$ so that there are no S^π or $\bar{S}^\pi$ orbitals.

The core and surface orbitals defined above by TSH theory can be related to the following aspects of the graph-theory derived model for the skeletal bonding in deltahedral boranes discussed above. (1) The lowest energy fully symmetric core orbital (A_{1g}, A_g, A_1, or A_1' depending upon the point group of the deltahedron) corresponds to the S^σ orbital in TSH theory. Since there are no S^π or $\bar{S}^\pi$ surface orbitals, this lowest energy core orbital cannot mix with any surface orbitals, so that it cannot become antibonding through core-surface mixing. (2) The three core orbitals of next lowest energy correspond to P^σ orbitals in TSH theory. These orbitals can mix with the P^π surface orbitals so that the P^σ core orbitals become antibonding with corresponding lowering of the bonding energies of the P^π surface orbitals below the energies of the other surface orbitals. This is why graph-theory-derived models of skeletal bonding in globally delocalized n-vertex deltahedra, which use the K_n graph to describe the multicenter core bond, give the correct numbers of skeletal bonding orbitals even for deltahedra whose corresponding deltahedral graph D_n has more than one positive eigenvalue. In this way, TSH theory can be used to justify important assumptions in the graph-theory-derived models for the chemical bonding in deltahedral boranes.

F. Dissection of Deltahedra into Rings and Caps: The Six Interstitial Electron Rule of Jemmis

Jemmis and collaborators[69] developed a different method for studying the aromaticity in certain borane polyhedra, which also shows an analogy between the three-dimensional borane structures and the planar two-dimensional structures of benzene and related aromatic hydrocarbons. The six interstitial electron rule dissects polyhedra conceptually into rings and caps and applies most obviously to pyramids and bipyramids (Figure 10b). For example, pentagonal bipyramidal $B_7H_7^{2-}$ can be divided into an equatorial B_5H_5 ring and two axial BH caps. If two electrons are assigned to each of the five B−B bonds in the equatorial ring of $B_7H_7^{2-}$ analogous to the five C−C bonds in the cyclopentadienyl anion, $C_5H_5^-$, there are no electrons available for π-bonding in the B_5H_5 ring. However, each of the axial BH groups in $B_7H_7^{2-}$ contributes two electrons to the ring-cap binding. The two BH caps and the -2 charge in $B_7H_7^{2-}$ combine to provide six electrons to bind the ring and the cap. Furthermore, three delocalized π-type bonding MOs are always available from the interaction of rings and caps in this manner. However, the electrons in these bonding MOs have been called *interstitial electrons* rather than π-electrons because of the three-dimensional nature of the structures.[70] This six interstitial electron rule may be related to Wade's rules for bipyramids by deleting the electrons corresponding

to the ring σ-bonds so that six interstitial electrons remain in the favorable structures. This dissection of polyhedral molecules into rings and caps is an artificial process which is particularly useful for understanding the bonding topology of electron-rich *nido* pyramidal boranes having $2n + 4$ skeletal electrons.

G. Fluxionality in Deltahedral Boranes: Diamond–Square–Diamond Rearrangements

An important property of some of the deltahedral boranes is the stereochemical nonrigidity or fluxionality of some of the polyhedra.[71] Such fluxionality can be recognized experimentally by nuclear magnetic resonance (NMR) spectra (e.g., ^{1}H or ^{11}B) with fewer distinct resonances than would be predicted by the symmetry of the deltahedron. In addition, fluxional deltahedra can exhibit a temperature-dependent NMR spectrum with all of the resonances predicted from the symmetry of the deltahedron being observed at low temperatures but coalescence of some of the sets of resonances into single resonances being observed at higher temperatures. The theory of polyhedral rearrangements is useful for understanding stereochemical nonrigidity in polyhedral structures.

The simplest approach for the study of polyhedral rearrangements dissects such rearrangements into elementary steps relating to the detailed topology of individual polyhedra. The most important elementary step is the *diamond−square−diamond* process which was first recognized in a chemical context by Lipscomb in 1966.[72] In this process (Figure 12a), a configuration such as p_1 can be called a *dsd situation* and the edge AB can be called a *switching edge*. If *a*, *b*, *c*, and *d* are taken to represent the degrees of the vertices A, B, C, and D, respectively, in p_1, then the *dsd type* of the switching edge AB can be represented as *ab*(*cd*). In this designation, the first two digits refer to the degrees of the vertices joined by AB but contained in the faces (triangles) having AB as the common edge (i.e., C and D in p_1). The quadrilateral face formed in structure p_2 may be called a *pivot face*.

Now consider a polyhedron having *e* edges. Such a polyhedron has *e* distinct dsd situations, one corresponding to each of the *e* edges acting as the switching edge. Applications of the dsd process at each of the dsd situations in a given polyhedron leads in each case to a new polyhedron. In some cases the new polyhedron is identical to the original polyhedron. In such cases, the switching edge can be said to be *degenerate* and the dsd type of a degenerate edge *ab*(*cd*) can be seen by application of the process $p_1 \rightarrow p_2 \rightarrow p_3$ to satisfy the following conditions

$$c = a - 1 \text{ and } d = b - 1 \text{ or } c = b - 1 \text{ and } d = a - 1 \quad (11)$$

A dsd process involving a degenerate switching edge represents a pathway for a degenerate polyhedral isomerization of the polyhedron. A polyhedron having one or more degenerate edges is inherently fluxional whereas a polyhedron without degenerate edges is inherently rigid.

This procedure can be used to check the borane deltahedra (Figure 3) for possible fluxionality with the following results. (1) Tetrahedron*:* No dsd process of any kind is possible since the tetrahedron is the complete graph K_4. A tetrahedron is therefore inherently rigid. (2) Trigonal bipyramid: The three edges connecting pairs of equatorial vertices are degenerate edges of the type 44(33). A dsd process using one of these degenerate edges as the switching edge and involving a square pyramid intermediate corresponds to a Berry pseudorotation (Figure 12b).[73,74] (3) Octahedron: The highly symmetrical octahedron has no degenerate edges and is therefore inherently rigid. (4) Pentagonal bipyramid: The pentagonal bipyramid has no degenerate edges and thus by definition is inherently rigid. However, a dsd process using a 45(44) edge of the pentagonal bipyramid (namely, an

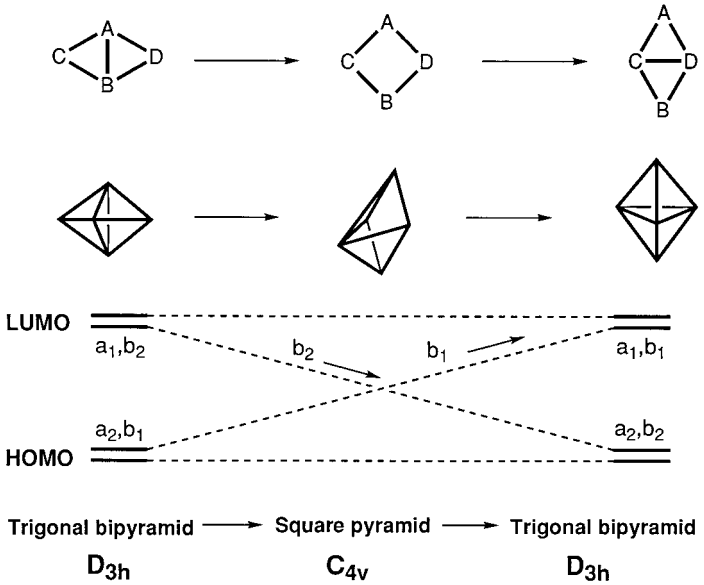

Figure 12. (a) Diamond−square−diamond (dsd) process. (b) A single dsd process interconverting two trigonal bipyramids through a square pyramid intermediate (Berry pseudorotation). (c) The HOMO−LUMO crossing occurring during the Berry pseudorotation process.

edge connecting an equatorial vertex with an axial vertex) gives a capped octahedron. The capped octahedron is a low energy polyhedron for ML_7 coordination complexes but an unfavorable polyhedron for boranes and carboranes because of its degree 3 vertex. (5) Bisdisphenoid: The 8-vertex bisdisphenoid has four pairwise degenerate edges, which are those of the type 55(44) located in the subtetrahedron consisting of the degree 5 vertices of the bisdisphenoid (Figure 3). Thus, two successive or more likely concerted (parallel) dsd processes involving opposite 55(44) edges (i.e., a pair related by a C_2-symmetry operation) converts one bisdisphenoid into another bisdisphenoid through a square antiprismatic intermediate. Thus, a bisdisphenoid, like the trigonal bipyramid discussed above, is inherently fluxional. (6) 4,4,4-Tricapped trigonal prism: The three edges of the type 55(44) corresponding to the "vertical" edges of the trigonal prism are degenerate. A dsd process using one of these degenerate edges as the switching edge involves a C_{4v} 4-capped square antiprism intermediate. Nine-vertex systems are therefore inherently fluxional. (7) 4,4-Bicapped square antiprism: This polyhedron has no degenerate edges and therefore is inherently rigid. (8) Edge-coalesced icosahedron: The four edges of the type 56(45) are degenerate. This 11-vertex deltahedron is therefore inherently fluxional. (9) Icosahedron: This highly symmetrical polyhedron, like the octahedron, has no degenerate edges and is therefore inherently rigid.

This simple analysis indicates that the 4-, 6-, 10-, and 12-vertex deltahedra are inherently rigid; the 5-, 8-, 9-, and 11-vertex deltahedra are inherently fluxional; and the rigidity of the 7-vertex structure depends on the energy difference between the two most symmetrical 7-vertex deltahedra, namely, the pentagonal bipyramid and the capped octahedron, which is large in the case of deltahedral boranes. This can be compared with experimental fluxionality observations by ^{11}B NMR on the deltahedral borane anions $B_nH_n^{2-}$ ($6 \leq n \leq 12$),[75] where the 6-, 7-, 9-, 10-, and 12-vertex structures are found to be rigid and the 8- and 11-vertex structures are found to be fluxional. The only discrepancy between experiment and these very simple topological criteria for fluxionality occurs in the 9-vertex structure $B_9H_9^{2-}$.

The discrepancy between the predictions of this simple topological approach and experimental data for $B_9H_9^{2-}$ has led to the search for more detailed criteria for the rigidity of the deltahedral boranes. In this connection, Gimarc and Ott studied orbital symmetry methods, particularly for the 5-,[76] 7-,[77] and 9-vertex[78] borane and carborane structures, recognizing that a topologically feasible dsd process is orbitally forbidden if crossing of occupied and vacant molecular orbitals (i.e., a "HOMO−LUMO crossing") occurs during the dsd process as illustrated in Figure 12c for the single dsd process of the trigonal bipyramid. For such an orbitally forbidden process, which occurs in the 5- and 9-vertex deltahedral boranes and carboranes, the activation barrier separating initial and final structures is likely to be large enough to prevent this polyhedral isomerization.

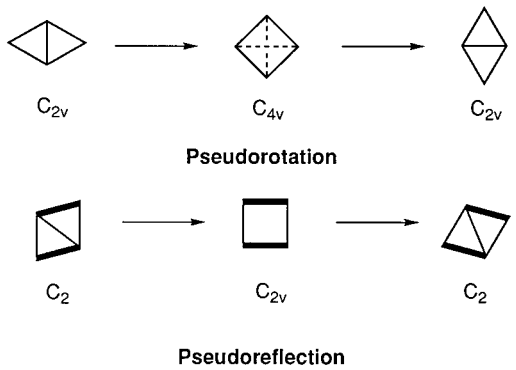

Figure 13. (a) Pseudorotation. (b) Pseudoreflection.

The fluxionality of the $B_9H_9^{2-}$ tricapped trigonal prism has also recently been studied by computational methods.[79] Thus, ab initio calculations at MP2/6-31G*, B3LYP/6-31G*, and B3LYP/6-311+G** levels indicate relatively high potential barriers for the intramolecular rearrangement of $B_9H_9^{2-}$ by the single dsd process (28.4 kcal/mol) or even a double dsd process (21.3 kcal/mol). However, its open-face protonated form $B_9H_{10}^-$ was calculated to be highly fluxional.

Some selection rules have been proposed for distinguishing between symmetry-allowed and symmetry-forbidden processes in deltahedral boranes, carboranes, and related structures. Thus, Wales and Stone[80] distinguish between symmetry-allowed and symmetry-forbidden processes by observing that a HOMO−LUMO crossing occurs if the proposed transition state has a single atom lying on a principal C_n rotational axis where $n \geq 3$. A more detailed selection rule was observed by Mingos and Johnston.[81] If the four outer edges of the two fused triangular faces (i.e., the "diamond") are symmetry equivalent, then a single dsd process results in a *pseudorotation* of the initial polyhedron by 90° (Figure 13a). However, if the edges are not symmetry equivalent, then the rearrangement results in a *pseudoreflection* of the initial polyhedron (Figure 13b). Pseudorotations are symmetry forbidden and have larger activation energies than pseudoreflections, which are symmetry allowed.

III. Computational Studies on Deltahedral Boranes

A. Early Computational Studies Based on Hückel Theory

The discovery of boron deltahedra in elemental boron and metal borides and later in polyhedral boranes generated an interest in computational studies on these structures as soon as suitable computational methods became available. The earliest computational work on boron deltahedra was the 1954 study by Longuet-Higgins and Roberts[13] on the B_6 octahedra found in metal boride studies using the secular determinants obtained from linear combinations of atomic orbitals (LCAO). This work was followed shortly by a study of boron icosahedra which predicted the existence of a stable anionic icosahedral

borane $B_{12}H_{12}^{2-}$ several years before it was discovered.[14]

The first systematic computational study on polyhedral boranes was reported in 1962 by Hoffmann and Lipscomb.[82] These authors studied a variety of actual and conceivable B_nH_n polyhedra including the tetrahedron ($n = 4$), octahedron ($n = 6$), cube ($n = 8$), bicapped square antiprism ($n = 10$), cuboctahedron ($n = 12$), and icosahedron ($n = 12$) using the LCAO-MO Hückel method. Because of the peculiarities of the polyhedral systems such as the inapplicability of the nearest neighbor assumptions of Hückel theory in two-dimensional systems and the increased number of parameters, new approaches to the factorization of the secular equation needed to be developed in order to make these calculations feasible with the limited computing power available at that time. In some of their calculations the full "5*n*" set of five orbitals per cage atom (i.e., the H 1s and all four B sp^3 orbitals) was simplified to only the four orbitals on each boron atom (the "4*n*" set) or even only the three skeletal orbitals from each boron atom (the "3*n*" set). Further simplification of the reduced 3*n* problem was gained by physical factorization of the secular equation. In their "in-surface factorization" method, the three boron sp^3 internal hybrid orbitals are rehybridized to give a radial orbital of mostly s character pointed toward the center of the polyhedron and two p orbitals directed arbitrarily perpendicular to the axial direction, i.e., tangential to the polyhedron circumsphere. The Hoffmann−Lipscomb "in-surface factorization" then separates the tangential ("surface") and radial ("in") interactions and neglects any "in-surface" interactions so that the 3*n* problem is factored into problems of degree *n* (radial) and degree 2*n* (tangential). In addition, Hoffmann and Lipscomb use an "equatorial-apex factorization" for the bicapped prisms and antiprisms to separate two apex atoms from $n - 2$ "equatorial" atoms and a "ring-polar factorization" for bipyramids and pyramids to separate the axial atom (pyramids) or atoms (bipyramids) from the "ring" atoms at the base of the pyramid or in the equatorial section of the bipyramid. This relates to the dissection of bipyramids and pyramids into rings and caps in order to apply the six interstitial electron rule of Jemmis (section II.F).[69]

The Hoffmann−Lipscomb calculations[82] predict filled electronic shells and hence stable structures for tetrahedral B_4H_4, octahedral $B_6H_6^{2-}$, pentagonal bipyramidal $B_7H_7^{2-}$, cubical $B_8H_8^{2-}$, bicapped trigonal antiprismatic $B_8H_8^{2-}$, bicapped square antiprismatic $B_{10}H_{10}^{2-}$, pentagonal prismatic $B_{10}H_{10}$, cuboctahedral $B_{12}H_{12}^{2-}$, and icosahedral $B_{12}H_{12}^{2-}$. At the time of these calculations, only the bicapped square antiprismatic $B_{10}H_{10}^{2-}$ and icosahedral $B_{12}H_{12}^{2-}$ structures were known experimentally, so that these Hoffmann−Lipscomb calculations predicted the stability of several of the other subsequently discovered deltahedral $B_nH_n^{2-}$ structures, e.g., those for $n = 6$ (octahedron) and 7 (pentagonal bipyramid). Subsequent computational work by Hoffmann and Lipscomb[83] using essentially the same methods were used to provide information on the charge distributions and overlap populations of the boranes that were then known. The Hoffmann−Lipscomb calculations also provide information on the energy parameters for both the bonding and antibonding orbitals which are useful for testing graph-theory-derived models for chemical bonding in deltahedral boranes.

These early Hoffmann−Lipscomb calculations on polyhedral boranes led to the development of extended Hückel methods which have been applied to a great variety of inorganic and organic structures. One direction of the development of such computational methods has been to improve the parametrization of the diagonal Hamiltonian matrix elements with numbers obtained from more exact model self-consistent field (SCF) MO calculations on relatively small molecules[84] such as diborane in the case of borane calculations.[85] Using these methods, improved results were obtained for calculations of experimental energy quantities (total energies and ionization potentials) for some of the simple boranes, e.g., BH_3, B_2H_6, B_4H_{10}, B_5H_9, and $B_{10}H_{14}$ (Figure 1). However, use of these methods for calculation of the formal charge distribution over the atoms turned out to be somewhat dependent on the detailed calculational technique owing partly to the noniterative nature of the calculations.

Lipscomb and co-workers in subsequent work investigated alternative computational methods for deltahedral boranes and carboranes. Thus, they used the "partial retention of diatomic differential overlap" (PRDDO) method[86] to examine the wave functions for the boranes $B_nH_n^{2-}$ and the corresponding carboranes $C_2B_{n-2}H_n$ in both canonical MOs and localized MOs (LMOs).[87] The value of the canonical MOs lies in examining molecular properties such as ionization potentials and reactivity sites based on charges. The use of LMOs provides a method for examining the relationship of rigorously computed valence structures to the simple valence bond structures predicted by the Lipscomb topological models. In general, the LMOs were found to correspond to delocalized topological structures or to sums of topologically allowed structures, the latter case occurring to increase the symmetry of the LMOs. Of interest is the observation that the LMOs for the 5-vertex structure 1,5-$C_2B_3H_5$ do not correspond to a structure with 3c-2e bonds but instead to a structure with only three bonds to each boron atom (Figure 10a).

Another approach for studying the electronic structure of boranes uses the localized three-center bonds arising from the Lipscomb topological models (section II.A) as the basis set for Hückel-type MO computations. Kettle and Tomlinson[88] showed that this method leads to the same pattern of MO energy levels as the LCAO methods of Lipscomb. Subsequent work[89] showed that this method is a topologically correct extension of Hückel theory to three dimensions.

The next computational studies on the deltahedral boranes were performed by Armstrong, Perkins, and Stewart,[90] who were the first to use iterative methods for borane calculations. Their calculations were also the first to consider all of the valence electrons and the terminal groups on the boron atoms so that

substituent effects, e.g., substitution of chlorine for hydrogen, could be examined. In the case of the deltahedral boranes, the closed-shell ground states for deltahedral $B_nX_n^{2-}$ (X = H, n = 6, 10, 12; X = Cl, n = 6, 12) were confirmed.[91] In $B_6H_6^{2-}$ and $B_{12}H_{12}^{2-}$, the excess negative charge from the dianion was distributed between boron and hydrogen with a preponderance toward the boron atom. This situation is changed by the substitution of chlorine for hydrogen so that in $B_6Cl_6^{2-}$ and $B_{12}Cl_{12}^{2-}$ the chlorine has the greater negative charge. Electron-density contours in $B_6H_6^{2-}$ show that the charge is concentrated both at the center of the cage and in the centers of the trigonal faces. This is consistent with more recent computational studies on $B_6H_7^-$, which favor a face-protonated structure over an edge-protonated structure.[92] In the larger $B_{10}H_{10}^{2-}$ and $B_{12}H_{12}^{2-}$ deltahedra, the electron density forms a symmetrical spherical shell inside the cage with the density decreasing toward the center. Thus, the electron densities from the core and surface bonding are distinctly separate in $B_6H_6^{2-}$, but in the large boranes the surface bonding, which involves $2n$ bonding electrons, dominates over the core bonding, which involves only two electrons, so that separate concentration of electron density for core bonding is no longer observed.

Because of the great conceptual value of Hückel theory, refinements of Hückel theory have continued even after the greatly improved availability of modern Gaussian ab initio computations. In this connection, Zhao and Gimarc[93] developed a version of three-dimensional Hückel theory developed from the approximations of simple Hückel theory plus a few additional assumptions but retaining the significance of molecular topology. Their theory differentiates between Coulomb integrals for radial (designated as α_R) and tangential orbitals (designated as α_T) rather than a single Coulomb integral α as used in eq 7. To readjust the zero of energy so that MOs can be interpreted as either bonding or antibonding orbitals by the sign of the energy, the equation $\alpha_R + 2\alpha_T = 0$ is used to recognize that there are twice as many tangential orbitals as radial orbitals. Application of this method to the $B_nH_n^{2-}$ polyhedra leads to the experimentally observed deltahedra (Figure 3) as the lowest energy polyhedra. Furthermore, the lowest energy structure for each n has $n + 1$ bonding MOs that are completely occupied by electrons where all antibonding MOs are vacant, thereby confirming the $n + 1$ cluster electron pair rule leading to the experimentally observed $2n + 2$ skeletal electrons.

Wade and collaborators[94] more recently continued to use extended Hückel MO methods to investigate stability patterns in deltahedral borane chemistry. Calculations were carried out for published experimental geometries and also for hypothetical structures in which all boron atoms lie on a spherical surface and all deltahedral faces are equilateral triangles with B−B = 1.70 Å and B−H = 1.19 Å. These calculations were found to reproduce at least semiquantitatively the patterns of chemical stability for the observed $B_nH_n^{2-}$ ($6 \le n \le 12$) ions and qualitatively the stoichiometries and stabilities of the observed B_nX_n neutral molecules. The authors suggest that the patterns of chemical stability of the deltahedral boranes are primarily the result of symmetry and topology and that while very sophisticated ab initio calculations are necessary to reproduce the detailed geometries of boranes, they are not needed in order to understand in MO terms the species observed (and not observed) as well as their relative stabilities.

The SCF-Xα scattered wave technique has been used by Basiri and Pan[95] for calculation of the MO energies of the octahedral boranes $B_6H_6^{z-}$ (z = 0, 2, and 4); this technique requires only a small fraction of the computer time of ab initio Hartree−Fock LCAO methods.[96] These calculations confirm the stability of $B_6H_6^{2-}$ by 110.8 kJ/mol with respect to the monoanion and by 176.8 kJ/mol with respect to the neutral molecule.

B. Semiempirical and Molecular Mechanics Calculations on Deltahedral Boranes

Semiempirical computational methods using some parameters determined by experiment were developed concurrently with ab initio methods. Although semiempirical methods have now been largely displaced by ab initio Gaussian methods using relatively large basis sets and corrections that can be handled by modern computers, the much smaller computational requirements for semiempirical methods still make them useful for simple and rapid initial structure optimizations.

Dewar and McKee[97] applied semiempirical computational methods to the study of boranes including those with deltahedral structures. Their attempts to parametrize the originally developed MINDO/3 method[98] for boron failed, apparently owing to inadequacies of the INDO approximation on which the MINDO/3 method is based. However, the more recently developed MNDO ("modified neglect of diatomic overlap") semiempirical method[99] based on the NDDO approximation[100] was parametrized successfully for boron, and calculations were reported for the deltahedral borane anions $B_nH_n^{2-}$ ($6 \le n \le 12$).[97] The MNDO calculations reproduced the observed deltahedral geometries for all of these borane anions except for $B_9H_9^{2-}$, where the MNDO calculations suggest a C_{2v} distorted capped square antiprism in contrast to the observed D_{3h} tricapped trigonal antiprism. This discrepancy has been attributed to the tendency of MNDO to underestimate the strengths of 3c-2e bonds.

Allinger and co-workers applied their MM3 molecular mechanics methods[101] to the study of deltahedral boranes having 7, 10, and 12 vertices. In the 7-vertex deltahedral boranes and derivatives,[102] the pentagonal bipyramidal cage was treated as a superimposition of a five-membered ring and apical (cap) groups similar to the methods of Jemmis (Figure 10b).[69] In the 10- and 12-vertex deltahedral boranes and carboranes, the deltahedral cages were treated analogously as a superposition of two rings and two caps[103,104] The chemical bonding between these structural building blocks was treated by Hill-like potentials such as those normally used for a description of nonbonded intra- and intermolecular interactions.

In general, these calculations gave good agreement with experimental data.

C. Gaussian ab Initio Computations on Deltahedral Boranes and Carboranes

The development of Gaussian approximations to atomic orbitals has had a major impact on the availability and reliability of ab initio computational methods. Computer programs for computational chemistry using Gaussian orbitals are now widely available. The first reported computation on polyhedral boranes using Gaussian methods, i.e., contracted Gaussian-type functions fitted to Slater-type orbitals, was described in 1973 by Guest and Hillier.[105] Integral evaluation was carried out by fitting each Slater-type orbital to three Gaussian-type functions. Extended basis set calculations on the $C_2B_4H_6$ isomers used double-ζ basis of carbon and boron 2p orbitals and hydrogen 1s orbitals. The electronic structures of the closed deltahedral carboranes 1,5-$C_2B_3H_5$, 1,2-$C_2B_4H_6$, 1,6-$C_2B_4H_6$, and 2,4-$C_2B_5H_7$ obtained from such ab initio Gaussian computations were compared with those obtained by semiempirical methods. The ab initio extended basis set SCF MO calculations were found to predict the observed order of stability for the isomers of $C_2B_4H_6$, whereas such calculations using a minimal basis set or semiempirical methods incorrectly predicted the 1,2 isomer to be the most stable. In these carboranes, the carbon was found to have considerable negative charge by a Mulliken analysis with the negative character increasing with an increased basis.

A much more comprehensive series of ab initio calculations on carboranes was reported in 1986 by Ott and Gimarc,[106] who used the Gaussian-80 program with an STO-3G basis set rather than a larger basis set for computations on 29 of the 52 possible carboranes of the type $C_2B_{n-2}H_n$ ($5 \leq n \leq 12$). All structures were optimized using a gradient optimization method starting with B−B distances of 1.69 Å and B−H distances of 1.11 Å in the obvious deltahedra for $n = 5$ (trigonal bipyramid), 6 (octahedron), 7 (pentagonal bipyramid), 10 (bicapped square antiprism), and 12 (octahedron) for the most regular deltahedra.[107] For carboranes derived from less regular deltahedra (n = 8, 9, and 11), averages of experimental distances were taken in the starting structures. The calculated bond distances in the optimized structures agreed with the experimental distances within ±0.04 Å for 82% of the B−B, C−B, C−H, and B−H bond distances. These ab initio results also agree with the predictions made by Williams[108] using empirical valence rules except in the case of the isomers of $C_2B_6H_8$. These calculations of Gimarc and co-workers were later[109] extended to the corresponding deltahedral boranes $B_nH_n^{2-}$ ($5 \leq n \leq 12$) in order to test graph-theory-derived models of three-dimensional aromaticity.

In 1986 Fowler[110] reported some Gaussian calculations on the octahedral borane $B_6H_6^{2-}$ using the 4-31G, 6-31G, and 6-31G* basis sets, with the largest set (6-31G*) containing a set of d polarization functions on each boron atom. The order of the MOs was the same for all of the basis sets and predict HOMO−LUMO gaps >14 eV for $B_6H_6^{2-}$. The shapes and locations of the nodes of the skeletal bonding MOs were consistent with the S^σ, P^σ, and D^σ designations of spherical harmonics predicted by tensor surface harmonic theory (section II.E).

Gaussian methods were also used in the restricted Hartree−Fock calculations for the isoelectronic series of icosahedral boranes and carboranes $B_{12}H_{12}^{2-}$, $CB_{11}H_{12}^{-}$, and 1,12-$C_2B_{10}H_{12}$ reported in 1988 by Green, Switendick, and Emin.[111] For $B_{12}H_{12}^{2-}$, the STO-3G basis set did not produce enough bonding MOs whereas the larger 3-21G and 4-31G* basis sets both produced the correct number of bound one-electron orbitals, namely, 37 corresponding to 12 bonding MOs for the external B−H bonds, 12 bonding MOs for the icosahedral surface bonding, 1 bonding MO for the icosahedral core bonding, and 12 orbitals for the inner boron 1s electrons. The two larger basis sets also produced identical valence MO energy orderings and energies which agreed to a few tenths of an electronvolt as well as very similar optimized geometries, thereby suggesting that the smaller 3-21G basis set without the boron and carbon polarization functions used in the larger 4-31G* basis set was adequate for the study of these icosahedral molecules.

Zahradnik, Balaji, and Michl[112] also reported an SCF study of 10-vertex and 12-vertex polyhedral boranes and heteroboranes. Thus, they obtained completely optimized geometries for $B_{10}H_{10}^{2-}$, $B_{12}H_{12}^{2-}$, and their isoelectronic analogues with a single heteroatom (C, N, O, Al, Si, P, S) using the 3-21G and 6-31G* basis sets. For the anionic and dianionic species, the geometry optimization was also carried out using the 6-31+G* basis set. The harmonic vibrational frequencies were obtained at the Hartree−Fock 3-21G level. The calculated results compared well with experiment.

Bader and Legare[113] used SCF calculations in Gaussian 88 with a contracted (9s,5p) basis set supplemented with polarization functions to calculate the energies, geometries, and charge distribution of diverse known boranes including the deltahedral $B_nH_n^{2-}$ (n = 6, 7, 12) and the carboranes $C_2B_{n-2}H_n$ (n = 5, 6). Good agreement was obtained between the experimental and calculated geometries. Molecular structures were assigned on the basis of the bond paths defined by the topology of the charge density using the theory of atoms in molecules.[114] The stability of the borane structures based on polyhedra and polyhedral fragments is considered to be a consequence of the delocalization of charge over the surfaces of the three- and four-membered rings of atoms that result from the formation of bonds of reduced order, a delocalization that is itself essential to the formation of the ring bonds and related to the concept of multicenter bonding (section II.A).

Jemmis and collaborators[115] extended the study of the topography of deltahedral boranes, carboranes, and silaboranes having 5−7 vertices using ab initio computations at the 6-31G* level with Gaussian 90. Single-point calculations using better quality triple-ζ basis[116] were then performed on the optimized structures. The resulting molecular wave functions were

used for the study of the topographical features such as the critical points, i.e., the point where the gradient of the scalar field is zero. No B−B bond critical points were found to exist in the equatorial plane for the 5-vertex deltahedra, suggesting localized bonding without any B−B equatorial interactions. The charge density was found to be larger on the exterior of the deltahedron than in the interior, indicative of the major role of surface-delocalized bonding. However, all of the borane anions exhibited some localization of the electron density in the centroid of the deltahedron corresponding to core bonding.

Another comprehensive computational study on the deltahedral boranes $B_nH_n^{2-}$ and carboranes $C_2B_{n-2}H_n$ ($5 \le n \le 12$) using ab initio restricted Hartree−Fock methods with STO-6G and MIDI-4 basis sets was reported by Takano, Izuho, and Hosoya[117] in 1992. By the use of double-ζ MOs of high quality, the electron densities in these compounds were calculated and analyzed in detail through spherical charge analysis[118] and electron density contour mapping. The external B−H bonds in the deltahedral boranes and carboranes were found to have almost similar homopolar bonding character of a typical 2c-2e bond. Inspection of the contour maps of the deformation electron density on a variety of planes in the deltahedral molecular skeleton reveals that the central planar ring in a deltahedral molecule (e.g., an equatorial square in an octahedron or an equatorial pentagon in a pentagonal bipyramid) has a charge distribution similar to that in two-dimensional planar cyclic conjugated systems. This is related to the six interstitial electron rule of Jemmis (section II.F)[69] discussed above.

Recently Schleyer and co-workers[119] used the calculation of nucleus-independent chemical shifts (NICS) of the deltahedral boranes $B_nH_n^{2-}$ ($5 \le n \le 12$) to investigate magnetic criteria for aromaticity. NICS is based on the absolute chemical shieldings computed at the cage centers. The quantitative correspondence of NICS, diamagnetic susceptibility exaltation (Λ), aromatic stabilization, and geometric criteria have been demonstrated for five-membered aromatic and antiaromatic heterocycles.[120] Such calculations on the deltahedral boranes indicate large negative NICS values at the cage centers suggesting pronounced three-dimensional delocalization in such structures. The most symmetric $B_{12}H_{12}^{2-}$ (I_h) and $B_6H_6^{2-}$ (O_h) have the largest NICS values followed by $B_{10}H_{10}^{2-}$.

Schleyer and Najafian[121] recently reported comprehensive ab initio calculations on the deltahedral boranes $B_nH_n^{2-}$ ($5 \le n \le 12$) using density functional methods at the B3LYP/6-311+G** level to examine the energetic relationships. The acetylene-like $B_2H_2^{2-}$ was employed and the BH_{inc} increment energy was taken as the difference between B_3H_5 (C_{2v}, planar) and B_2H_4 (D_{2h}, ethylene-like) in order to study the energies of the following reaction

$$B_2H_2^{2-} + (n-2)\,BH_{inc} \rightarrow B_nH_n^{2-} \quad (5 \le n \le 12) \tag{12}$$

All such reaction energies were found to be exothermic. Furthermore, the stabilities of the deltahedral boranes were found to fall into the following four groups of generally decreasing stability: (1) $B_{12}H_{12}^{2-}$ and $B_6H_6^{2-}$; (2) $B_{10}H_{10}^{2-}$ and $B_7H_7^{2-}$; (3) $B_8H_8^{2-}$ and $B_9H_9^{2-}$; (4) $B_{11}H_{11}^{2-}$ and $B_5H_5^{2-}$.

Schleyer and Najafian[122] also recently performed ab initio calculations at the RMP2(fc)/6-31G* level on the deltahedral carboranes $CB_{n-1}H_n^-$ and $C_2B_{n-2}H_n^{2-}$ ($5 \le n \le 12$). As was the case with the isoelectronic carbon-free deltahedral boranes, the stabilities of the members of these series of carboranes were found to increase with increasing cluster size from 5 to 12 vertices characteristic of three-dimensional aromaticity. The rather large NICS and the magnetic susceptibilities, which correspond well with one another, also show all of these deltahedral carboranes to exhibit three-dimensional aromaticity.

Jemmis and collaborators found through ab initio computations using Gaussian 90 and 94 that the relative isomer stabilities of some deltahedral heteroboranes change drastically upon substitution of carbon by silicon.[123−125] In the case of octahedral $E_2B_4H_6$, the antipodal (1,6) carborane (E = C) is found to be more stable than the adjacent (1,2) isomer, whereas these relative stabilities are reversed for the silicon analogues (E = Si).[123] Similarly, for the 7-vertex pentagonal bipyramidal $E_2B_5H_7$, the relative stabilities for the carborane isomers (E = C) are nonadjacent (2,4) > adjacent (1,2 and 2,3) > antipodal (1,7) whereas the stability sequence for the corresponding silaborane isomers is exactly the opposite.[123] For the 8-vertex $E_2B_6H_8$ isomers (E = C, Si, Ge, Sn, Pb), the most stable isomer in all cases is the 1,7-bisdisphenoidal isomer with the heteroatoms at nonadjacent degree 4 vertices. However, a hexagonal bipyramidal isomer of $Si_2B_6H_8$ with the silicon atoms at the degree 6 axial vertices is found to be only 17.2 kcal/mol higher in energy than the most stable 1,7-bisdisphenoidal isomer.[124] For the icosahedral heteroboranes $E_2B_{10}H_{12}$, the relative isomer stabilities remain antipodal (1,12) > nonadjacent (1,7) > adjacent (1,2) when carbon is replaced by silicon, although the energy differences are significantly smaller for the silicon derivatives.[125]

McKee, Bühl, Charkin, and Schleyer used Gaussian methods at the MP2/6-31G* level to study four-center two-electron (4c-2e) bonding in deltahedral boranes and carboranes.[92] They found face-capping using a 4c-2e B_3H bond to be more favorable than edge-capping using a 3c-2e B_2H bond in the octahedral boranes $B_6H_7^-$ and CB_5H_7 by 12.1 and 16.8 kcal/mol, respectively.

In very recent work, McKee, Wang, and Schleyer[126] reported computational studies on the neutral boranes B_nH_n (n = 5−13, 16, 19, 22) and the borane radical anions $B_nH_n^-$ (n = 5−13) at the B3LYP/6-31G* and higher levels of density functional theory. The favored structures for the neutral boranes B_nH_n with $n = 3p + 1$ (p = 2−7) were all found to have one boron atom on a 3-fold axis. Thus, the favored structure for B_7H_7 is a capped octahedron rather than the pentagonal bipyramid experimentally observed for the dianion $B_7H_7^{2-}$. Loss of one electron from

$B_nH_n^{2-}$ ($n = 5-13$) is predicted to be exothermic except for $B_{12}H_{12}^{2-}$.

Computational studies have also been used to test mechanistic models of deltahedral borane isomerizations. In this connection, McKee[127] has shown by ab initio calculations using Gaussian 82 or 86 program systems at several levels up to MP4/6-31G*+ZPC//6-31G* that the isomerization of 1,2-$C_2B_4H_6$ to 1,6-$C_2B_4H_6$ proceeds in two steps with a benzvalene-like intermediate. The first step, the rate-determining step, is a modified dsd step where the symmetry of the transition state is reduced from C_{2v} to C_2, thereby changing the step from orbitally forbidden (in C_{2v} symmetry) to orbitally allowed (in C_2 symmetry). The second step is a concerted dsd step which is also known as a local bond rotation. The activation barrier was calculated to be 44.7 kcal/mol, in good agreement with an experimental estimate (42−45 kcal/mol).

D. Computational Studies of "Classical" versus "Nonclassical" Bonding Models for 5-Vertex Deltahedral Boranes

Computational methods have recently been used to study bonding delocalization in 5-vertex deltahedral boranes in which the two degree 3 axial vertices of the trigonal bipyramid suggest localized "classical" bonding models with three-coordinate boron similar to $(CH_3)_3B$ (section II.D and Figure 10a). Geometrical optimizations using ab initio MO calculations of Burdett and Eisenstein[128] at the Hartree−Fock and MP2 level on bipyramidal $(BX)_n(Y)_2$ systems ($n = 3$ [trigonal bipyramid] and 4 [octahedron]) suggest that the equatorial B−B distances for a given polyhedron correlate broadly with the electronegativity of the axial atoms. For the trigonal bipyramidal molecules, the B−B distances for $(BH)_3N_2$ are calculated to be quite short (1.65 Å), suggesting a globally delocalized structure, whereas the B−B distances for $(BNH_2)_3(SiH)_2$ are calculated to be significantly longer (1.96 Å), suggesting a localized bonding model with three-coordinate boron in the latter case. This approach for the study of trigonal bipyramidal boranes was extended by Subramanian, Schleyer, and Dransfeld,[129] who performed bonding (NLMO bond orders and Bader's topographical analysis[113,114]), energetic (homodesmotically computed stabilization energies), and magnetic (diamagnetic susceptibility exaltation and NICS) analyses for the trigonal bipyramidal 1,5-$X_2B_3Y_3$ (X = N, CH, P, SiH; Y = NH_2, CH_3, H). Their work suggests that "nonclassical" versus "classical" bonding for 5-vertex trigonal bipyramidal boranes (Figure 10a) is determined by the substituents on the equatorial boron atoms.

Another recent computational study on 5-vertex boranes used SCF, DFT, MP2 CCSD, and CCSD(T) calculations with three different basis sets and the three-parameter hybrid exchange-correlation function of Becke (B3LYP) for the DFT calculations.[130] For the investigation of the deformability of the polyhedron of $C_2B_3H_5$, the equilibrium structures together with the B−B bond strengths and the chemical shifts for $C_2B_3H_3Li_2$, $C_2B_3H_2Li_3$, $C_2B_3H_2F_3$, $C_2B_3F_5$, $C_2B_3H_3Cl_2$, $C_2B_3H_2Cl_3$, $C_2B_3H_3(NH_2)_2$, and $C_2B_3H_2(NH_2)_3$ were calculated. The calculated B−B distances were found to vary from 1.775 Å in $C_2B_3H_3Li_2$ to 1.9523 Å in $C_2B_3F_5$. The molecules $C_2B_3H_3F_2$, $C_2B_3H_2F_3$, $C_2B_3F_5$, $C_2B_3H_2Cl_3$, and $C_2B_3H_2(NH_2)_3$ were all suggested by these calculations to exhibit "classical" structures without multicenter bonding, whereas the lithium-substituted derivatives $C_2B_3H_3Li_2$ and $C_2B_3Li_5$ were all suggested to have "nonclassical" structures (Figure 10a). The remaining 5-vertex boranes appeared to exhibit bonding intermediate between the "classical" and "nonclassical" models.

A recent ab initio computational study by McKee[131] on B_nH_n and $B_n(NH_2)_n$ ($n = 3-6$) species at the HF/6-31G(d), MP2/6-31G(d), and B3LYP/6-31G(d) levels provides a comparison of "classical" and "nonclassical" structures for some of the smaller deltahedral boranes with only $2n$ rather than the $2n + 2$ skeletal electrons required for global delocalization. For early members of the B_nH_n series ($n = 3-5$), the lowest energy isomer contains one or more 3c-2e B−B−B bonds. Closed deltahedral structures become more stable only with B_6H_6, again suggesting the role of degree 3 vertices in preventing global delocalization of deltahedra. When hydrogens are replaced by amino groups, the classical nonplanar ring structure becomes more stable than the nonclassical deltahedron for $B_n(NH_2)_n$ ($n = 4-6$).

The question of "classical" versus "nonclassical" bonding in 5-vertex deltahedral boranes was studied experimentally by determining the molecular and crystal structures and electron density distribution for a single crystal of 1,5-$Et_2C_2B_3H_3$ using high-resolution X-ray diffraction at 120 K.[132] The mean B−C and B−B distances were found to be 1.571 and 1.876 Å, respectively, and the axial C···C distance was 2.272 Å. Deformation electron density maps showed charge accumulation in the skeletal B−C bonds, and these bonds were found to be essentially bent outward of the C_2B_3 cage. However, no charge accumulation was detected in the B−B bonds, thus indicating the absence of direct B−B interactions. Positive and delocalized deformation electron density was found in all of the B_2C triangular faces of the C_2B_3 trigonal bipyramid, thereby indicating a contribution of the multicenter bonding in the electronic structure of 1,5-$Et_2C_2B_3H_3$.

E. Use of Computations to Test Topological Models for the Chemical Bonding in Deltahedral Boranes

The results from some of the less complicated computations of MO energy parameters of deltahedral boranes can be used to test topological models of their chemical bonding (section II.C). Thus, the MO energy parameters for structures exhibiting delocalized bonding such as the deltahedral boranes can be related to the eigenvalues of the adjacency matrix of the underlying graph G by eq 7 (section II.D). However, any actual structure provides too few relationships to determine fully all of the three parameters α, β, and S in this equation. Therefore, some assumptions concerning the values of α, β, and S are necessary for any comparisons to be feasible. The generally used approach first assumes a zero value for S and then determines α from the midpoint of all of the molec-

Table 3. Orbital Representations for Deltahedra

deltahedron	Γ_σ (core and external orbitals)	Γ_π (surface orbitals)
octahedron	$A_{1g}+T_{1u}+E_g$	$T_{1u}+T_{2g}*+T_{2u}*+T_{1g}*$
pentagonal bipyramid	$2A_1'+E_1'+E_2'+A_2''$	$A_2'*+2E_1'+E_2'+A_2''+2E_1''*+E_2''*$
bisdisphenoid	$2A_1+2B_2+2E$	$2A_1+2A_2*+2B_1*+2B_2+4E$
4,4,4-tricapped trigonal prism	$2A_1'+2E'+A_2''+E''$	$A_1'+2A_2'*+3E'+A_1''*+2A_2''+3E''$
4,4 bicapped square antiprism	$2A_1+2B_2+E_1+E_2+E_3$	$A_2+A_2*+B_1*+B_2+3E_1+2E_2+3E_3$
icosahedron	$A_g+T_{1u}+T_{2u}+H_g$	$T_{1u}+H_g+G_u*+G_g*+H_u*+T_{1g}*$

ular energies by taking an appropriately weighted average so that eq 7 is reduced to

$$E_k \approx x_k\beta \tag{12}$$

The third parameter, β, can then be determined from specific orbital energies.

To relate a given computation on a deltahedral borane to topological models for its chemical bonding, computed values for all of the molecular orbital energy parameters are required including those for the unfilled antibonding (virtual) orbitals.[109] Having such information, the first step is to calculate α, the energy "zero point" (eq 7). In the case of a deltahedral borane anion $B_nH_n^{2-}$, this can be done by taking the mean of the energy parameters for all $5n$ molecular orbitals arising from the $4n$ atomic orbitals of the n sp^3 boron manifolds and the n s orbitals of the n hydrogen atoms. In taking this mean, the degenerate orbitals of the E, T, G, and H representations are given the weights 2, 3, 4, and 5, respectively, corresponding to their degeneracies. Hence, the parameter α becomes

$$\alpha = \frac{\sum_k g_k E_k}{\sum_k g_k} \tag{13}$$

In eq 13, g_k is the degeneracy of energy level k and the summation is over all molecular orbitals k. It is convenient to tabulate orbital energies as $E_k' = E_k - \alpha$, such that

$$\sum_k E_k' = 0 \tag{14}$$

The surface energy unit, β_s, can also be estimated at this stage as the degeneracy-weighted average distance of the pure surface orbitals from the energy zero point α. At this stage an unavoidable sampling error is introduced since only the pure surface orbitals can be included in the averages. The energy parameters of the other surface orbitals must be excluded from this average since they are distorted by substantial core−surface and external−surface mixing.

Further analysis of the computed energy parameters either requires some special symmetry such as that found in octahedral $B_6H_6^{2-}$ or icosahedral $B_{12}H_{12}^{2-}$ or some further assumptions concerning the chemical bonding topology for less symmetrical systems in order to minimize the number of independent unknowns to be determined. In the cases of $B_6H_6^{2-}$ and $B_{12}H_{12}^{2-}$, the core energy units β_c and the nonadjacent atom unique internal orbital interactions can be estimated from the energy parameters of the principal core orbital and a second core orbital, which does not mix with the surface orbitals. Possible errors arising from core−external orbital interactions do not appear to be large.

Table 4. Analysis of Computations[a] on Octahedral $B_6H_6^{2-}$

	HL5n	APS	GD
	core orbitals		
A_{1g} (principal)	+3.210	−50.3	−1.126
E_g	−0.888	+13.6	+0.470
T_{1u} (actual)	−0.844	11.3	−0.848
T_{1u} (effect of mixing removed)	(−0.478)	(10.1)	
	pure surface orbitals		
T_{2g}	+0.493	−5.5	−0.486
T_{2u}	−0.416	+9.8	+0.198
T_{1g}	−0.671	+11.7	+0.548
	derived parameters		
α	0	+7.2	+0.675
β_s	0.527	−8.1	−0.429
β_c	0.683	−10.7	−0.266
β_c/β_s	1.296	1.320	0.620
t	0.700	0.700	0.233
$\Delta E(T_{1u})$	0.366	−1.2	

[a] Energy units: GD, hartrees; APS, electronvolts; HL5N, dimensionless quantities given by $(\alpha-E_k)/(K-E_k)$ where K is the proportionality constant between resonance integral β and overlap S: $\beta_{rs} = KS_{rs}$.

To apply this method it is necessary to know the irreducible representations corresponding to Γ_σ for the core and external orbitals and Γ_π for the surface orbitals for the deltahedra of interest (Table 3). The pure surface orbitals are starred in Table 3; these orbitals correspond to irreducible representations found in Γ_π but not in Γ_σ.

The following computations on $B_6H_6^{2-}$ and $B_{12}H_{12}^{2-}$ have been analyzed by this method:[109] (1) Early extended Hückel computations by Hoffmann and Lipscomb[82] using a Slater orbital basis set (HL5n in Table 4); (2) Self-consistent molecular orbital computations by Armstrong, Perkins, and Stewart[90] also using a Slater orbital basis set (APS in Table 4); (3) Ab initio self-consistent field molecular orbital computations by Gimarc and collaborators[109] using a Gaussian 82 program with a STO-3G basis set (GD in Table 4).

The method for analyzing these computations on $B_6H_6^{2-}$ is summarized below, and the results are given in Table 4. An analogous but more complicated method can be used to analyze similar computations of icosahedral boranes such as $B_{12}H_{12}^{2-}$. Similar analyses of the computations on less symmetrical $B_nH_n^{2-}$ deltahedra do not appear to be feasible since the lower symmetry leads to a larger number of independent parameters and thus highly underdetermined systems of equations.

To study the data for octahedral $B_6H_6^{2-}$, consider an octahedrally weighted K_6 graph (Figure 9) having 12 edges of unit weight corresponding to the octahedron edges (cis interactions) and the remaining 3 edges of weight t corresponding to the three octahedron antipodal vertex pairs (trans interactions).[109] The spectrum of this graph has a nondegenerate eigenvalue $4 + t$ corresponding to the A_{1g} principal core orbital, a triply degenerate eigenvalue $-t$ corresponding to the triply degenerate T_{1u} core molecular orbital, and a doubly degenerate $-2 + t$ eigenvalue corresponding to the doubly degenerate E_g core molecular orbital (Figure 9). Note that any positive value of t (up to $+2$) is sufficient to lead to only one positive eigenvalue, namely, the $4 + t$ eigenvalue of the A_g orbital, and five negative eigenvalues, namely, the $-t$ eigenvalues of the triply degenerate T_{1u} orbital and the $-2 + t$ eigenvalues of the doubly degenerate E_g orbital. This indicates that any reasonable positive trans interaction in an octahedron gives the same distribution of bonding and antibonding orbitals, namely, 1 and 5, respectively, as an unweighted ($t = 1$) K_6 graph. Thus, for octahedral boranes, the numbers of bonding and antibonding orbitals are insensitive to the value taken for t. Note also that setting $t = 0$ leads to the spectrum of the octahedron (+4, 0, 0, 0, −2, −2) which is the D_6 graph whereas setting $t = 1$ leads to the spectrum of the K_6 complete graph (+5, −1, −1, −1, −1, −1).

The spectrum of the octahedrally weighted K_6 complete graph indicates that in the absence of core−surface mixing, eq 13 for the energy parameters of the octahedral core orbitals in $B_6H_6^{2-}$ relative to α becomes the equations

$$E(A_{1g}) = (4 + t)\beta_c \quad (15a)$$

$$E(T_{1u})_c = -t\beta_c \quad (15b)$$

$$E(E_g) = (-2 + t)\beta_c \quad (15c)$$

Since the A_{1g} and E_g orbitals are pure core orbitals (i.e., there are no surface orbitals having these irreducible representations, see Table 3), eqs 15a and 15c can be used to calculate the two parameters t and β_c corresponding to the $E(A_{1g})$ bonding and $E(E_g)$ antibonding energy parameters from a given computation, provided $\alpha = 0$ or is already known. Substitution of these calculated values for t and β_c in eq 15b then gives a hypothetical value for $E(T_{1u})_c$ in the absence of core−surface mixing. Comparison of this hypothetical value with the computed value for the T_{1u} core orbitals determines $\Delta E(T_{1u})$.

A related approach can be used to compare the computed octahedral surface orbital energy parameters with the ideal values arising from the graph-theory-derived method. In this case, the ideal surface orbital energy parameters are the following, with β_s designating the surface orbital energy unit

$$E(T_{2g}) = E(T_{1u})_s = \beta_s \quad (16a)$$

$$E(T_{2u}) = E(T_{1g}) = -\beta_s \quad (16b)$$

The following appropriately weighted mean of the *pure* surface orbitals T_{2g}, T_{2u}, and T_{1g} derived from eq 14 can be used to determine β_s

$$\beta_s = {}^1/_2\{-{}^1/_2[E(T_{2u}) + E(T_{1g})] + E(T_{2g})\} \quad (17)$$

The energy parameter $E(T_{1u})_s$ is not included in this mean because of the uncertainty in the core−surface mixing parameter $\Delta E(T_{1u})$, obtained as outlined above, which must be subtracted from the value of $E(T_{1u})$ obtained from the actual computation.

Application of these methods for the topological analysis of various computations on octahedral $B_6H_6^{2-}$ (Table 4) and icosahedral $B_{12}H_{12}^{2-}$ leads to the following observations. (1) The Hoffmann−Lipscomb LCAO-MO extended Hückel computations[82] and the Armstrong−Perkins−Stewart self-consistent molecular orbital computations,[90] both of which use Slater-type orbitals directly, give very similar values of β_c/β_s and t, particularly in the case of octahedral $B_6H_6^{2-}$. (2) The SCF-MO ab initio Gaussian 82 computations, which approximate Slater-type orbitals with a sum of Gaussians,[109] give much lower values of both β_c/β_s and the nonadjacent core orbital interaction parameters (t for $B_6H_6^{2-}$ and m for $B_{12}H_{12}^{2-}$) than the computations using Slater orbitals directly. This indicates that the representation of Slater-type orbitals by a sum of Gaussians as is typical in modern ab initio computations leads to significantly weaker apparent core bonding approximated more closely by deltahedral (D_n) rather than complete K_n topology, probably because Gaussian functions of the type $e^{\alpha r^2}$ fall off more rapidly at longer distances than Slater functions of the type $e^{-\zeta r}$. (3) The T_{1u} orbitals, which, if pure, would be nonbonding in octahedral (D_6) core bonding topology for $B_6H_6^{2-}$ and bonding in icosahedral (D_{12}) core bonding topology for $B_{12}H_{12}^{2-}$ become antibonding through core−surface mixing. Because of this feature, the simpler graph-theory-derived model using complete core bonding topology where $G_c = K_n$ (section II.D) gives the correct numbers of bonding and antibonding orbitals for the deltahedral boranes, even though analyses of MO energy parameters from computations suggest that the complete graph K_n is a poor approximation of the actual G_c corresponding to the computations using Gaussian orbitals.

Qualitative TSH theory (section II.E) has also been tested computationally by using it as a basis for so-called extended tensor surface harmonic (ETSH) calculations of the electronic structure and bonding in deltahedral boranes.[133] The borane deltahedron is treated as pseudospherical, but in ETSH, individual orbital energies are calculated including surface−core interaction effects. The assumptions of TSH theory are then justified by showing that whereas inclusion of core−surface interaction is necessary for correct electron counts, the tight-binding approximation does not lead to incorrect results. The results from the ETSH calculations were found to be compatible with qualitative TSH theory but of extended Hückel accuracy. Energy levels of the correct numbers and degeneracies were obtained for deltahedral boranes giving theoretical and computational support for the

empirical electron-counting rules and rationalizations of departures from them.

F. Some Experimental Tests of Computational and Topological Models of Deltahedral Borane Chemical Bonding

Photoelectron spectroscopy is a useful method for determining MO energy parameters experimentally for comparison with computational results and topological bonding models. In this connection, Vondrák and collaborators[134] measured the He I photoelectron spectra of a variety of 10- and 12-vertex deltahedral carboranes and thiaboranes. Semiempirical calculations suggest that the low ionization energy bands correspond predominantly to B−H and C−H MOs. In deltahedral carboranes with chlorines, experimental evidence for conjugative interaction of cluster π-type orbitals with the Cl nonbonding orbitals was obtained. The icosahedral thiaborane 1-$SB_{11}H_{11}$ exhibited five well-resolved band systems that were assigned to *F*(surface), *D*(surface + B−H), *F*(surface), *P*(B−H), and *F*(B−H) orbitals of TSH theory in the limit of spherical symmetry.

The oscillator strength spectra in the region of boron and carbon 1s excitations in the three isomeric icosahedral carboranes $C_2B_{10}H_{12}$ have been derived from inner-shell electron energy loss spectra (ISEELS) recorded under electric dipole-scattering conditions.[135] The spectral features were assigned on the basis of comparisons with spectral predictions derived from the results of ab initio and extended Hückel MO calculations. The isomeric and core level variations in the discrete core excitations were related to changes in orbital symmetries as well as variations in electron localization in these isomers. The ionization efficiency in the region of the boron and carbon 1s edges was determined.

A topological analysis of the electron density distribution, $\rho(\mathbf{r})$, in crystalline icosahedral 8,9,10,12-$C_2B_{10}H_8F_4$ has been performed using high-resolution low-temperature (120 K) X-ray diffraction data and a multipole model for data refinement.[136] Deformation electron density maps as well as maps of the Laplacian of $\rho(\mathbf{r})$ showed that the electron density is essentially delocalized over the surface of the cage and locally depleted in the center, suggesting the dominance of surface bonding involving 24 bonding electrons relative to core bonding involving only 2 bonding electrons. All B−B and B−C bonds in the icosahedron were characterized by significant bending, which was evident by shifts of their bond critical points from the straight lines between bonded atoms. Comparison of these data with corresponding ab initio calculations on small deltahedral boranes suggested that the electron-withdrawing of the fluorine substituents causes considerable redistribution of the electron density in the molecule, which, in particular, is reflected in the shift of $\rho(\mathbf{r})$ from the more electron-rich C−C bonds to the B−C bonds.

McLemore, Dixon, and Strauss[137] also reported some ab initio DFT calculations on fluorinated carboranes for comparison with experimental data on the site of fluorine substitution upon polyfluorination of $CB_{11}H_{12}^-$ and $CB_9H_{10}^-$. These calculations predict that 2-$CB_{11}H_{11}F^-$ is marginally more stable than 7-$CB_{11}H_{11}F^-$ or 12-$CB_{11}H_{11}F^-$ despite the observation that 12-$CB_{11}H_{11}F^-$ (the "antipodal" or "para" isomer) is the only isomer formed when $CB_{11}H_{12}^-$ is fluorinated with liquid anhydrous HF. These calculations thus suggest kinetic rather than thermodynamic control for the regioselective fluorination of $CB_{11}H_{12}^-$.

IV. Other Polyhedral Boron Derivatives

A. Electron-Rich (Hyperelectronic) Polyhedral Boranes: *Nido* and *Arachno* Structures

Electron-rich or hyperelectronic polyhedral boranes are those containing more than the $2n + 2$ skeletal electrons required for globally delocalized *n*-vertex deltahedra without vertices of degree 3. Electron-rich boranes include the well-known families of *nido* compounds having $2n + 4$ skeletal electrons and *arachno* compounds having $2n + 6$ skeletal electrons (Figure 14).[38] Examples of *nido* boranes include several relatively stable neutral binary boron hydrides of the general formula B_nH_{n+4} with $2n + 4$ skeletal electrons, e.g., B_5H_9, B_6H_{10}, and $B_{10}H_{14}$ (Figure 1) originally discovered by Stock.[1] Several *arachno* neutral binary boron hydrides of the general formula B_nH_{n+6}, such as B_4H_{10} and B_5H_{11}, were also discovered by Stock. Even at the time of their discovery, they were recognized to be generally less stable than the binary *nido* boron hydrides. Thus, in the early days of borane chemistry,[1] B_5H_9 was called

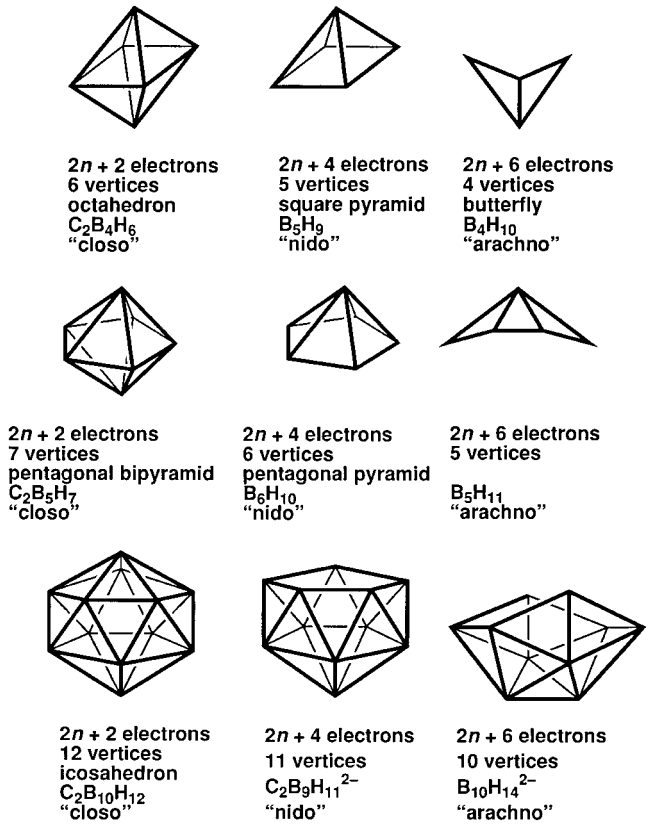

Figure 14. Hyperelectronic (electron-rich) polyhedra or polyhedral fragments having $2n + 4$ (*nido*) or $2n + 6$ (*arachno*) skeletal electrons obtained by excision of one or two vertices from an octahedron, pentagonal bipyramid, or icosahedron.

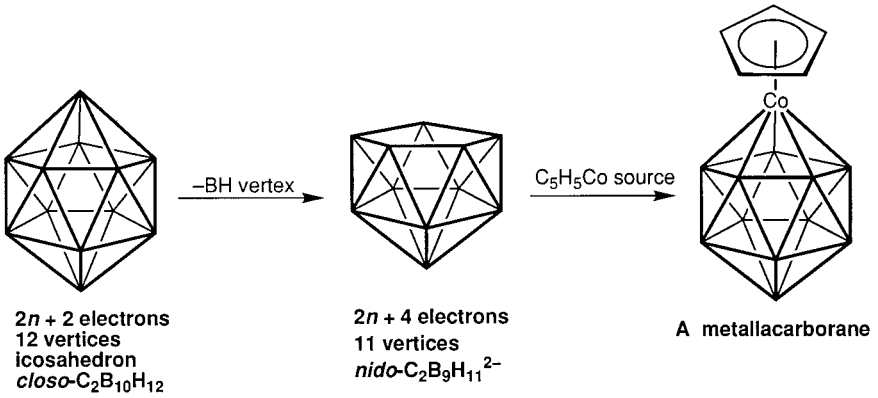

Figure 15. Conversion of an icosahedral carborane to an icosahedral metallacarborane by removal of a BH vertex followed by introduction of a transition-metal (C_5H_5Co) vertex.

"stable pentaborane" and B_5H_{11} was called "unstable pentaborane".

The *nido* boranes all have structures derived from the most spherical deltahedra (Figure 3) by loss of a vertex of highest degree (i.e., highest connectivity). In the resulting *nido* polyhedron, all but one of the faces are triangular; the unique nontriangular face may be regarded as a hole. Analogously, the *arachno* polyhedra are derived from the most spherical deltahedra (Figure 3) by loss of two adjacent vertices of relatively high connectivity. They have either two nontriangular faces or one large nontriangular face (i.e., two holes or one large bent hole). Thus, successive additions of electron pairs to a closed $2n + 2$ skeletal electron deltahedron result in successive punctures of the deltahedral surface to give holes (faces) having more than three edges by a process conveniently called *polyhedral puncture*. The open polyhedral networks can also be considered to arise by excision of one or more vertices along with all of the edges leading to them from a closed deltahedron having $m > n$ vertices by a process conveniently called polyhedral excision (Figure 14).

Treatment of the skeletal bonding topology in electron-rich polyhedra, even the *nido* polyhedra with only one nontriangular face and $2n + 4$ skeletal electrons, is considerably more complicated than the treatment of the skeletal bonding topology of deltahedra discussed above. The vertex atoms in electron-rich polyhedra may be divided into the following two sets: border vertex atoms which are vertices of the one face containing more than three edges (i.e., they are at the border of the single hole) and interior vertex atoms which form vertices of only triangular faces. For example, in a square pyramid (e.g., B_5H_9 in Figure 14), which is the simplest example of a *nido* polyhedron, the four basal vertices are the border vertices since they all border the square "hole", i.e., the base of the square pyramid. However, the single apical vertex of the square pyramid is an interior vertex since it is a vertex where only triangular faces meet. The external and twin internal orbitals of the border vertex atoms are taken to be sp^2 hybrids. The unique internal orbitals of the border vertex atoms will thus be p orbitals. The external and unique internal orbitals of the interior vertex atoms are taken to be sp hybrids in accord with the treatment of closed deltahedra discussed in section II.D. The twin internal orbitals of the interior vertex atoms must therefore be p orbitals. Note that in the *nido* polyhedra the hybridization of the border vertex atoms is the same as that of the vertex atoms of polygonal systems (e.g., benzene) whereas the hybridization of the interior vertex atoms is the same as that of the vertex atoms of deltahedral systems. A chemical consequence of the similar vertex atom hybridizations in polygons and the borders of *nido* polyhedra is the ability of both planar polygonal hydrocarbons (e.g., cyclopentadienyl and benzene) and the border atoms of *nido* carboranes[138] to form chemical bonds with transition metals of similar types involving interaction of the transition metal with *all* of the atoms of the planar polygon or the border atoms of the polygonal hole of the *nido* polyhedron (Figure 15).

Nido polyhedra can be classified into two fundamental types: the pyramids with only one interior vertex (the apex) and the nonpyramids with more than one interior vertex. If n is the total number of vertices and v is the number of interior vertices in a *nonpyramidal nido* polyhedron, the interactions between the internal orbitals which generate bonding orbitals are of the following three different types. (1) The $2(n - v)$ twin internal orbitals of the border atoms and the $2v$ twin internal orbitals of the interior atoms interact along the polyhedral surface to form n bonding orbitals and n antibonding orbitals. (2) The v unique internal orbitals of the interior vertex atoms all interact with each other at the core of the structure in a way which may be represented by the complete graph K_v to give a single bonding orbital and $v - 1$ antibonding orbitals. (3) The $n - v$ unique internal orbitals of the border atoms interact with each other across the surface of the hole in a way which may be represented by the complete graph K_{n-v} to give a single bonding orbital and $n - v - 1$ antibonding orbitals.

The above interactions in *nido* systems of the first two types correspond to the interactions found in the closed deltahedral systems discussed in the previous section, whereas the interactions of the third type can only occur in polyhedra containing at least one hole such as the nonpyramidal *nido* systems. Furthermore, the values of v and $n - v$ in the second and third types of interactions are immaterial as long as they both are greater than 1, since any complete

graph K_i ($i > 1$) has exactly one positive eigenvalue, namely, $i - 1$. The total number of skeletal bonding orbitals in nonpyramidal *nido* systems with n vertices generated by interactions of the three types listed above are n, 1, and 1, respectively, leading to a total of $n + 2$ bonding orbitals holding $2n + 4$ skeletal electrons in accord with experimental observations.

Pyramidal *nido* polyhedra having only one interior vertex require a somewhat different treatment because the eigenvalue of the 1-vertex no-edge complete graph K_1 is 0, leading to ambiguous results for the second type of interaction listed above. This difficulty can be circumvented by realizing that the only types of pyramids relevant to polyhedral borane chemistry are square pyramids, pentagonal pyramids, and hexagonal pyramids, and bonding schemes for these types of pyramids can be constructed which are completely analogous to well-known[139] transition-metal complexes of cyclobutadiene, cyclopentadienyl, and benzene, respectively. In applying this analogy, the interior vertex atom plays the role of the transition metal and the planar polygon of the border vertex atoms plays the role of the planar polygonal ring in the metal complexes. Furthermore, the $n - 1$ unique internal orbitals of the border vertex atoms interact cyclically leading to three "submolecular" orbitals which may be used for bonding to the single interior vertex atom as represented by the three nonnegative eigenvalues of the corresponding C_{n-1} cyclic graph ($n = 5, 6, 7$). Of these three polygonal orbitals, one orbital, the A_1 orbital, has no nodes perpendicular to the polygonal plane whereas the other two remaining orbitals, the degenerate E orbitals, each have one node perpendicular to the polygonal plane with the two nodes from pair of degenerate E orbitals being mutually perpendicular. This method is equivalent to the Jemmis method[69] of dissecting pyramids into "rings" and "caps" (section II.F).

The following three interactions are used to generate the skeletal bonding orbitals in *nido* pyramids. (1) The $2(n - 1)$ twin internal orbitals of the border atoms interact along the edges of the base of the pyramid to form $n - 1$ bonding orbitals and $n - 1$ antibonding orbitals analogous to the σ bonding and σ^* antibonding orbitals, respectively, of planar polygonal hydrocarbons. (2) The unique internal orbital of the single interior vertex atom (the apex of the pyramid) interacts with the A_1 orbital to give one bonding orbital and one antibonding orbital. (3) The twin internal orbitals of the apex of the pyramid interact with the two orthogonal E orbitals in two separate pairwise interactions to give two bonding and two antibonding orbitals.

The total numbers of skeletal bonding orbitals in pyramidal *nido* systems generated by these three interactions are $n - 1$, 1, and 2, respectively, leading to a total of $n + 2$ bonding orbitals holding $2n + 4$ skeletal electrons. Thus, the graph-theoretical treatment of nonpyramidal and pyramidal *nido* polyhedra with n vertices leads to the prediction of the same numbers of skeletal bonding orbitals, namely, $n + 2$, in accord with experimental observations. However, the partitionings of these bonding orbitals are different for the two types of *nido* systems, namely, (n, 1, 1) for the nonpyramidal systems and ($n - 1$, 1, 2) for the pyramidal systems.

The process of polyhedral puncture, which forms *nido* polyhedra with one hole and $2n + 4$ skeletal electrons from closed deltahedra with $2n + 2$ skeletal electrons, can be continued further to give polyhedral fragments containing two or more holes or one larger hole. Such boranes having $2n + 6$ and $2n + 8$ skeletal electrons are called *arachno* and *hypho* boranes, respectively (Figure 14). Formation of a new hole by such polyhedral puncture splits the complete graph formed by interactions at the polyhedral core between the unique internal orbitals of the interior vertex atoms into two smaller complete graphs. One of these new complete graphs involves interaction at the polyhedral core between the unique internal orbitals of the vertex atoms which are still interior atoms after creation of the new hole or expansion of the existing hole. The second new complete graph involves interaction above the newly created hole between the unique internal orbitals of the vertex atoms which have become border atoms of the newly created hole. Since each new complete graph contributes exactly one new skeletal bonding orbital to the polyhedral system, each application of polyhedral puncture to give a stable system requires addition of two skeletal electrons.

B. Metallaboranes: the "Isocloso Problem"

The boron vertices in borane polyhedra can be replaced with isolobal transition-metal vertices bearing sufficient external ligands, e.g., carbonyl groups or perhapto planar polygons, to give the transition metal a suitable electronic configuration, most frequently the 18-electron configuration of the next noble gas. Examples of transition-metal vertices isoelectronic and isolobal with a BH vertex and thus donors of two skeletal electrons include $Fe(CO)_3$, (η^6-C_6H_6)Fe, and (η^5-C_5H_5)Co as well as corresponding derivatives of their heavier congeners. Similarly $Co(CO)_3$, (η^6-C_6H_6)Co, and (η^5-C_5H_5)Ni and corresponding derivatives of their heavier congeners are donors of three skeletal electrons similar to a CH vertex in polyhedral carboranes. The hydrogen atoms in BH and CH vertices as well as in the η^5-C_5H_5 and η^6-C_6H_6 rings bonded to transition-metal vertices in metallaboranes can be replaced by other monovalent groups, such as halogen, alkyl, aryl, etc., and the carbonyl groups in $M(CO)_3$ can be replaced by other two-electron donor ligands such as tertiary phosphines or isocyanides.

Deltahedral metallaboranes having n vertices, besides being derived from the corresponding deltahedral boranes by suitable isolobal/isoelectronic substitution of transition-metal vertices for boron vertices as noted above, can also be regarded as metal complexes of *nido* borane ligands with $n - 1$ vertices. For example, removal of one BH vertex from the icosahedral carborane $C_2B_{10}H_{12}$ (formally as BH^{2+}) gives an 11-vertex nido species, $C_2B_9H_{11}^{2-}$, having an open pentagonal face (Figure 15). Complexing a transition metal (e.g., a C_5H_5Co unit) to the open

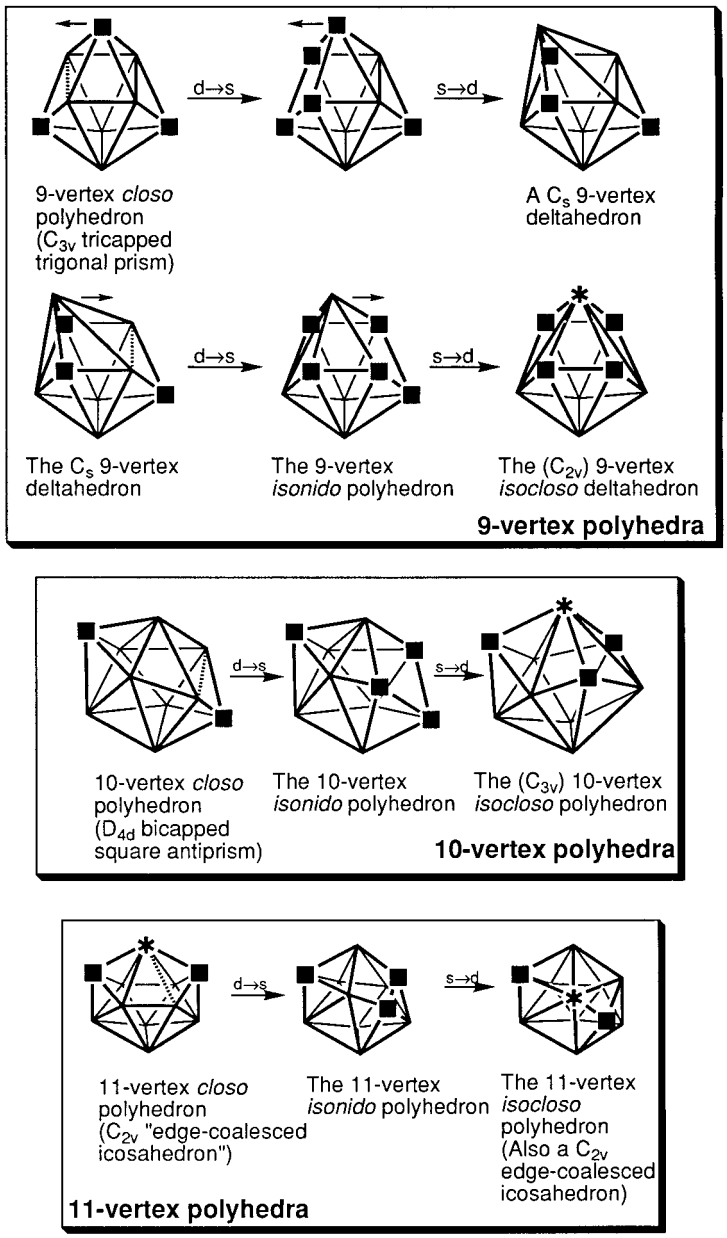

Figure 16. Diamond−square−diamond (dsd) processes leading from 9-, 10-, and 11-vertex *closo* 9-vertex deltahedra to the corresponding *isocloso* deltahedra. For clarity, the degree 4 and 6 vertices are indicated by solid squares (■) and six-pointed asterisks (*), respectively, and the edges broken in the d → s stage of the dsd process are indicated by hatched lines.

pentagonal face of $C_2B_9H_{11}^{2-}$ reconstitutes the icosahedral structure in the form of a metallacarborane (i.e., $C_5H_5CoC_2B_9H_{11}$ in the case of a C_5H_5Co vertex). The bonding of the cobalt atom to the pentagonal face of $C_2B_9H_{11}^{2-}$ is analogous to the pentahapto bonding of a cobalt atom to pentagonal $C_5H_5^-$.

Initially it was assumed that the polyhedra in metallaboranes would be the same as the polyhedra in isoelectronic metal-free boranes using the isolobal/isoelectronic relationships noted above. However, as metallaborane chemistry was developed further, particularly by Kennedy and co-workers,[140] a variety of deltahedral metallaborane structures were discovered based on deltahedra topologically distinct from the deltahedra found in simple metal-free boranes and carboranes. Of particular interest was the discovery of 9- and 10-vertex metallaboranes based on deltahedra with the transition metal at a degree 6 vertex whereas the corresponding metal-free deltahedron has only degree 4 and 5 vertices. Even more interesting was the observation that such "anomalous" metallaborane deltahedra are also "disobedient" in having electron counts corresponding to only $2n$ skeletal electrons rather than the expected $2n + 2$ skeletal electrons. Such metallaborane deltahedra are called *isocloso* structures and can be derived from the *closo* deltahedron with the same number of vertices by diamond−square−diamond (dsd) rearrangements (Figure 16). In such dsd rearrangements the intermediate polyhedron with a single quadrilateral face looks like a *nido* polyhedron but one obtained by removal of a vertex of degree 4 rather than a larger degree from a deltahedron having $n + 1$ vertices. However, such apparent *nido* polyhedra do not have the expected $2n + 4$ skeletal electrons but instead have only $2n + 2$ skeletal electrons and

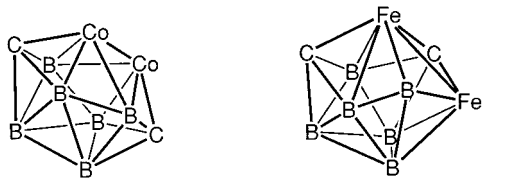

Figure 17. The 10-vertex metallacarborane deltahedra in the $(C_5H_5M)_2C_2B_6H_8$ (M = Fe, Co) complexes discovered by Hawthorne and co-workers in the 1970s showing the contrast between the *closo* dicobalt derivative with 22 skeletal electrons and the *isocloso* diiron derivative with only 20 skeletal electrons. Hydrogen atoms on the boron and carbon atoms and cyclopentadienyl rings on the metal atoms are not shown.

accordingly have been called *isonido* polyhedra. The 11-vertex *closo*/*isocloso* pair is different from the 9- and 10-vertex *closo*/*isocloso* pairs in that the 11-vertex *closo* and *isocloso* polyhedra are topologically equivalent with a single degree 6 vertex even though they are related by a diamond−square−diamond rearrangement like the 9- and 10-vertex *closo*/*isocloso* deltahedral pairs. This relates to the topological impossibility of an 11-vertex deltahedron having only degree 4 and 5 vertices,[23] so that the favored 11-vertex deltahedron for the metal-free boranes such as $B_{11}H_{11}^{2-}$ and $C_2B_9H_{11}$ is the edge-coalesced icosahedron with a single degree 6 vertex (Figure 3).

An interesting *closo*/*isocloso* pair of 10-vertex metallacarboranes was discovered by Hawthorne and co-workers in the 1970s (Figure 17) before the existence of *isocloso* deltahedra was recognized. Reduction of 1,7-$C_2B_6H_8$ with sodium naphthalenide followed by addition of NaC_5H_5 and $CoCl_2$ gave a mixture from which a 7% yield of 2,9,1,10-$(C_5H_5Co)_2C_2B_6H_8$ could be isolated.[141] X-ray diffraction of this compound indicated a structure (Figure 17) based on the 10-vertex *closo* deltahedron, namely, the 4,4-bicapped square antiprism (Figure 3), with the carbon atoms at the two degree 4 (axial) vertices and the cobalt atoms at degree 5 vertices[142] in accord with the 22 skeletal electrons (= $2n + 2$ for $n = 10$) expected for such a *closo* structure noting that C_5H_5Co vertices are donors of two skeletal electrons each. In contrast to this result, reduction of 4,5-$C_2B_7H_9$ with sodium followed by addition of NaC_5H_5 and $FeCl_2$ gave a mixture from which a 5% yield of 1,6,2,3-$(C_5H_5Fe)_2C_2B_6H_8$ could be isolated.[143] The substitution of two cobalt atoms by iron atoms in a polyhedral cluster with otherwise the same stoichiometry and bonding to external groups reduces the number of skeletal electrons by two so that 1,6,2,3-$(C_5H_5Fe)_2C_2B_6H_8$ has 20 skeletal electrons (= $2n$ for $n = 10$), which is now recognized to be correct for *isocloso* geometry. The structure of 1,6,2,3-$(C_5H_5Fe)_2C_2B_6H_8$ found by X-ray diffraction[143] corresponds to what is now recognized as the 10-vertex *isocloso* deltahedron with one iron atom at the degree 6 vertex and the other iron atom at a degree 5 vertex adjacent to the degree 6 vertex and with carbon atoms at two of the three degree 4 vertices (Figure 17). Since *isocloso* deltahedra were not recognized at the time of this experimental work, Hawthorne and co-workers[143] as well as subsequently Nishimura[144] rationalized the different geometry of the cobalt and iron complexes by assuming that the C_5H_5Fe vertices each donated the same two skeletal electrons as a C_5H_5Co vertex but that there was an Fe−Fe bond in addition to the usual 10-vertex deltahedral skeletal bonding to give the iron atoms the favored 18-electron configuration. A distortion arising from this extra Fe−Fe bond was assumed to account for the observed change in the deltahedral geometry in going from the cobalt to the iron complex of the same stoichiometry except for the change in the transition-metal atoms. With the additional information on metallaborane structures in the quarter century since this experimental work by Hawthorne and co-workers,[141−143] we can now interpret 2,9,1,10-$(C_5H_5Co)_2C_2B_6H_8$ as a *closo* deltahedral complex and 1,6,2,3-$(C_5H_5Fe)_2C_2B_6H_8$ as an *isocloso* deltahedral complex in accord with their respective skeletal electron counts.

The reason for the anomalous electron counts in the *isocloso* structures (i.e., two electrons less than the $n + 2$ skeletal electrons expected from "Wade's rules")[25] has been the cause for some speculation. Ideas to rationalize this anomaly include postulation of Jahn−Teller distortions removing orbital degeneracies in the HOMO/LUMO region[145,146] and postulating four-orbital rather than the usual three-orbital involvement of the transition-metal vertex to provide the "extra" electron pair.

A more direct rationalization for the anomalous electron counts in *isocloso* deltahedra describes the chemical bonding topology in isocloso deltahedra in terms of exclusively 3c-2e B−B−B bonds in deltahedral faces without any 2c-2e bonds or two-electron bonds involving more than three orbitals such as the *n*-center two-electron core bonds in the deltahedral boranes $B_nH_n^{2-}$ ($6 \le n \le 12$) discussed above (section II.D).[147] Thus, consider the bonding topology in a an *isocloso* metallaborane deltahedron with *n* vertices, which can be shown by Euler's theorem[55] to have $2n - 4$ faces and $3n - 6$ edges such as the corresponding *closo* deltahedron with the same number of vertices. If each vertex (e.g., a neutral BH vertex or isoelectronic/isolobal equivalent) contributes three skeletal (internal) orbitals and two skeletal electrons (i.e., a $2n$ skeletal electron system), then the numbers of skeletal orbitals and electrons are correct for 3c-2e bonds in *n* of the $2n - 4$ faces leaving $n - 4$ faces without 3c-2e bonds.

A more detailed understanding of this chemical bonding topology for *isocloso* metallaboranes can be obtained by removing the metal vertex leaving a metal-free borane unit with an open hexagonal face like a *nido* structure but a skeletal electron count like a *closo* structure. Thus, consider the 11-vertex ruthenium complexes of the type (arene)$RuB_{10}H_{10}$ (arene = *p*-cymene, hexamethylbenzene, etc.),[148] which may be considered to have 22 skeletal electrons, two from each vertex. The ruthenium atom in the (arene)-Ru vertex may be considered to have a typical +2 formal oxidation state like the stable $[(arene)Ru^{II}Cl_2]_2$ compounds so that removal of this vertex as (arene)-Ru^{2+} leaves behind a $B_{10}H_{10}^{2-}$ ligand with all of the 22 skeletal electrons. These skeletal electrons are used to form eight 3c-2e B−B−B bonds in 8 of the

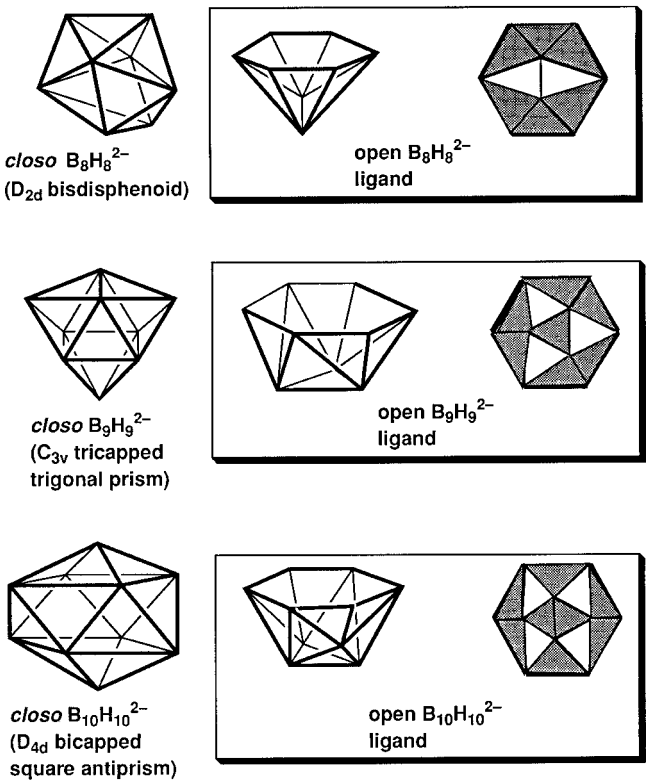

Figure 18. (a) Comparison of the structures of the *closo* boranes $B_nH_n^{2-}$ (n = 8, 9, 10) with the $B_nH_n^{2-}$ ligands containing an open hexagonal face found in *isocloso* metal complexes. (b) Viable arrangements of 3c-2e B−B−B bonds in the triangular faces of the open $B_nH_n^{2-}$ ligands; the shaded faces contain the 3c-2e B−B−B bonds.

12 triangular faces of the open $B_{10}H_{10}^{2-}$ unit and three 2c-2e B−B bonds in alternating edges of the open hexagonal face similar to the alternating C=C double bonds in a Kekulé structure of benzene (Figure 18). Reconstituting the *isocloso* metallaborane (arene)$RuB_{10}H_{10}$ from the open $B_{10}H_{10}^{2-}$ ligand with this bonding topology and the (arene)Ru^{2+} vertex with three internal orbitals converts the 2c-2e bonds on the open hexagonal face of $B_{10}H_{10}^{2-}$ into 3c-2e bonds leading to 11 3c-2e bonds and no 2c-2e bonds in the skeletal bonding framework of the reconstituted (arene)$RuB_{10}H_{10}$ structure in accord with its 22 skeletal electrons provided by the 33 internal orbitals of the 11 vertex atoms. The $B_{10}H_{10}^{2-}$ dianion ligand in (arene)$RuB_{10}H_{10}$, which can be considered as a hexahapto ligand, can be seen to be analogous to an arene ligand with the three 2c-2e B−B bonds on alternating edges of the open hexagon of $B_{10}H_{10}^{2-}$ functioning like the three alternating C=C double bonds of benzene in metal complexation.

Isocloso metallaboranes with 9 and 10 vertices can be considered analogously to be transition-metal derivatives of open $B_8H_8^{2-}$ and $B_9H_9^{2-}$ anions with one hexagonal face and $2n - 10$ triangular faces (Figure 18). However, in many cases one or more of the external hydrogen atoms in the open $B_{n-1}H_{n-1}^{2-}$ ligand are replaced by either Lewis base ligands (e.g., phosphines or isocyanides) or monovalent groups [e.g., Cl in $(Me_3P)_2HIrB_8H_7Cl$ (ref 149)] and/or a boron atom is replaced by a carbon atom with the necessary adjustments in electron count. In all cases the open $B_{n-1}H_{n-1}^{2-}$ ligand (Figure 18) can be regarded as a hexahapto ligand toward the transition-metal vertex with metal−ligand bonding similar to arene metal complexes. Furthermore, the triangular faces of the open $B_{n-1}H_{n-1}^{2-}$ ligand containing 3c-2e B−B−B bonds (i.e., the shaded faces in Figure 18) are situated so that three such shaded faces meet at each interior vertex and two such shaded faces meet at each vertex of the open hexagon in accord with the availability of three internal orbitals from each vertex atom but the involvement of one internal orbital from the open hexagon vertex boron atoms in the hexahapto bonding of the $B_{n-1}H_{n-1}^{2-}$ ligand to the transition metal.

C. Boron Allotropes: The Truncated Icosahedron in a Boron Structure

Elemental boron exists in a number of allotropic forms of which four (two rhombohedral forms and two tetragonal forms) are well established (Table 5).[150−152] The structures of all of these allotropic forms of boron are based on various ways of joining B_{12} icosahedra using the external orbitals on each boron atom. The chemical bonding topology in these B_{12} icosahedra appears to be exactly analogous to that found in the discrete $B_{12}H_{12}^{2-}$ anion, so that elemental boron provides an example of three-dimensional aromaticity in a refractory material.

The structures of the two rhombohedral forms of elemental boron (Table 5) are of interest in illustrating what can happen when icosahedra are packed into an infinite three-dimensional lattice. In these rhombohedral structures the local symmetry of a B_{12} icosahedron is reduced from I_h to D_{3d} because of the loss of the 5-fold rotation axis when packing icosahedra into a crystal lattice. The 12 vertices of an icosahedron, which are all equivalent under I_h local symmetry, are split under D_{3d} local symmetry into two nonequivalent sets of six vertices each (Figure 19a). The six rhombohedral vertices (labeled R in Figure 19a) define the directions of the rhombohedral axes. The six equatorial vertices (labeled E in Figure 19a) lie in a staggered belt around the equator of the

Table 5. Well-Characterized Allotropes of Elemental Boron

allotrope	atoms per unit cell	structural units in the unit cell
α-rhombohedral boron	12	one B_{12} icosahedron
β-rhombohedral boron	105	one B_{84} unit, two B_{10} groups, and one B atom
α-tetragonal boron	50	four B_{12} icosahedra and two B atoms
β-tetragonal boron	188	$B_{21}{\cdot}2B_{12}{\cdot}B_{2.5}$

Table 6. Analogies between the Packing of Units of Icosahedral Symmetry in α- and β-Rhombohedral Boron

	α	β
icosahedral unit	icosahedron	truncated icosahedron
number of vertices	12	60
rhombohedral linkages	two-center bonds	icosahedral cavities
equatorial linkages	three-center bonds	ideal B_{28} polyhedron from three fused icosahedra

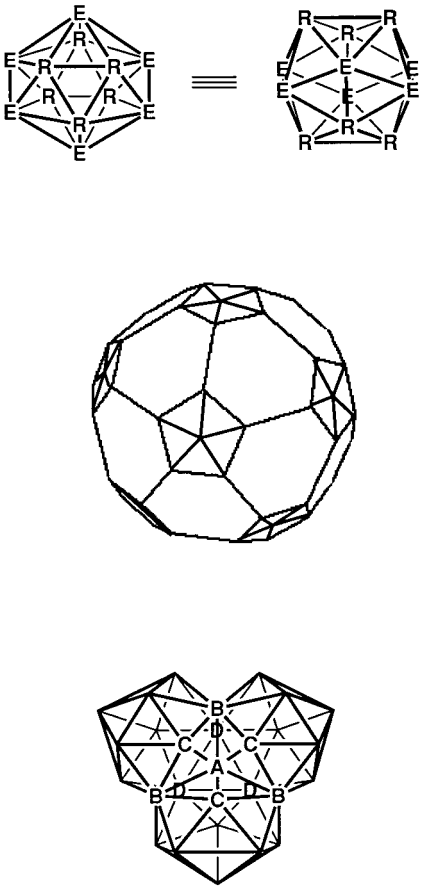

Figure 19. (a) Two views of the partitioning of the 12 vertices of a regular icosahedron into six rhombohedral vertices (R) and six equatorial vertices (E) upon reduction from I_h to D_{3d} symmetry. (b) The Samson complex derived from a truncated icosahedron, which is found in the β-rhombohedral boron structure. (c) The 28-vertex polyhedral cavities formed by overlap of the equatorial pentagonal pyramidal cavities of three Samson complexes in the β-rhombohedral boron structure.

icosahedron. The six rhombohedral and six equatorial vertices form prolate (elongated) and oblate (flattened) trigonal antiprisms, respectively.

In the simple (α) rhombohedral allotrope of boron (Table 5), all boron atoms are part of discrete icosahedra. In a given B_{12} icosahedron, the external orbitals of the rhombohedral boron atoms form 2c-2e bonds with rhombohedral boron atoms of an adjacent B_{12} icosahedron and the external orbitals of the equatorial boron atoms form 3c-2e bonds with equatorial boron atoms of two adjacent B_{12} icosahedra. Of the available (12)(3) = 36 electrons from an individual B_{12} icosahedron in α-rhombohedral boron, 26 electrons are used for the skeletal bonding (one 12-center core bond and 12 surface bonds) and the remaining 10 electrons are parts of external bonds, namely, $^1/_2$ of six 2c-2e bonds from the rhombohedral boron atoms and $^1/_3$ of six 3c-2e bonds from the equatorial boron atoms. Thus, α-rhombohedral boron has a closed-shell electronic configuration just like $B_{12}H_{12}^{2-}$. This bonding scheme for α-rhombohedral boron is supported by experimental determination of its electron density distribution using the maximum entropy method with synchrotron radiation powder data.[153]

The structure of the energetically more favorable β-rhombohedral boron avoids the 3c-2e intericosahedral bonding of α-rhombohedral boron and thus is energetically more favorable. The structure of β-rhombohedral boron may be described as a rhombohedral packing of B_{84} polyhedral networks known as Samson complexes (Figure 19b).[154] These B_{84} Samson complexes have an outer B_{60} surface with the same truncated icosahedral geometry that has become famous in recent years in the C_{60} fullerene structure. Inside the B_{60} truncated icosahedron surfaces of the Samson complexes are two nested B_{12} icosahedra with the inner B_{12} icosahedra being similar to the B_{12} icosahedra in α-rhombohedral boron or $B_{12}H_{12}^{2-}$.

The truncated icosahedral surfaces of the B_{84} Samson complexes in the β-rhombohedral boron structure have 12 pentagonal faces which are the bases of 12 pentagonal pyramidal cavities (indentations or "dimples") where the apices correspond to the 12 vertices of the Samson complex of the larger of the two internal icosahedra (Figure 19b).[155] These 12 pentagonal pyramidal cavities, which necessarily are located at the vertices of a large icosahedron, can be partitioned into a set of six rhombohedral cavities and a set of six equatorial cavities just as the 12 vertices of a B_{12} icosahedron in α-rhombohedral boron can be partitioned into sets of six rhombohedral and six equatorial vertices as noted above. The rhombohedral cavities overlap with the rhombohedral cavities of an adjacent Samson complex in a staggered manner to form new icosahedral cavities analogous to the 2c-2e external bonds of α-rhombohedral boron. The equatorial cavities overlap with the equatorial cavities of two adjacent Samson complexes by means of an additional B_{10} unit to form new polyhedral cavities with 28 vertices (Figure 19c). These B_{28} cavities have local C_{3v} symmetry and are constructed by fusion of three icosahedra so that in each icosahedron one vertex is shared by all three icosahedra and four vertices are shared by two of the icosahedra so that $3(B_7B_{4/2}B_{1/3}) = B_{28}$. The structures of α-rhombohedral and β-rhombohedral boron are quite analogous as illustrated in Table 5, where the B_{12} icosahedra in α-rhombohedral boron play roles analogous to the B_{60} truncated icosahedra in β-rhombohedral boron. Despite the complexity of the structure and bonding model for β-rhombohedral boron with the added complication of partial occupancies of some of the sites in the B_{28} cavities, the number of skeletal electrons works out to be within 1% of that required by reasonable bonding models based on the observed geometry.[155]

Bullett[156] performed some electronic structural calculations on both α-rhombohedral and β-rhombohedral boron as well as on the less well-characterized α-tetragonal boron[157] (Table 5). The results show that a band picture can provide a description of the bonding in these solids. The α-rhombohedral structure is found to produce semiconducting properties, with an indirect band gap of 1.7 eV. The ordering of bands was qualitatively interpreted in terms of the skeletal molecular orbitals of a B_{12} icosahedron and the 2c-2e and 3c-2e external bonds linking neighboring icosahedra in accord with the topological bonding

model discussed above. In the case of β-rhombohedral boron, a forbidden gap of ~2.7 eV was found to occur in the spectrum of electron states. Some degree of defect- or impurity-induced disorder appeared to be essential to stabilize the structure, since the valence band of the "ideal" structure can accommodate 320 electrons per B_{105} unit cell compared with the 315 electrons available. These calculations questioned the suggested α-tetragonal modification of pure boron (Table 5), since the electron deficit in the suggested structure should be so severe that the presence of a more electron-rich atom than boron such as carbon or nitrogen would be required leading to stoichiometries such as $B_{50}C_2$ and $B_{50}N_2$. Thus, the so-called α-tetragonal boron is probably an impurity-stabilized phase.

Computational studies based on density functional theory have been used by Boustani to investigate a variety of possible structures of elemental boron that have not yet been realized experimentally. Small boron clusters B_n ($2 \leq n \leq 14$)[158,159] appear to prefer structures based on planar or quasiplanar triangular networks which can be considered to be fragments of a planar surface or segments of the surface of a sphere. Low-energy structures of larger boron clusters, e.g., B_{21} and B_{24}, can also consist of interpenetrating icosahedral structural units.[160] Larger boron aggregates such as quasiplanar surfaces[161] and nanotubes[162] also appear to form similar triangulated networks. The fundamental building blocks of all of these computationally discovered but not yet experimentally realized structures of boron aggregates consist of B_6 pentagonal pyramids and B_7 hexagonal bipyramids having local environments of the central vertices similar to the boron atoms at vertices of degrees 5 and 6, respectively, of borane deltahedra (e.g., Figure 3).[163] The B_6 pentagonal pyramids found in Boustani's structures for boron aggregates are also similar to the pentagonal pyramidal cavities on the surface of a Samson complex in β-rhombohedral boron discussed above (Figure 19b).

D. Boron-Rich Metal Borides

The structures of binary metal borides are relatively complicated.[164−166] The metal borides with the highest boron content, i.e., those with boron/metal ratios of 4.0 or more, contain polyhedra of boron atoms, e.g., B_6 octahedra in MB_4 and MB_6 (M = La), B_{12} cuboctahedra in YB_{12}, B_{12} icosahedra in $NaB_{14.5}$ or C_3B_{12}, or $B_{12}(B_{12})_{12}$ "icosahedra of icosahedra" in YB_{66} (Figures 8−3).[167,168]

The structures of a few of these boron-rich metal borides were determined by X-ray diffraction long before the discovery of any of the deltahedral borane anions $B_nH_n^{2-}$ ($6 \leq n \leq 12$). It is therefore not surprising that the first computational studies on boron deltahedra were performed on the deltahedra in solid-state boride structures rather than the deltahedral borane anions. Thus, already in 1954, Longuet-Higgins and Roberts[13] showed that the B_6 octahedra in the CaB_6 structure, which are linked to adjacent B_6 octahedra through B−B 2c-2e external bonds, are stable as the dianions $[B_6^{2-}]$. In 1960 Lipscomb and Britton[167] reported an extension of the topological methods that they had developed for the study of polyhedral boranes for the study of boron-rich metal borides. They used the following approach. (1) The boron framework is dissected into polyhedra which are connected to each other by localized bonds, occasionally with the use of multicentered orbitals. (2) The skeletal bonding of the individual polyhedra is then investigated leading to determination of their MO energy parameters. (3) Electrons are transferred from the more electropositive element, typically an alkali metal, an alkaline-earth metal, or a lanthanide, to the boron framework until the bonding orbitals are filled. (4) Excess valence electrons on the metal atoms are regarded as metallic and presumed to lead to metallic optical and electrical properties.

The band structures of some metal borides containing B_6 octahedra were subsequently studied by Perkins, Armstrong, and Breeze.[169] The alkaline-earth metal hexaborides AeB_6 (Ae = Ca, Sr, Ba) were shown to have small band gaps in accord with the closed-shell nature of $[B_6^{2-}]$ in a solid-state structure with each boron of a B_6 octahedron linked through a 2c-2e bond to a boron atom in an adjacent B_6 octahedron and thus isoelectronic with the discrete ion $B_6H_6^{2-}$. Similarly, the metallic conductivity of LaB_6 was attributed to the extra electron remaining on each lanthanum after filling the bonding orbitals in the boron cages to give $[B_6^{2-}]$ structural units. Typical metallic properties of LaB_6 were investigated by these authors,[169] including the Hall coefficient and the Fermi surface.

Boron icosahedra are also found in many boron-rich borides of the most electropositive metals such as Li, Na, Mg, and Al.[170] An important structural unit in such borides is B_{14}^{4-}, which may be written more precisely as $(B_{12}^{2-})(B^-)_2$. Thus, consider the magnesium boride $Mg_2B_{14} = (Mg^{2+})_2(B_{12}^{2-})(B^-)_2$ (ref 171). One-half of the external bonds from the B_{12} icosahedra are direct bonds to other B_{12} icosahedra, whereas the other half of these external bonds are to the isolated boron atoms. Closely related structures are found in $LiAlB_{14}$ (ref 172) and the so-called "$MgAlB_{14}$". However, "$MgAlB_{14}$" is actually $MgAl_{2/3}B_{14}$ because of partial occupancy of the aluminum sites and thus can be formulated with the same B_{14}^{2-} unit as Mg_2B_{14}.[173] A less closely related structure is $NaB_{14.5}$, which has two types of interstitial boron atoms as well as the same B_{12}^{2-} icosahedra.[174,175]

The lanthanides are also examples of electropositive metals that form boron-rich borides having boron subnetworks constructed from B_{12} icosahedra. An example of an extremely boron-rich metal boride is YB_{66}.[176,177] The structure of YB_{66} is very complicated with a unit cell containing approximately 24 yttrium atoms and 1584 boron atoms. The majority of the boron atoms (1248 = (8)(156)) are contained in 13-icosahedron units of 156 atoms each. In each 13-icosahedron unit a central B_{12} icosahedron is surrounded by 12 icosahedra leading to a B_{156} "icosahedron of icosahedra". The remaining boron atoms are statistically distributed in channels that result from the packing of the 13-icosahedron units and from nonicosahedral cages that are not readily char-

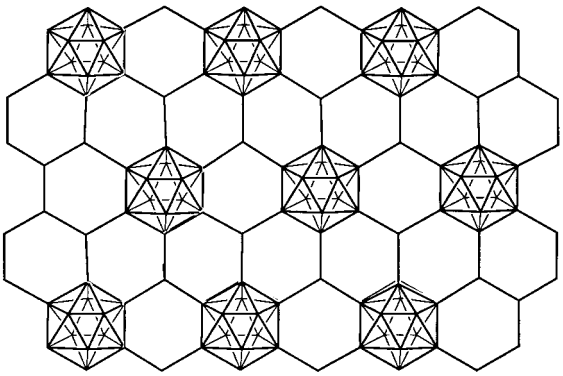

Figure 20. Schematic representation of the boron carbide structure showing the B_{12} icosahedra and the C_2B_4 six-membered rings.

acterized. The complexity of this structure and the uncertainty in the positions of the "interstitial" boron atoms clearly preclude any serious attempts at electron counting.

Another interesting boron-rich solid-state compound is the refractory material boron carbide, which exhibits stoichiometries between B_4C (= $B_{12}C_3$)[178] and $B_{13}C_2$.[179] These materials have interesting structures in which B_{12} icosahedra are linked by C_2B_4 six-membered rings similar to the six-membered rings in the planar graphite (Figure 20). Thus, the structure of $B_{12}C_3$ can be derived from the structure of α-rhombohedral boron by replacement of the 3c-2e bonds linking B_{12} icosahedra with the linear C_3 bridging units. The planarity of the six-membered C_2B_4 rings suggests "benzenoid-type" aromaticity. Additional carbon (in $B_{12}C_3$) or boron (in $B_{13}C_2$) atoms link the carbon atoms to form allene-like C_3 or CBC chains, respectively, in directions perpendicular to the planes of the C_2B_4 rings. Thus, the structure of $B_{12}C_3$ can be derived from the structure of α-rhombohedral boron by replacement of the 3c-2e bonds linking B_{12} icosahedra with the linear C_3 bridging units; computational studies[156] lead to a direct band gap of 3.8 eV relative to an indirect band gap of 1.7 eV for α-rhombohedral boron. The combination of the very stable "aromatic" hexagonal C_2B_4 rings fused to the likewise very stable B_{12} icosahedra can account for the observed stability and strength of the $B_{12}C_3$ and $B_{13}C_2$ structures including the extreme hardness and high melting points of these boron carbides.

E. Supraicosahedral Boranes

A question of interest in deltahedral borane chemistry is whether supraicosahedral boranes $B_nH_n^{2-}$ ($n \geq 13$) can be synthesized and whether the Frank−Kasper polyhedra (Figure 11) are suitable models for their structures. The 14-vertex supraicosahedral metallacarborane $(C_5H_5)_2Co_2B_{10}C_2H_{12}$ is known[180] and has a structure based on the Frank−Kasper bicapped hexagonal antiprism with the cobalt atoms at the degree 6 vertices.

The first detailed theoretical study on the supraicosahedral boranes $B_nH_n^{2-}$ ($13 \leq n \leq 24$) was performed by Brown and Lipscomb,[181] who investigated possible deltahedra and performed simple SCF calculations on the structures with up to 17 boron atoms. The proposed structures were found to resemble solutions to problems of arranging objects which repel one another on the surface of a sphere, which were studied in the prequantum mechanics days by the mathematician Föppl.[182,183] The observed deltahedra conform to the following generalizations. (1) There may be boron atoms at a pole or both poles and on latitudinal rings perpendicular to the polar axis. (2) The latitudinal rings are rotated (twisted) so that arrangements of boron atoms are not coincident between neighboring rings to minimize boron−boron repulsion. (3) There exist special values of n corresponding to special arrangements.

In subsequent work shortly after this original report, Lipscomb and co-workers[184,185] performed partial retention of diatomic differential overlap (PRDDO) calculations on these supraicosahedral boranes. This work identified three examples of supraicosahedral boranes, namely, $B_{16}H_{16}^{z-}$, $B_{19}H_{19}^{z-}$, and $B_{22}H_{22}^{z-}$, where the dianions (i.e., $z = 2$) were found to undergo Jahn−Teller distortions. The full molecular symmetries were obtained by considering the structure to be a neutral one with only $2n$ skeletal electrons.

These supraicosahedral boranes were subsequently investigated by Fowler[186] using the pairing principle from tensor surface harmonic theory (section II.E). The predicted anomalous electron counts for $B_{16}H_{16}^{z-}$, $B_{19}H_{19}^{z-}$, and $B_{22}H_{22}^{z-}$, namely, $2n$ or $2n + 4$ rather than $2n + 2$ skeletal electrons, were shown to be forced by symmetry for either T or T_d clusters with an odd number of sets of four equivalent cage atoms or C_m or C_{mv} ($m \geq 3$) clusters with an odd number of cage atoms on the C_m axis.

More recently, the still experimentally unknown supraicosahedral boranes $B_nH_n^{2-}$ ($n = 13-17$) were evaluated by Schleyer, Najafian, and Mebel[187] at the B3LYP/6-31G* level of density functional theory. Calculations of the nucleus-independent chemical shifts suggested that all of these deltahedral boranes should exhibit three-dimensional aromaticity. The supraicosahedral boranes $B_nH_n^{2-}$ ($n = 13-17$) were found to be thermodynamically more stable than the subicosahedral boranes $B_nH_n^{2-}$ ($n = 9-11$) but less stable than the icosahedral $B_{12}H_{12}^{2-}$, which has the lowest energy on a per vertex basis of any of the deltahedral boranes. The formation of $B_{13}H_{13}^{2-}$ from $B_{12}H_{12}^{2-}$ was found to be especially unfavorable thermodynamically, which may account for the fact that no metal-free binary supraicosahedral boranes are known. The geometry optimization in these computations led to the Frank−Kasper polyhedra (Figure 11) for $B_{14}H_{14}^{2-}$ and $B_{15}H_{15}^{2-}$ but not for $B_{16}H_{16}^{2-}$, which had an optimized structure with two square faces. This computational study suggests that the supraicosahedral boranes $B_nH_n^{2-}$ ($n = 13-17$) should be stable compounds, but a successful method for their synthesis must find a way of avoiding being trapped in the icosahedral $B_{12}H_{12}^{2-}$ energy sink.

Recent calculations by McKee, Wang, and Schleyer[126] suggest the possibility of synthesizing neutral supraicosahedral boranes of the type B_nH_n. In particular, a C_{3v} capped icosahedral structure of neutral

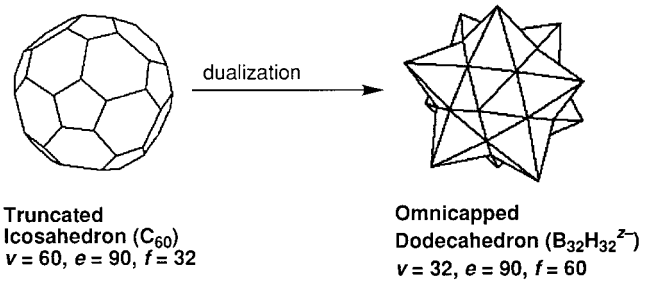

Figure 21. Dual relationship between the truncated icosahedron of C_{60} and the omnicapped (stellated) dodecahedron proposed for $B_{32}H_{32}^{z-}$.

$B_{13}H_{13}$ is expected to be exceptionally stable for a supraicosahedral borane since it combines the high stability of the $B_{12}H_{12}^{2-}$ icosahedron with a BH^{2+} cap.

Recent work by Dopke, Powell, and Gaines[188] led to the synthesis of the dianion $B_{19}H_{19}^{2-}$ by cage expansion of $M_2[B_{18}H_{20}]$ (M = Na, K) with $H_2BCl{\cdot}SMe_2$ or $HBCl_2{\cdot}SMe_2$ in diethyl ether followed by deprotonation of the intermediate $B_{19}H_{20}^-$ ion with Proton Sponge (1,8-bis(dimethylamino)naphthalene). The intermediate $B_{19}H_{20}^-$ ion as its crystalline $(Ph_3P)_2N^+$ salt was found by X-ray diffraction to exhibit a structure consisting of edge-sharing *nido* 10- and 11-vertex fragments rather than a single 19-vertex deltahedron. This result provides experimental evidence that structures containing large deltahedra for boranes $B_nH_n^{2-}$ are not favorable relative to structures constructed by fusing 10- to 12-vertex polyhedra. The dianion $B_{19}H_{19}^{2-}$ was not isolated as a crystalline salt but instead characterized by ^{11}B NMR of the deprotonation reaction mixture.

An even larger deltahedral boron cage of interest is $B_{32}H_{32}^{z-}$, since this is the first possible deltahedron after $B_{12}H_{12}^{2-}$ of icosahedral (I_h) symmetry. Such an omnicapped dodecahedral structure for $B_{32}H_{32}^{z-}$ turns out to be the dual of the famous C_{60} truncated icosahedron (Figure 21). This structure for $B_{32}H_{32}^{z-}$ was first proposed by Lipscomb and co-workers in 1978[185] but subsequently studied in more detail by Fowler and co-workers.[186] A qualitative extended Hückel treatment of $B_{32}H_{32}^{z-}$ indicated an accidental degeneracy at the nonbonding level from which charges of +4, −2, or −8 might be deduced. Subsequent ab initio calculations[189] using an STO-3G basis set suggested that $B_{32}H_{32}^{z-}$ is most stable as a dianion similar to the smaller deltahedral boranes. The absolute value of the energy of $B_{32}H_{32}^{2-}$ per BH unit was found to be intermediate between that of the octahedral $B_6H_6^{2-}$ and the icosahedral $B_{12}H_{12}^{2-}$.

V. Summary

Chemical bonding models based on graph theory or tensor surface harmonic theory demonstrate the analogy between the aromaticity in two-dimensional planar polygonal hydrocarbons such as benzene and that in three-dimensional deltahedral borane anions of the type $B_nH_n^{2-}$ ($6 \le n \le 12$). Such models are supported both by diverse computational studies and experimental determinations of electron density distribution. Related methods can be used to study the chemical bonding in the boron polyhedra found in other structures including neutral binary boron hydrides, metallaboranes, various allotropes of elemental boron, and boron-rich solid-state metal borides.

VI. Acknowledgment

I am indebted to the Petroleum Research Fund of the American Chemical Society for partial support of this work.

VII. References

(1) Stock, A. *Hydrides of Boron and Silicon*; Cornell University Press: Ithaca, NY, 1933.
(2) Dilthey, W. *Z. Angew. Chem.* **1921**, *34*, 596.
(3) Bell, R. P.; Longuet-Higgins, H. C. *Proc. R. Soc. (London) A* **1945**, *183*, 357.
(4) Price, W. C. *J. Chem. Phys.* **1947**, *15*, 614.; Price, W. C. *J. Chem. Phys.* **1948**, *16*, 894.
(5) Laszlo, P. *Angew. Chem., Int. Ed.* **2000**, *39*, 2071.
(6) Hedberg, K.; Schomaker, V. *J. Am. Chem. Soc.* **1951**, *73*, 1482.
(7) Lipscomb, W. N. *Boron Hydrides*; W. A. Benjamin: New York, 1963.
(8) Pitzer, K. S. *J. Am. Chem. Soc.* **1945**, *67*, 1126.
(9) Eberhardt, W. H.; Crawford, B.; Lipscomb, W. N. *J. Chem. Phys.* **1954**, *22*, 989.
(10) Williams, R. E. *Inorg. Chem.* **1971**, *10*, 210.
(11) Allard, G. *Bull. Soc. Chim. Fr.* **1932**, *51*, 1213.
(12) Pauling, L.; Weinbaum, S. *Z. Kristallogr.* **1943**, *87*, 181.
(13) Longuet-Higgins, H. C.; Roberts, M. de V. *Proc R. Soc. (London)* **1954**, *224A*, 336.
(14) Longuet-Higgins, H. C.; Roberts, M. de V. *Proc R. Soc. (London)* **1955**, *230A*, 110.
(15) Hoard, J. L.; Geller, S.; Hughes, R. E. *J. Am. Chem. Soc.* **1951**, *73*, 1892.
(16) Hawthorne, M. F.; Pitochelli, A. R. *J. Am. Chem. Soc.* **1960**, *82*, 3328.
(17) Hawthorne, M. F.; Pitochelli, A. R. *J. Am. Chem. Soc.* **1959**, *81*, 5519.
(18) Wunderlich, J.; Lipscomb, W. N. *J. Am. Chem. Soc.* **1960**, *82*, 4427.
(19) Kaczmarczyk, A.; Dobrott, R. D.; Lipscomb, W. N. *Proc. Natl. Acad. U.S.A.* **1962**, *48*, 729. Dobrott, R. D.; Lipscomb, W. N. *J. Chem. Phys.* **1962**, *37*, 1779.
(20) Klanberg, F.; Muetterties, E. L. *Inorg. Chem.* **1966**, *5*, 1955.
(21) Klanberg, F.; Eaton, D. R.; Guggenberger, L. J.; Muetterties, E. L. *Inorg. Chem.* **1967**, *6*, 1271.
(22) Boone, J. L. *J. Am. Chem. Soc.* **1964**, *86*, 5036.
(23) King, R. B.; Duijvestijn, A. J. W. *Inorg. Chim. Acta* **1990**, *178*, 55.
(24) Wade, K. *Chem. Commun.* **1971**, 792.
(25) Wade, K. *Adv. Inorg. Chem. Radiochem.* **1976**, *18*, 1.
(26) Mingos, D. M. P. *Acc. Chem. Res.* **1984**, *17*, 311.
(27) Mingos, D. M. P.; Johnston, R. L. *Struct. Bonding* **1987**, *68*, 29.
(28) Grimes, R. N. *Carboranes*; Academic Press: New York, 1970.
(29) Shapiro, I.; Good, C. D.; Williams, R. E. *J. Am. Chem. Soc.* **1962**, *84*, 3837. Shapiro, I.; Keilin, B.; Williams, R. E.; Good, C. D. *J. Am. Chem. Soc.* **1963**, *85*, 3167.
(30) Potenza, J. A.; Lipscomb, W. N. *Inorg. Chem.* **1964**, *3*, 1673. Voet, D.; Lipscomb, W. N. *Inorg. Chem.* **1964**, *3*, 1679. Potenza, J. A.; Lipscomb, W. N. *J. Am. Chem. Soc.* **1964**, *86*, 1874. Potenza, J. A.; Lipscomb, W. N. *Inorg. Chem.* **1966**, *5*, 1483.
(31) Stanko, V. I.; Struchkov, Yu. T. *Zh. Obshch. Khim.* **1965**, *35*, 930. Andrianov, V. G., Stanko, V. I.; Struchkov, Yu. T.; Klimova, A. L. *Zh. Strukt. Khim.* **1967**, *8*, 707.
(32) Aihara, J.-i *J. Am. Chem. Soc.* **1978**, *100*, 3339.
(33) King, R. B.; Rouvray, D. H. *J. Am. Chem. Soc.* **1977**, *99*, 7834.
(34) Stone, A. J.; Alderton, M. J. *Inorg. Chem.* **1982**, *21*, 2297.
(35) Dickerson, R. E.; Lipscomb, W. N. *J. Chem. Phys.* **1957**, *27*, 212.
(36) Lipscomb, W. N. In *Boron Hydride Chemistry*; Muetterties, E. L., Ed.; Academic Press: New York, 1975; pp. 30−78.
(37) Williams, R. E. *Chem. Rev.* **1992**, *92*, 177.
(38) Rudolph, R. W.; Pretzer, W. R. *Inorg. Chem.* **1972**, *11*, 1974.
(39) Rudolph, R. W. *Acc. Chem. Res.* **1976**, *9*, 446.
(40) Mingos, D. M. P. *Nature Phys. Sci.* **1972**, *99*, 236.
(41) Mingos, D. M. P. *Acc. Chem. Res.* **1984**, *17*, 311.
(42) Gutman, I.; Cyvin, S. J. *Introduction to the Theory of Benzenoid Hydrocarbons*; Springer: Berlin, 1989. Gutman, I. *Topics Curr. Chem.* **1992**, *153*, 1−18.
(43) Dixon, D. A.; Kleier, D. A.; Halgren, T. A.; Hall, J. H.; Lipscomb, W. N. *J. Am. Chem. Soc.* **1977**, *99*, 6226.
(44) O'Neill, M.; Wade, K. *Polyhedron* **1984**, *3*, 199.
(45) Morrison, J. A. *Chem. Rev.* **1991**, *91*, 35.
(46) Bowser, J. R.; Bonny, A.; Pipal, J. R.; Grimes, R. N. *J. Am. Chem. Soc.* **1979**, *101*, 6229.

(47) Gillespie, R. J.; Porterfield, W. W.; Wade, K. *Polyhedron* **1987**, *6*, 2129.
(48) Ruedenberg, K. *J. Chem. Phys.* **1954**, *22*, 1878.
(49) Schmidtke, H. H. *J. Chem. Phys.* **1966**, *45*, 3920. *Coord. Chem. Rev.* **1967**, *2*, 3.
(50) Biggs, N. L. *Algebraic Graph Theory*; Cambridge University Press: London, 1974.
(51) King, R. B. In *Chemical Applications of Topology and Graph Theory*; King, R. B., Ed.; Elsevier: Amsterdam, 1983; pp 99−123.
(52) King, R. B. In *Molecular Structure and Energetics*; Liebman, J. F., Greenberg, A., Ed.; VCH: Deerfield Beach, FL, 1976; pp 123−148.
(53) King, R. B. *Rep. Mol. Theor.* **1990**, *1*, 141.
(54) Mansfield, M. J. *Introduction to Topology*; Van Nostrand: Princeton, NJ, 1963; p 40.
(55) Grünbaum, B. *Convex Polytopes*; Interscience: New York, 1967; p 138.
(56) Hückel, E. *Z. Physik.* **1932**, *76*, 628.
(57) Beinecke, L. W.; Wilson, R. J. *Selected Topics in Graph Theory*; Academic Press: New York, 1978; Chapter 1.
(58) Chisholm, C. D. H. *Group Theoretical Techniques in Quantum Chemistry*; Academic Press: New York, 1976; Chapter 6.
(59) Aihara, J.-i. *Bull. Chem. Soc. Jpn.* **1979**, *52*, 2202.
(60) Kuratowski, K. *Fundam. Math.* **1930**, *15*, 271.
(61) Kettle, S. F. A.; Tomlinson, V. *J. Chem. Soc. A* **1969**, 2002, 2007.
(62) McNeill, E. A.; Gallaher, K. L.; Scholer, F. R.; Bauer, S. H. *Inorg. Chem.* **1973**, *12*, 2108.
(63) King, R. B. In *Contemporary Boron Chemistry*; Davidson, M. G., Hughes, A. K., Marder, T. B., Wade, K., Eds.; Royal Society of Chemistry: Cambridge, U.K., 2000; pp 506−509.
(64) Frank, F. C.; Kasper, J. S. *Acta Crystallogr.* **1958**, *11*, 184.
(65) King, R. B. *Inorg. Chim. Acta* **1995**, *235*, 111.
(66) Middaugh, R. L. In *Boron Hydride Chemistry*; Muetterties, E. L., Ed.; Academic Press: New York, 1975; p 283.
(67) Stone, A. J. *Mol. Phys.* **1980**, *41*, 1339. Stone, A. J. *Inorg. Chem.* **1981**, *20*, 563. Stone, A. J.; Alderton, M. J. *Inorg. Chem.* **1982**, *21*, 2297. Stone, A. J. *Polyhedron* **1984**, *3*, 1299.
(68) Johnston, R. L.; Mingos, D. M. P. *Theor. Chim. Acta* **1989**, *75*, 11.
(69) Jemmis, E. D. *J. Am. Chem. Soc.* **1982**, *104*, 7017. Jemmis, E. D.; Schleyer, P. v. R. *J. Am. Chem. Soc.* **1982**, *104*, 4781. Jemmis, E. D.; Pavankumar, P. N. V. *Proc. Indian Acad. Sci.* **1984**, *93*, 479.
(70) Collins, J. B.; Schleyer, P. v. R. *Inorg. Chem.* **1977**, *16*, 152.
(71) McKee, M. L. Fluxional Processes in Boranes and Carboranes. In *The Encyclopedia of Computational Chemistry*; Schleyer, P. v. R., Ed.; Wiley: New York, 1998; pp 1002−1013.
(72) Lipscomb, W. N. *Science* **1966**, *153*, 373.
(73) Berry, R. S. *J. Chem. Phys.* **1960**, *32*, 933.
(74) Holmes, R. R. *Acc. Chem. Res.* **1972**, *5*, 296.
(75) King, R. B. *Inorg. Chim. Acta* **1981**, *49*, 237.
(76) Gimarc, B. M.; Ott, J. J. *Inorg. Chem.* **1966**, *25*, 83.
(77) Ott, J. J.; Brown, C. A.; Gimarc, B. M. *Inorg. Chem.* **1989**, *28*, 4269.
(78) Gimarc, B. M.; Ott, J. J. *Inorg. Chem.* **1986**, *25*, 2708.
(79) Mebel, A. M.; Schleyer, P. v. R.; Najafian, K.; Charkin, O. P. *Inorg. Chem.* **1998**, *37*, 1693.
(80) Wales, D. J.; Stone, A. J. *Inorg. Chem.* **1987**, *26*, 3845.
(81) Mingos, D. M. P.; Johnston, R. J. *Polyhedron* **1988**, *7*, 2437.
(82) Hoffmann, R.; Lipscomb, W. N. *J. Chem. Phys.* **1962**, *36*, 2179.
(83) Hoffmann, R.; Lipscomb, W. N. *J. Chem. Phys.* **1962**, *37*, 2872.
(84) Newton, M. D.; Boer, F. P.; Lipscomb, W. N. *J. Am. Chem. Soc.* **1966**, *88*, 2353.
(85) Boer, F. P.; Newton, M. D.; Lipscomb, W. N. *J. Am. Chem. Soc.* **1966**, *88*, 2361.
(86) Halgren, T. A.; Lipscomb, W. N. *Proc. Natl. Acad. Sci. U.S.A.* **1972**, *69*. 652; *J. Chem. Phys.* **1974**, *61*, 3905.
(87) Dixon, D. A.; Kleier, D. A.; Halgren, T. A.; Hall, J. H.; Lipscomb, W. N. *J. Am. Chem. Soc.* **1977**, *99*, 6226.
(88) Kettle, S. F. A.; Tomlinson, V. *J. Chem. Soc. A* **1969**, 2002.
(89) Kettle, S. F. A.; Tomlinson, V. *Theor. Chim. Acta* **1969**, 175.
(90) Armstrong, D. R.; Perkins, P. G.; Stewart, J. J. *J. Chem. Soc. A* **1971**, 3674.
(91) Armstrong, D. R.; Perkins, P. G.; Stewart, J. J. *J. Chem. Soc. A* **1973**, 627.
(92) McKee, M. L.; Bühl, M.; Charkin, O. P.; Schleyer, P. v. R. *Inorg. Chem.* **1993**, *32*, 4549.
(93) Zhao, M.; Gimarc, B. M. *Inorg. Chem.* **1993**, *32*, 4700.
(94) Porterfield, W. W.; Jones, M. E.; Gill, W. R.; Wade, K. *Inorg. Chem.* **1990**, *29*, 2914, 2919, 2923, 2927. Gill, W. R.; Jones, M. E.; Wade, K.; Porterfield, W. W.; Wong, E. H. *J. Mol. Struct. (THEOCHEM)* **1992**, *261*, 161.
(95) Basiri, H. G.; Pan, Y.-K. *J. Electron Spectrosc. Relat. Phenom.* **1989**, *48*, 137.
(96) Slater, J. C. *Quantum Theory of Molecules and Solids*; McGraw-Hill: New York, 1974; Vol. 4.
(97) Dewar, M. J. S.; McKee, M. L. *Inorg. Chem.* **1978**, *17*, 1569.
(98) Bingham, R. C.; Dewar, M. J. S.; Lo, D. H. *J. Am. Chem. Soc.* **1975**, *97*, 1285, 1294, 1302, 1307.
(99) Dewar, M. J. S.; Thiel, W. *J. Am. Chem. Soc.* **1977**, *99*, 4899, 4907.
(100) Pople, J. A.; Santry, J. P.; Segal, G. A. *J. Chem. Phys.* **1965**, *43*, S129.
(101) Allinger, N. L.; Yuh, Y. H.; Lii, J. H. *J. Am. Chem. Soc.* **1989**, *111*, 8551.
(102) Timofeeva, T. V.; Mazurek, U.; Allinger, N. L. *J. Mol. Struct. (THEOCHEM)* **1996**, *363*, 35.
(103) Timofeeva, T. V.; Suponitsky, K. Yu.; Yanovsky, A. I.; Allinger, N. L. *J. Organomet. Chem.* **1997**, *536*−*537*, 481.
(104) Suponitsky, K. Yu.; Timofeeva, T. V.; Allinger, N. L. *Inorg. Chem.* **2000**, *39*, 3140.
(105) Guest, M. F.; Hillier, I. H. *Mol. Phys.* **1973**, *26*, 435.
(106) Ott, J. J.; Gimarc, B. M. *J. Comput. Chem.* **1986**, *7*, 673.
(107) Pulay, P. *Mol. Phys.* **1969**, *17*, 197.
(108) Williams, R. E. *Adv. Inorg. Chem. Radiochem.* **1976**, *18*, 67.
(109) King, R. B.; Dai, B.; Gimarc, B. M. *Inorg. Chim. Acta* **1990**, *167*, 213.
(110) Fowler, P. W. *J. Chem. Soc., Faraday Trans. 2* **1986**, *82*, 61.
(111) Green, T. A.; Switendick, A. C.; Emin, D. *J. Chem. Phys.* **1988**, *89*, 6815.
(112) Zahradnik, R.; Balaji, V.; and Michl, J. *J. Comput. Chem.* **1991**, *12*, 1147.
(113) Bader, R. F. W.; Legare, D. A. *Can. J. Chem.* **1992**, *70*, 657.
(114) Bader, R. F. W. *Atoms in Molecules*—*A Quantum Theory*; Oxford University Press: Oxford, U.K., 1990. Bader, R. F. W. *Chem. Rev.* **1991**, *91*, 893.
(115) Jemmis, E. D.; Subramanian, G.; Srivastava, I. H.; Gadre, S. R. *J. Phys. Chem.* **1994**, *98*, 6445.
(116) Ahrlichs, R.; Bär, M.; Häser, M.; Kölmel, C. *Chem. Phys. Lett.* **1989**, *162*, 165.
(117) Takano, K.; Izuho, M., Hosoya, H. *J. Phys. Chem.* **1992**, *96*, 6962.
(118) Takano, K.; Hosoya, H.; Iwata, S. *J. Am. Chem. Soc.* **1984**, *106*, 2787. Takano, K.; Hosoya, H.; Iwata, S. *J. Chem. Soc. Jpn.* **1986**, 1395. Takano, K.; Okamoto, M.; Hosoya, H. *J. Phys. Chem.* **1988**, *92*, 4869.
(119) Schleyer, P. v. R.; Subramanian, G.; Jiao, H.; Najafian, K.; Hofmann, M. In *Advances in Boron Chemistry*; Siebert, W., Ed.; Royal Society of Chemistry, Cambridge, U.K., 1997; pp 3−14.
(120) Schleyer, P. v. R.; Maerker, C.; Dransfeld, A.; Jiao, H.; Hommes, N. J. R. v. E. *J. Am. Chem. Soc.* **1996**, *118*, 6317.
(121) Schleyer, P. v. R.; Najafian, K. In *The Borane-Carborane-Carbocation Continuum*; Casanova, J., Ed.; Wiley: New York, 1998; Chapter 7, pp 169−190.
(122) Schleyer, P. v. R.; Najafian, K. *Inorg. Chem.* **1998**, *37*, 3454.
(123) Jemmis, E. D.; Subramanian, G.; Radom, L. *J. Am. Chem. Soc.* **1992**, *114*, 1481.
(124) Jemmis, E. D.; Subramanian, G.; McKee, M. L. *J. Phys. Chem.* **1996**, *100*, 7014.
(125) Jemmis, E. D.; Kiran, B.; Coffey, D., Jr. *Chem. Ber.* **1997**, *130*, 1147.
(126) McKee, M. L.; Wang, Z.-X.; Schleyer, P. v. R. *J. Am. Chem. Soc.* **2000**, *122*, 4781.
(127) McKee, M. L. *J. Am. Chem. Soc.* **1988**, *110*, 5317; **1992**, *114*, 879.
(128) Burdett, J. K.; Eisenstein, O. *J. Am. Chem. Soc.* **1995**, *117*, 11939.
(129) Subramanian, G.; Schleyer, P. v. R., Dransfeld, A. *Organometallics* **1998**, *17*, 1634.
(130) Dyczmons, V.; Horn, M.; Botschwina, P.; Meller, A. *J. Mol. Struct. (THEOCHEM)* **1998**, *431*, 137.
(131) McKee, M. L. *Inorg. Chem.* **1999**, *38*, 321.
(132) Antipin, M.; Boese, R.; Bläser, D.; Maulitz, A. *J. Am. Chem. Soc.* **1997**, *119*, 326.
(133) Fowler, P. W.; Porterfield, W. W. *Inorg. Chem.* **1985**, *24*, 3511.
(134) Vondrák, T. *Polyhedron* **1987**, *6*, 1559; Vondrák, T.; Heřmánek, S.; Plešek, J. *Polyhedron* **1993**, *12*, 1301.
(135) Hitchcock, A. P.; Urquhart, S. G.; Wen, A. T.; Kilcoyne, A. L. D.; Tyliszczak, T.; Rühl, E.; Kosugi, N.; Bozek, J. D.; Spencer, J. T.; McIlroy, D. N.; Dowben, P. A. *J. Phys. Chem. B* **1997**, *101*, 3483.
(136) Lyssenko, K. A.; Antipin, M. Yu.; Lebedev, V. N. *Inorg. Chem.* **1998**, *37*, 5834.
(137) McLemore, D. K.; Dixon, D. A.; Strauss, S. H. *Inorg. Chim. Acta* **1999**, *294*, 193.
(138) Hawthorne, M. F. *Acc. Chem. Res.* **1988**, *1*, 281.
(139) King, R. B. *Transition Metal Organometallic Chemistry: An Introduction*; Academic Press: New York, 1969.
(140) Bould, J.; Kennedy, J. D.; Thornton-Pett, M. *J. Chem. Soc., Dalton* **1992**, 563; Kennedy, J. D.; Štibr, B. In *Current Topics in the Chemistry of Boron*; Kabalka, G. W., Ed.; Royal Society of Chemistry: Cambridge, 1994; pp 285−292. Kennedy, J. D. In *The Borane-Carborane-Carbocation Continuum*; Casanova, J., Ed.; Wiley: New York, 1998; Chapter 3, pp 85−116. Štibr, B.; Kennedy, J. D.; Drdáková, E.; Thornton-Pett, M. *J. Chem. Soc., Dalton* **1994**, 229.

(141) Dunks, G. B.; Hawthorne, M. F. *J. Am. Chem. Soc.* **1970**, *92*, 7213.
(142) Hoel, E. L.; Strouse, C. E.; Hawthorne, M. F. *Inorg. Chem.* **1974**, *13*, 1388.
(143) Callahan, K. P.; Evans, W. J.; Lo, F. Y.; Strouse, C. E.; Hawthorne, M. F. *J. Am. Chem. Soc.* **1975**, *97*, 296.
(144) Nishimura, E. K. *Chem. Commun.* **1978**, 858.
(145) Baker, R. T. *Inorg. Chem.* **1986**, *25*, 109.
(146) Johnston, R. L.; Mingos, D. M. P. *Inorg. Chem.* **1986**, *25*, 3321. Johnston, R. L.; Mingos, D. M. P. *J. Chem. Soc., Dalton* **1987**, 647. Johnston, R. L.; Mingos, D. M. P. *Polyhedron* **1986**, *5*, 2059.
(147) King, R. B. *Inorg. Chem.* **1999**, *38*, 5151.
(148) Bown, M.; Fontaine, X. L. R.; Greenwood, N. N.; Kennedy, J. D.; Thornton-Pett, M. *J. Chem. Soc., Dalton* **1990**, 3039.
(149) Bould, J.; Crook, J. E.; Greenwood, N. N.; Kennedy, J. D.; McDonald, W. S. *Chem. Commun.* **1982**, 346.
(150) Lipscomb, W. N.; Britton, D. *J. Chem. Phys.* **1960**, *33*, 275.
(151) Hoard, J.; Hughes, R. E. In *The Chemistry of Boron and its Compounds*; Muetterties, E. L., Ed.; Wiley: New York, 1967; pp 25−154.
(152) *Boron-Rich Solids*; Emin, D., Aselage, T., Beckel, C. L., Howard, I. A., Woods, C. D., Eds.; American Institute of Physics: New York, 1986.
(153) Fujimori, M.; Nakata, T.; Nakayama, T.; Nishibori, E.; Kimura, K.; Takata, M.; Sakata, M. *Phys. Rev. Lett.* **1999**, *82*, 4452.
(154) Pauling, L. *Phys. Rev. Lett.* **1987**, *58*, 365.
(155) King, R. B. *Inorg. Chim. Acta* **1991**, *181*, 217.
(156) Bullett, D. W. *J. Phys. C: Solid State Phys.* **1982**, *15*, 415.
(157) Hoard, J. L.; Geller, S.; Hughes, R. E. *J. Am. Chem. Soc.* **1951**, *73*, 1892; Hoard, J. L.; Hughes, R. E.; Sands, D. E. *J. Am. Chem. Soc.* **1958**, *80*, 4507.
(158) Boustani, I. *Chem. Phys. Lett.* **1995**, *240*, 135.
(159) Boustani, I. *Phys. Rev. B* **1997**, *55*, 16426.
(160) Boustani, I.; Quandt, A.; Kramer, P. *Europhys. Lett.* **1996**, *36*, 583.
(161) Boustani, I. *Surf. Sci.* **1997**, *370*, 355.
(162) Boustani, I.; Quandt, A. *Europhys. Lett.* **1997**, *39*, 527.
(163) Boustani, I. *J. Solid State Chem.* **1997**, *133*, 182.
(164) Rogl, P.; Nowotny, H. *J. Less Common Met.* **1978**, *61*, 39.
(165) Étourneau, J.; Hagenmuller, P. *Philos. Mag. B* **1985**, *52*, 589.
(166) Albert, B. *Eur. J. Inorg. Chem.* **2000**, 1679.
(167) Lipscomb, W. N.; Britton, D. *J. Chem. Phys.* **1960**, *33*, 275.
(168) Lipscomb, W. N. *J. Less Common Met.* **1981**, *82*, 1.
(169) Perkins, P. G.; Armstrong, D. R.; Breeze, A. *J. Phys. C: Solid State Phys.* **1975**, *8*, 3558.
(170) Naslain, R.; Guette, A.; Hagenmuller, *J. Less-Common Met.* **1976**, *47*, 1.
(171) Guette, A.; Barret, M.; Naslain, R.; Hagenmuller, P.; Tergenius, L. E.; Lundström, T. *J. Less-Common Met.* **1981**, *82*, 325.
(172) Higashi, I. *J. Less-Common Met.* **1981**, *82*, 317.
(173) Matkovich, V. I.; Economy, J. *Acta Crystallogr., Sect. B* **1969**, *26*, 616.
(174) Naslain, R.; Kasper, J. S. *J. Solid State Chem.* **1970**, *1*, 150.
(175) Albert, B.; Hofmann, K.; Fild, C.; Eckert, H.; Schliefer, M.; Gruehn, R. *Chem. Eur. J.* **2000**, *6*, 2531.
(176) Richards, S. M.; Kasper, J. S. *Acta Crystallogr., Sect. B* **1969**, *25*, 257.
(177) Kasper, J. S. *J. Less-Common Met.* **1976**, 17.
(178) Clark, K. H.; Hoard, J. L. *J. Am. Chem. Soc.* **1943**, *65*, 2115.
(179) Will, G.; Kossobutzki, K. H. *J. Less-Common Met.* **1976**, *44*, 87.
(180) Evans, W. J.; Hawthorne, M. F. *J. Chem. Soc. Chem. Commun.* **1974**, 38.
(181) Brown, L. D.; Lipscomb, W. N. *Inorg. Chem.* **1977**, *16*, 2989.
(182) Föppl, *J. Reine. Angew. Math.* **1912**, *141*, 251.
(183) Whyte, L. *Am. Math. Monthly* **1952**, *59*, 606. Jeech, L. *Math. Gazette* **1957**, *41*, 81. Coxeter, H. S. M. *Trans. N.Y. Acad. Sci.* **1962**, *24*, 320.
(184) Bicerano, J.; Marynick, D. S.; Lipscomb, W. N. *Inorg. Chem.* **1978**, *17*, 2041.
(185) Bicerano, J.; Marynick, D. S.; Lipscomb, W. N. *Inorg. Chem.* **1978**, *17*, 3443.
(186) Fowler, P. W. *Polyhedron* **1985**, *4*, 2051.
(187) Schleyer, P. v. R.; Najafian, K.; Mebel, A. M. *Inorg. Chem.* **1998**, *37*, 6765.
(188) Dopke, J. A.; Powell, D. R.; Gaines, D. F. *Inorg. Chem.* **2000**, *39*, 463.
(189) Fowler, P. W.; Lazzeretti, P.; Zanasi, R. *Inorg. Chem.* **1988**, *27*, 1298.

CR000442T